NON-ACTIVATION LOOP PHOSPHORYLATION AND DOWNSTREAM SIGNALING OF AGC1-3, THE *ARABIDOPSIS THALIANA* HOMOLOGUE OF THE TOMATO CELL DEATH SUPPRESSOR ADI3

A Dissertation

by

JOEL WILLIAM GRAY

Submitted to the Office of Graduate Studies of
Texas A&M University
in partial fulfillment of the requirements for the degree of

DOCTOR OF PHILOSOPHY

Chair of Committee,	Timothy Devarenne
Committee Members,	David Peterson
	Thomas McKnight
	J. Martin Scholtz
Head of Department,	Gregory Reinhart

August 2013

Major Subject: Biochemistry

ABSTRACT

Programmed cell death (PCD) is a fundamentally important process delicately coordinated throughout an organism's life cycle. In plants, PCD is an integral part of development, reproduction, and pathogenesis. Numerous types of proteins are involved in regulation of PCD in plants, like phosphatases, metacaspases, and protein kinases. In tomato resistance to the pathogen *Pseudomonas syringae* pv. *tomato* (*Pst*), a Ser/Thr protein kinase, Adi3 (AvrPto-dependent Pto-interacting protein 3), interacts with the pathogen's avirulence protein AvrPto and the tomato resistance protein Pto. Adi3 is a member of the AGC protein kinase family, a group known to transmit signals via the secondary messengers cAMP, cGMP, and phospholipids. In an unchallenged system, the master regulator of AGC kinases, Pdk1, activates Adi3. Activation of Adi3 enables nuclear localization and cell death suppression – all of which is prevented when challenged by *Pst*.

A BLASTp search of the *Arabidopsis thaliania* genome with the amino acid sequence of Adi3 identified a 67% identical match, AGC1-3. Like Adi3, AGC1-3 at its activation-loop serine and another site, by Pdk1. With N-terminal deletions of AGC1-3, Pdk1 was found to phosphorylate AGC1-3 at two serines – one serine conserved among all *Arabidopsis* AGC kinases, the other a serine on the N-terminus of the kinase domain. The non-activation loop serine in AGC1-3, Ser269, is conserved at Ser212, in Adi3. Phosphorylation at Ser212 does not impact auto-catalytic activity of Adi3. However it does enhance trans-catalytic activity. Analysis of AGC1-4 and AGC1-7, two proteins

closely related to AGC1-3, reveals that phosphorylation of non-activation loop residues by Pdk1 is not restricted to AGC1-3 and Adi3. Functional analysis of AGC1-3 in *Arabidopsis* protoplasts revealed that like Adi3, nuclear localization and activation-loop phosphorylation are essential for cell viability.

In an effort to elucidate a signaling network controlled by AGC1-3, the KiC (Kinase-client) assay was employed. In the KiC assay, a 2,100-member peptide library was assayed against AGC1-3 and the constitutively active mutant AGC1-3^{S596D}. By MS analysis, AGC1-3 and AGC1-3^{S596D} phosphorylated 26 and 19 substrate peptides, respectively. Substrate peptides were mapped to proteins involved in central metabolism, transcription, and protein metabolism.

The work presented in this dissertation provides conclusive evidence that Pdk1 phosphorylates AGC1-3 and Adi3 at a non-activation loop residue. The work also supports AGC1-3 as the *Arabidopsis* homologue of Adi3 and presents novel phosphorylation data of potential AGC1-3 substrates.

DEDICATION

This dissertation is dedicated to the three most important people in my life, my heroes and role models.

My brother, Jeremiah.

My father, Thomas.

My mother, RuthAnn.

Thank you, I love you all.

ACKNOWLEDGEMENTS

First I would like to thank my boss, Tim. Thank you for taking me into your lab and for your patience. I greatly appreciate your mentorship as well as your friendship.

I would like to thank former lab mates – Dr. Anna Nelson Dittrich, Dr. Julian Avila, and Dr. Taylor Weiss. Likewise, I would be remiss if I did not mention the de facto Devarenne lab member, Andrew "The Mandrew" Nelson.

Thank you to the members of my dissertation committee – Dr. McKnight, Dr. Scholtz, and Dr. Peterson. Dr. Peterson, your mentorship means a great deal to me, not to mention you shared the sage wisdom with me of "maybe your results are right."

Current Devarenne lab graduate students – Hem and Dongyin, I have enjoyed researching and teaching with you, and getting to know you better over the past year, I wish you the best in your careers. Dan and Mehmet as you begin your graduate careers, I wish you the best of luck – you've entered a great learning environment.

All of the high school and undergraduate student workers who have passed through our lab during my time as a graduate student you always brought levity to the lab, which was appreciated by everyone.

Thank you as well to Dr. Mullins, Dr. Miles, and Dr. Funkhouser for helping me develop as an educator. Likewise, thank you to Dr. Park for helping me develop as an educator and for helping me learn to be more patient – as well as for your calming influence.

I would also like to acknowledge Dr. Nagib Ahsan at the University of Missouri-Columbia for collaborative work that will help this project continue on for years to come.

Finally, I would like to thank Dr. Gary Kunkel; you've been a great role model and friend – I have great respect for you as a scientist and a man. I am deeply thankful for my friends who have supported and encouraged me – Denton and Lindsey, John-Robert and Diana, Doug and Nichole, and Matt.

NOMENCLATURE

Adi3	AvrPto-dependent Pto-interacting protein 3
Pdk1	3-Phosphoinositide dependent protein kinase 1
PFP	Pyrophosphate-dependent phosphofructokinase
PFK1	Phosphofructokinase
KiC	Kinase client
HR	Hypersensitive response
Pst	*Pseudomonas syringae* pv. *tomato*
Sl	*Solanum lycopersicum* (Tomato)
At	*Arabidopsis thaliana*

TABLE OF CONTENTS

Page

LIST OF FIGURES

Page

LIST OF TABLES

Page

CHAPTER I

INTRODUCTION AND LITERATURE REVIEW

1.1 History and significance

1.1a Phosphorylation of proteins: 1900-1940

Many of the contemporary rules for protein nomenclature were agreed upon during a joint meeting of the American Physiological Society and the American Biochemical Society in 1907. *Phosphoprotein* was established to describe a "…protein molecule with some, as yet undefined, phosphorous containing substance other than a nucleic acid…" (Chittenden et al., 1908). Although phosphoproteins were given a classification, the chemical and biological relevance of phosphoproteins was unknown. Early experiments showed proteins were *phosphorised* after incubation with phosphorus oxychloride and *dephosphorised* after incubation with hydrochloric acid. Identifying phosphate, not inorganic phosphorus, as the molecule being added and removed from the protein was the key discovery from these experiments (Rimington and Kay, 1926).

Investigation into protein phosphorylation was an early foray into the ever-expanding field of post-translational modifications. Many inquiries dissected the highly abundant milk protein casein as their model. Phosphopeptide analysis of the trypsin digestion products of casein indicated that phosphate groups were covalent modifications of amino acids with hydroxyl groups (Rimington, 1927). Notably, the physical properties of solutions of phosphorylated and non-phosphorylated albumin were markedly different from one another. In addition to having different KOH titration

curves, a solution with poly-phosphorylated albumin exhibited decreased viscosity (Heidelberger, 1941).

1.1b Enzymatic phosphorylation by protein kinases: 1940-1960

By the 1940s, phosphorylation of proteins by chemical treatment had become an established technique and deemed essential for phosphoprotein studies. While studying the immunological impact of protein phosphorylation, an investigator recovered less of the phosphoprotein than expected and concluded that "…[enzymatic] removal of [phosphate] from phosphorylated proteins… could not be excluded…" (Boursnell et al., 1948). Though it was merely speculation in the early 1940s, this idea was part of the basis for the entire study of reversible-protein phosphorylation.

Ongoing studies of phosphoproteins presented two questions: how was the phosphate group added to the protein of interest and from whence did it originate? In response to the first question, a 1950 publication proposed that the addition of a phosphate group to a protein was only possible when that protein was in the presence of a phosphorylated protein (Barth and Jaeger, 1950) (Figure 1B). This publication suggested that phosphates are transferred from one protein to another. However, this proposal failed to address how the first phosphoprotein was phosphorylated. In the years that followed, a model for protein phosphorylation was finally proposed. An experiment was designed to test this new model – two substrates were utilized: radiolabeled ATP and highly pure casein, the enzyme was an extract from mitochondria purified from rat liver. At the conclusion of the experiment, a radioactive phosphate group was transferred from ATP to casein.

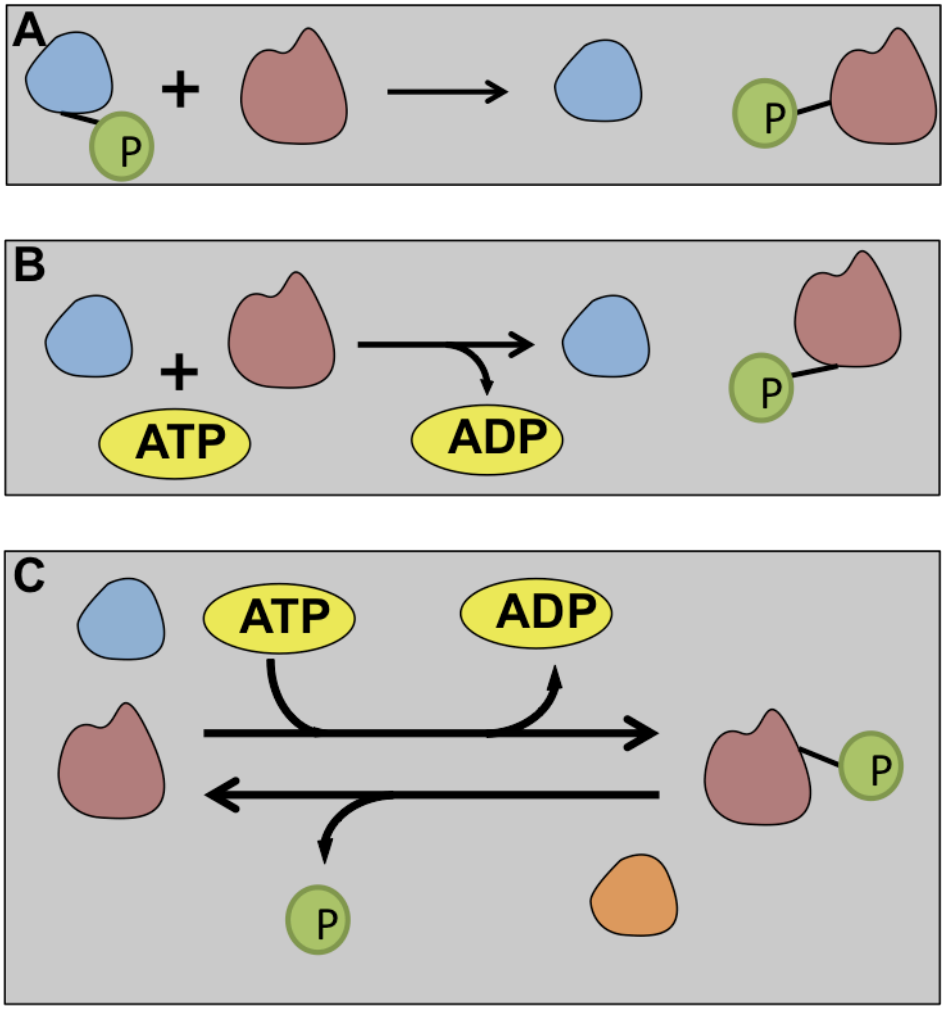

Figure 1. Early models of protein kinase function. *A*, An initial model for protein phosphorylation required a phosphoprotein to transfer its phosphate group to a non-phosphorylated protein. *B*, A later model of protein phosphorylation consisted of ATP as the phosphate donor, one protein transfers a phosphate group from ATP and another protein receives that phosphate group. *C*, Reversible protein phosphorylation consists of a protein kinase that transfers a phosphate group from ATP to a substrate protein, meanwhile a protein phosphatase is responsible for dephosphorylating a phosphorylated protein, liberating inorganic phosphate in the process.

The presence of a radiolabeled phosphate on the casein indicated that the phosphate group must have come from the ATP, and it meant that some agent in the mitochondrial extract was responsible for this transfer (Burnett and Kennedy, 1954) (Figure 1A). In their manuscript, the authors acknowledge that although casein is unlikely a physiologically relevant substrate to mitochondrial protein kinases, in an *in vitro* setting it can serve as a substrate. This is because they believed that the amino acid sequence was responsible for determining whether or not a protein can be phosphorylated. The prediction that casein is phosphorylated based on its amino acid sequence was the initial foray into the complicated field of phosphorylation site prediction.

1.1c Structure of protein kinases and processes they regulate: 1960-1990

The field of protein phosphorylation was still in its infancy when Edwin Krebs and Edmond Fischer started contributing; however by the end of their careers, Krebs and Fischer would be well known for their contributions to reversible protein phosphorylation. Krebs and Fischer joined the field in the early 1950s as junior faculty members at the University of Washington – the duo chose glycogen phosphorylase as their model to study. Phosphorylase exists in two different states – phosphorylated and non-phosphorylated. Krebs and Fischer's work is summarized in a simple, yet profound concept that is fundamental for all young biology students - protein kinases transfer a phosphate from ATP and protein phosphatases remove phosphates from proteins (Figure 1C).

Phosphorylation and dephosphorylation of proteins are of considerable importance because of their impact on fundamental biological processes. For example, the enzyme muscle phosphorylase fluctuates between active and inactive states, in part based on its phosphorylation status. Glycogen phosphorylase breaks glycogen into glucose 1- phosphate monomers; therefore, protein phosphorylation is related to carbohydrate metabolism (Newgard et al., 1989). In addition to carbohydrate metabolism, other metabolic processes are impacted by reversible protein phosphorylation. Hormone-sensitive lipase is activated by phosphorylation along with many other metabolism-related proteins (Krebs and Beavo, 1979). Considering that these fundamental processes are related to protein phosphorylation, the regulation of protein phosphorylation is distinctly correlated to cell health and viability.

Since the addition of phosphate groups to proteins can alter their activity, understanding the protein kinases responsible for this phosphorylation is just as important as understanding the proteins that receive the phosphate groups. Continual studies of phosphorylated casein inadvertently identified which of casein's amino acids were phosphorylated. The work of Claude Rimington in 1927 showed that the casein derived phosphopeptide his group analyzed consisted of a pair of serines, three hydroxyglutamic acids, and four hydroxyaminobutyric acid residues. Rimington concluded that the phosphate groups were on two hydroxyglutamic acid residues and a third phosphate molecule made a phosphodiester linkage existed between a hydroxyglutamic acid and a hydroxybutyric acid residue (Rimington, 1927). Continued phosphopeptide analysis only confirmed Rimington's conclusion that serine was phosphorylated (Burnett and

Kennedy, 1954). As the field grew, other phosphorylated amino acids were identified and now data supports the phosphorylation of threonine, tyrosine, histidine, arginine, lysine, as well as glutamic and aspartic acids (Paoletti and Moss, 1972; Eckhart et al., 1979; Huebner and Matthews, 1985; Besant et al., 2009; Attwood et al., 2011). Although many different variants of these amino acids have been identified, serine, threonine, and tyrosine are the most commonly phosphorylated residues (Figure 2).

As of 1988, more than 100 eukaryotic protein kinases had been identified, and as sequencing technology improved over the years the number of annotated protein kinases expanded. At the time of preparation of this manuscript in the *Arabidopsis thaliana* genome, there are 1,357 loci annotated with kinase activity (http://www.arabidopsis.org). By the textbook definition, a protein kinase is made up of a catalytic domain and a regulatory domain. The catalytic domain of a protein kinase consists of 11 subdomains with various functions in enzyme catalysis (Hanks et al., 1988). Of the domains, 1-5 are involved in ATP binding and the remaining subdomains are responsible for substrate peptide binding and transfer of the phosphate group (Hanks, 2003) (Figure 3).

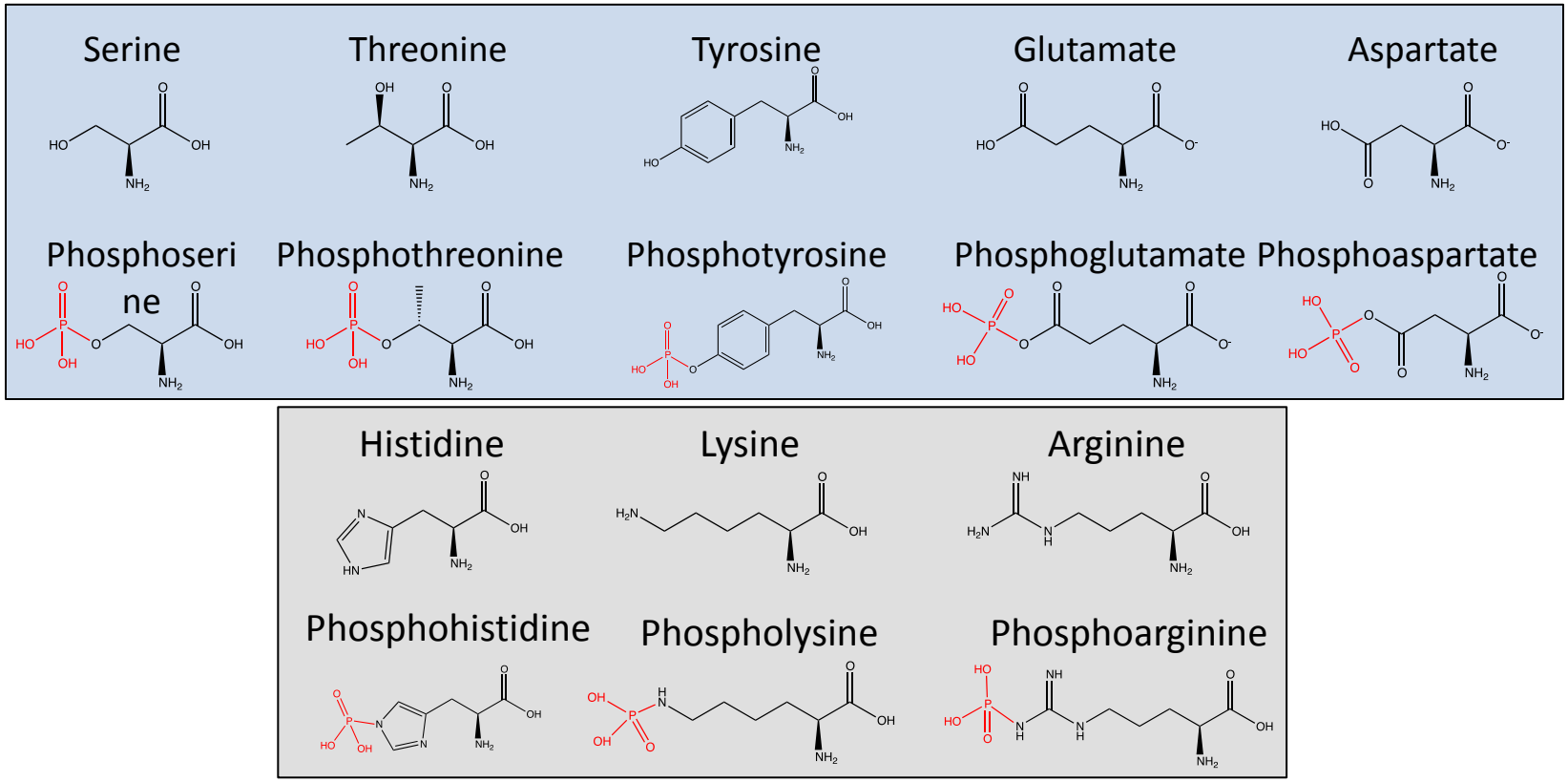

Figure 2. Phosphorylated amino acids. Although serine, threonine, and tyrosine are the most commonly phosphorylated amino acids, there are 5 other amino acids that can be phosphorylated. The hydroxyl groups of glutamate and aspartate can be phosphorylated, likewise phosphoramidate bonds are formed to produce phosphohistidine, phospholysine, and phosphoarginine.

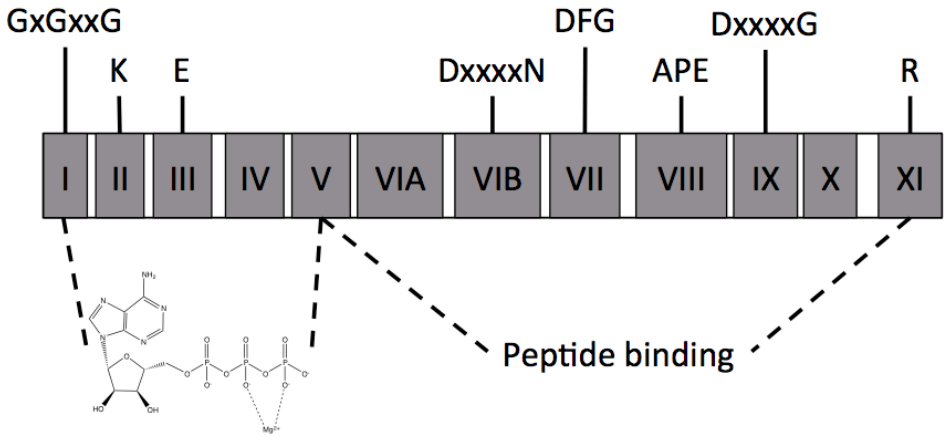

Figure 3. Conserved subdomains of protein kinases. The 12 conserved subdomains of protein kinases are defined above with the invariant residues within each subdomain. Subdomains 1-5 are involved ATP binding whereas subdomains 5-11 are involved in substrate peptide binding and phosphate transfer.

Perception and transmission of signals is the essential role of protein kinases; these diverse signals include biotic and abiotic stimuli (Hanks et al., 1988). One example of a response to an abiotic stimulus is the phenomenon known as phototropism, the movement or growth of a plant toward a light source (Briggs and Christie, 2002). The *Arabidopsis thaliana* protein kinases, PHOT1 and PHOT2 mediate photoresponses by perception of light through chromophore-binding LOV domains (light-oxygen-voltage) (Briggs and Christie, 2002). The chromophore receives light energy and induces a conformational change in the protein, which activates the protein's kinase activity (Okajima et al., 2012). The protein ATP-binding cassette B19 (ABCB19), a transporter of the growth hormone auxin, is one of the proteins phosphorylated by PHOT1 (Christie et al., 2011). Phosphorylation by PHOT1 inhibits ABCB19 transporter activity (Christie et al., 2011). Considering that knockout mutants of PHOT1/PHOT2 and ABCB19 do not exhibit the same phototropic phenotype, other substrates of PHOT1/PHOT2 are likely involved in the phototropism as controlled by PHOT1/PHOT2 (Briggs and Christie, 2002; Christie et al., 2011). With an understanding of the protein kinases that perceive signals as well as substrates of those kinases, the signaling cascade that a plant uses to mediate a response to abiotic and biotic signals can be clearly defined.

1.1d Contemporary problem – protein kinase substrates: 1990-Present

Kinase subdomains as described by Hanks et al. describe what constitutes a protein kinase, but identifying substrates of protein kinases is a different challenge. Protein kinases regulate a range of processes from metabolism to light signaling, and the proteins involved in these processes are drastically different and have different

sequences. In previously described experiments with rat liver mitochondria, Burnett and Kennedy attempted to phosphorylate casein and several other proteins, including lysozyme (Burnett and Kennedy, 1954). Casein, but not lysozyme, was phosphorylated indicating that the mitochondrial proteins discriminated between lysozyme and casein (Burnett and Kennedy, 1954). The discrimination between these proteins was based on their amino acid sequence – simply having a phosphorylatable residue does not mean that it will be phosphorylated.

Identifying protein kinases can be done more readily as whole genome sequencing technology has advanced. Although annotation of protein kinases has accelerated, identifying substrates of protein kinases still relies on assays based on protein-protein interaction. Protein kinase substrates have dissimilar phosphorylation motifs – specific to the upstream kinase. Protein kinase B (PKB), also known as Akt, receives a great deal of attention based on its implications in cancer and other diseases. Many substrates of PKB have been identified, and ultimately the optimal phosphorylation motif for PKB was identified as RXRXX(S/T) with X indicating any amino acid (Obata et al., 2000). However if a protein kinases' phosphorylation motif can be deduced, sequence data can be utilized to identify additional potential substrates.

1.2 PDK1

1.2a Structural features of PDK1

One of the most well-studied protein kinases is the previously mentioned PKB – at the time of this manuscript preparation, Pubmed searches for PKB and Akt return total of 41,963 citations (http://www.pubmed.gov). This overwhelming amount of research is

in part because impaired PKB signaling in mice has been implicated in compromised glucose homeostasis whereas uncontrolled activation of PKB signaling leads to cancer (Hill and Hemmings, 2002; Calleja et al., 2007). A thorough understanding of PKB's role in the cell as well as its regulation is essential for understanding numerous diseases. One avenue to begin that investigation is to determine how PKB is activated. Activation of PKB has been observed in mammalian cells treated with the hormone insulin as well growth factors and that activation is correlated with trans-phosphorylation of PKB at Thr308 and Ser473 (Alessi et al., 1997). In order to understand the activation of PKB it is important to understand how insulin actually is involved in the activation of PKB. Insulin is first perceived by the insulin receptor which upon binding insulin phosphorylates several of its own tyrosine residues (Czech et al., 1988). The auto-activation of the insulin receptor enables the protein's insulin receptor substrate-1 & -2 to bind the insulin receptor (Alessi et al., 1997). IRS-1 and IRS-2 are phosphorylated by the insulin receptor and are then able to interact with a number of different proteins (Metz and Houghton, 2011). IRS-1 interacts with the p85 subunit of phosphatidylinsositol 3-kinase (PI3K), a protein which phosphorylates PtdIns(4,5)P_2 (phosphatidylinositol (4,5) diphosphate) to produce the secondary messenger PtdIns(3,4,5)P_3 (PIP_3) (Alessi et al., 1997). The production of the secondary messenger PIP_3 is significant because it activates the protein PDK1 (3-phosphoinositol dependent protein kinase 1) (Metz and Houghton, 2011). Upon binding of PIP_3, PDK1 activates PKB by phosphorylation at Thr308 (Carnero, 2010). In *in vitro* experiments, recombinant PDK1 incubated with PKB and PI(3,4,5)P_3 resulted in significantly higher

activation of PKB than when other phospholipids were utilized like $PI(3,5)P_2$ or $PI(3,4)P_2$ (Alessi et al., 1997). The significance is that PDK1 and PKB both bind PIP_3 and are recruited to the plasma membrane where their interaction takes place (Currie et al., 1999; Carnero, 2010). PDK1 is known as the master regulator of AGC kinases and is conserved throughout many eukaryotes (Mora et al., 2004). The AGC kinase family is named after cAMP-dependent protein kinases, cGMP-dependent protein kinases, and phospholipid-dependent protein kinase C (Bogre et al., 2003).

Binding of phospholipids by the PH domain determines subcellular localization of PDK1 (Currie et al., 1999). GFP fusions of wild type and a mutant PDK1, lacking the PH domain present different localization patterns (Currie et al., 1999). In human cells, the PDK1 mutant is seen throughout the cell whereas the wild type protein specifically localizes to the plasma membrane (PM) where many phospholipids are located (Currie et al., 1999). Change in localization dependent on the lipid binding by the PH domain is a characteristic not unique to PDK1; PKB also has a PH domain and GFP fusions of PKB with and without the PH domain exhibit different localization patterns (Currie et al., 1999). Both the PH-domain mutant and wild type PKB proteins are found at the PM, however the concentration of the mutant at the PM is much lower (Currie et al., 1999). As an agonist, insulin activates the insulin receptor, which phosphorylates IRS-1, enabling the activation of PI3K to produce $PI(3,4,5)P_3$ from $PI(3,4)P_2$ (Alessi et al., 1997). Production of $PI(3,4,5)P_3$ facilitates the activation of PDK1 and its co-localization with PKB (Currie et al., 1999). Understanding the control and regulation of this pathway continues to be an avenue for research as well as a drug target for diseases.

PDK1 has been investigated in many different eukaryotes. In mice $PDK1^{+/-}$ were setup in mating groups and no $PDK1^{-/-}$ were identified, indicating that the homozygous mutant for PDK1 was embryonic lethal (Lawlor et al., 2002). In the budding yeast, *Saccharomyces cerevisiae* the closest homologues of mammalian PDK1, were identified as PKB-activating kinase homologues 1 & 2 (Pkh1 and Pkh2) (Casamayor et al., 1999). The Pkh1 & Pkh2 kinase domains are 72% identical to one another and are 50% identical to mammalian PDK1 – a noteworthy difference, however, is the absence of the PH domain (Casamayor et al., 1999). Analysis of Pkh1 and Pkh2 reveal proteins that are functionally redundant, capable of phosphorylating mammalian PKB, and are essential for viability (Casamayor et al., 1999). In addition to homologues of PDK1 being lethal in yeast and mice, the homologue in *Caenorhabditis elegans* appears to be developmentally essential. The loss-of-function mutant of *C elegans* PDK1 results in arrested development in the dauer stage, a developmental phase in which the worms do not feed or reproduce (Paradis et al., 1999). Given the sequence similarity and necessity for viability, it appears possible that PDK1 serves similarly important roles in eukaryotes.

1.2b PDK1 interaction with substrates

As previously mentioned, PDK1 is the master regulator of AGC kinases, a family of protein kinases of which PDK1 is itself a member (Pearce et al., 2010). AGC kinases have a diverse set of responsibilities, as previously mentioned. PKB has been implicated in cancer; from a molecular standpoint, one of the activities of PKB is prevention of caspase activation (Yamaguchi and Wang, 2001). In addition to preventing caspase activity, PKB regulates apoptosis by preventing the pro-apoptotic protein Bax from

undergoing a conformational change and subsequent transport into the mitochondria (Yamaguchi and Wang, 2001). Although PKB is one of the thoroughly investigated AGC kinases, many others have been investigated for their roles in diseases. AGC kinases have a number of common features, for example activation consists of phosphorylation within the activation loop of the protein and phosphorylation in the hydrophobic motif of the protein (Pearce et al., 2010). In addition to PKB, serum- and glucocorticoid-induced kinase (SGK) is an AGC kinase implicated in Huntington's disease (Pearce et al., 2010). SGK inhibits neuronal toxicity associated with Huntington's disease by phosphorylation of the Huntington's disease protein polyQ-huntingtin (Rangone et al., 2004). An understanding how AGC kinases are regulated as well as how they regulate substrates as well as the identity of those substrates can contribute to a greater understanding of numerous diseases.

The structure of an AGC kinase domain consists of a pair of lobes (N- terminal "N" lobe and C-terminal "C" lobe) folded such that ATP is positioned by the consensus Mg^{2+} coordinating DFG motif between the lobes (Pearce et al., 2010). Phosphorylation of the activation loop of AGC kinases leads to conformational changes in the protein. In particular, phosphorylation of the activation loop of AGC kinases facilitates hydrogen bonding between an α-helix on the C-lobe and the N-lobe of the protein which results in the kinase adopting its active state (Pearce et al., 2010).

As stated above, co-localization is important for PDK1 to interact with PKB. However, PKB has a PH domain enabling it to bind phospholipids and come in close proximity to PDK1 but not all AGC kinases have PH domains. Many of the interactions

between AGC kinases and PDK1 are dependent on the hydrophobic motif at the C-terminus of the protein, known as the PIF (PDK1-interacting fragment) (Calleja et al., 2007). The PIF is a 4-7 AA motif with a consensus sequence of FxxF(S/T)(F/Y) or F(D/E)xF (Biondi et al., 2000; Biondi et al., 2001; Bogre et al., 2003). In the 7 AA long motif, the S/T is phosphorylated or a phosphomimetic residue is present in its place which is their role in the 4 AA long motif (Pearce et al., 2010). Both PDK1 substrates S6K1 and PKB have PIF motifs. However the interaction between PDK1 and S6K1 is PIF dependent while the PDK1-PKB interaction is PIF-independent (Biondi et al., 2001; Calleja et al., 2007). In PIF-dependent interactions, the PIF of the substrate enters a hydrophobic pocket of PDK1 known as the PIF binding pocket (Biondi et al., 2002). The PIF binding pocket is in the C-lobe of PDK1 and is a 5 Å pocket formed by an alpha-helix and a beta-sheet (Biondi et al., 2002). Within the PIF binding pocket of PDK1, the roles of several residues in PIF binding have been ascribed. With the human PDK1 PIF binding pocket as the model for PIF binding, the first two Phe of the PIF (**F**xx**F**(S/T)(F/Y)) bind to four pocket residues (Lys115, Ile119, Gln150, and Leu155), the phosphorylated Ser/Thr or acidic PIF residue (FxxF(**S**/**T**)(F/Y)) binds four pocket residues (Arg75, Lys76, Lys77, and Arg131), and finally the last Phe/Tyr(FxxF(S/T)(**F**/**Y**)) binds three pocket residues (F81, F146, and F148) (Frodin et al., 2002) (Figure 4A). Mutations within the PDK1 PIF binding pocket as well as mutations within the substrate's PIF can impede PDK1 from interacting with its substrates (Balendran et al., 1999; Biondi et al., 2001).

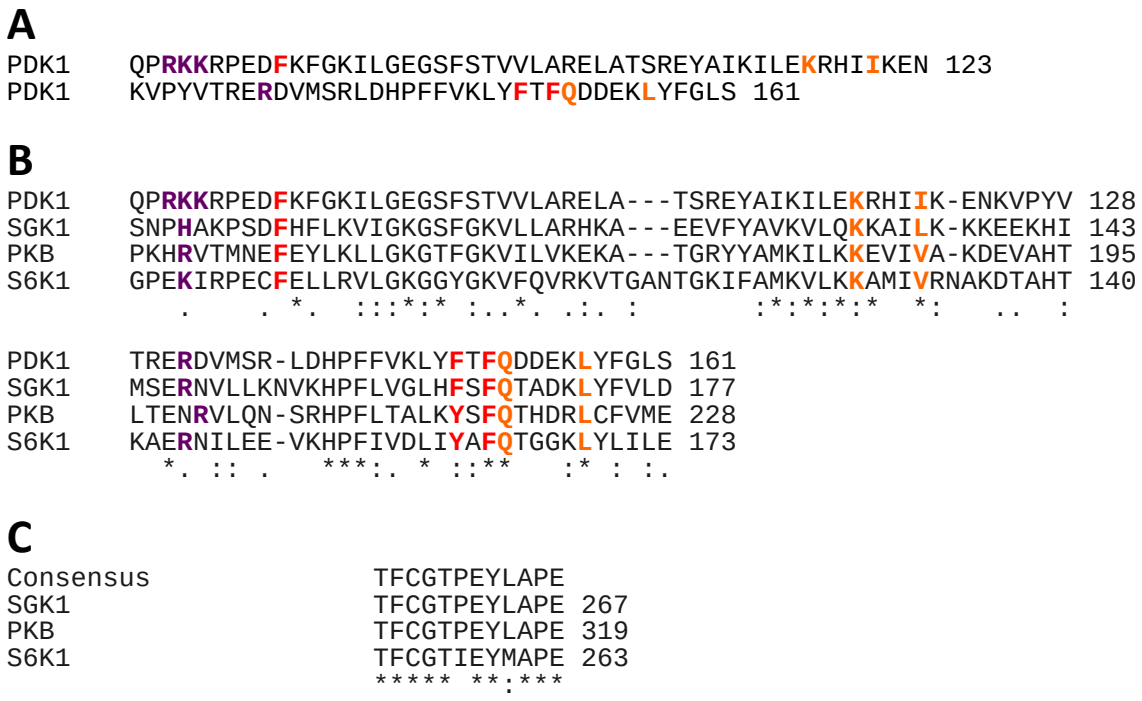

Figure 4. Sequence of human PDK1 PIF binding pocket. *A*, The PIF binding pocket of PDK1 is presented, residues involved in PIF binding are specified. Residues in purple are involved in binding the phosphorylated S/T (FxxF(**S**/**T**)(F/Y)) in the PIF, residues in red are involved in binding the Phe/Tyr (FxxF(S/T)(**F**/**Y**)) of the PIF, residues in orange are involved in binding the first two Phe (**F**xx**F**(S/T)(F/Y)) of the PIF. *B*, Sequences of the PDK1-PIF binding pocket are aligned with similar regions within SGK1, PKB, and S6K1. *C*, The consensus PDK1 phosphorylation motif is aligned with the corresponding sites in SGK1, PKB, and S6K1 – the first Thr in the motif is phosphorylated by PDK1.

Sequence alignment of PDK1 with other AGC kinases reveals conservation of residues within the kinase domain that constitute the PIF binding pocket (Frodin et al., 2002) (Figure 4B). In the model for AGC kinase activation, after the PIF of a substrate enters the PIF binding pocket of PDK1 (Figure 5A), the substrate is phosphorylated at a conserved Ser/Thr within the activation loop of the protein (Belham et al., 1999) (Figure 4C & Figure 5B). Upon trans-phosphorylation by PDK1 the substrate kinase will undergo a conformational change resulting in the PIF of the substrate entering the PIF binding pocket of the substrate (Frodin et al., 2002) (Figure 5C). After the conformational change has occurred and the AGC kinase's PIF has entered it's own PIF binding pocket, the kinase autophosphorylates and move on to phosphorylate substrates (Biondi and Nebreda, 2003) (Figure 5D). Therefore, the PIF can serve two purposes – first by mediating an interaction with PDK1 and by enabling autophosphorylation.

1.2c Arabidopsis *Pdk1*

PDK1 is conserved through many eukaryotes, however its essential role for viability varies. In *Arabidopsis thaliana* there are two copies of PDK1, *Pdk1-1* (At5g04510) and *Pdk1-2* (At3g10540), a pair of proteins that are 92% identical (Camehl et al., 2011). Contrary to knockouts of the mammalian counterparts, *Arabidopsis* has two copies of Pdk1 and a double knockout of *Pdk1-1* and *Pdk1-2* is still viable – a notable phenotypic difference between the double knockout and wild type is the reduced silique size observed in the mutant plants (Camehl et al., 2011). An earlier investigation into *Arabidopsis Pdk1* revealed that it was able to complement the *Pkh1*/*Pkh2* double mutant (Deak et al., 1999). This analysis of *Arabidopsis Pdk1* focused on *Pdk1-1*,

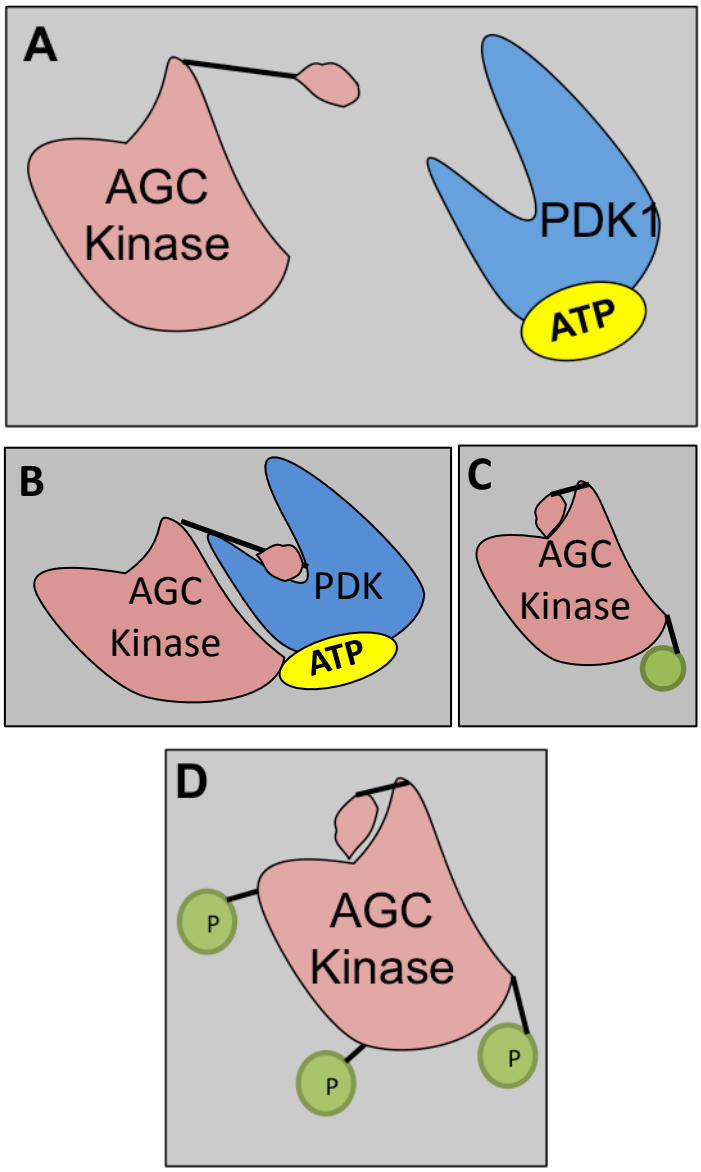

Figure 5. Model of AGC kinase activation by PDK1. *A*, the substrate AGC kinase and PDK1 prior to interaction, the PIF pocket of PDK1 is accessible to the substrate kinase. *B*, the PIF of the substrate kinase enters the PIF-binding pocket of PDK1 at which time PDK1 can phosphorylate and activate the substrate. *C*, the PIF of the phosphorylated substrate kinase folds back on itself, entering its own PIF binding pocket. *D*, with the trans-phosphorylation by PDK1, the PIF in its own PIF-binding pocket, the AGC kinase can auto-phosphorylate and activate itself and is capable of phosphorylating substrates of its own.

in addition to its ability to complement the *pkh1*Δ *pkh2*Δ mutant, *Arabidopsis* Pdk1-1 was also able to phosphorylate mammalian PDK1 substrate PKB (Deak et al., 1999). Similar to its mammalian counterpart, *Arabidopsis* Pdk1 has a phospholipid binding PH domain.

This domain binds phospholipids, and binding of phosphatidic acid and PtdIns(4,5)P_2 activates *Arabidopsis* Pdk1 (Deak et al., 1999; Anthony et al., 2004). The presence of the PH domain and absence of one in Pkh1 and Pkh2 is interesting considering that *Arabidopsis Pdk1* was able to complement *pkh1*Δ *pkh2*Δ with and without it (Deak et al., 1999). Considering that homologues of *Pdk1* are essential for several organisms, it is likely that in *Arabidopsis* the substrates that it activates are different or at least have different functions.

1.2d Plant AGC kinases

Plant AGC protein kinases are involved in a diverse array of activities – blue-light responses, auxin transport, and root hair growth (Bogre et al., 2003). In *Arabidopsis* there are a total of 39 AGC kinases, including both isoforms of *Pdk1* (Bogre et al., 2003). The two isoforms of *Pdk1* are a group separate from the others, while the remaining 37 are divided into 5 different groups (Bogre et al., 2003). The 37 non-*Pdk1* AGC kinases are separated based on sequence comparison to other eukaryotic protein kinases, these groups are designated as subfamilies AGC VI, Other, VII, VIIIb, and VIIIa (Bogre et al., 2003) (Figure 6A). The VIIIa and VIIIb subfamilies are subdivisions of the VIII family, made up of genes with highest similarity to protein kinase A (Bogre et al., 2003). The AGC VIII family is unique in several respects – the DFG

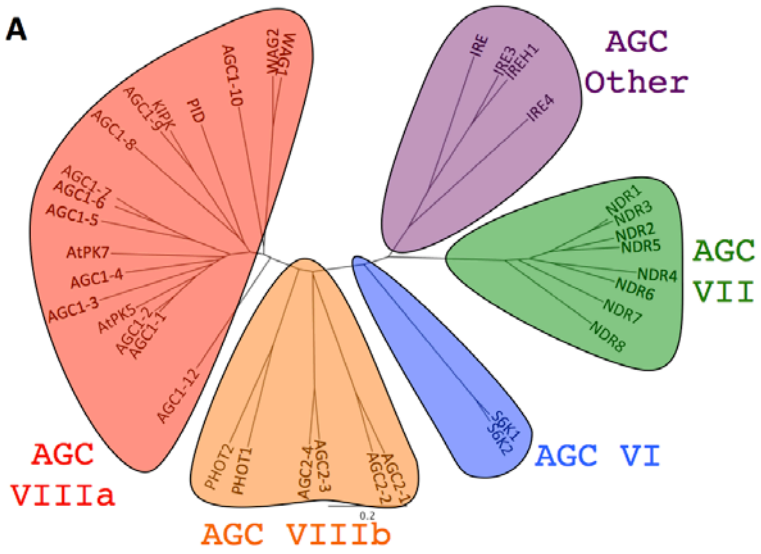

B

Consensus	TFCGTPEYLAPE
AGC1-3	TRSMSFVGTHEYLAPE
AtPK5	ARSMSFVGTHEYLAPE
PHOT1	RASNSFVGTEEYIAPE
AGC2-3	ERSNSFVGTDEYISPE
S6K1	TRSNSMCGTTEYMAPE
S6K2	TRSNSMCGTTEYMAPE
NDR1	MLAYSTVGTPDYIAPE
NDR7	TLAFSTVGTPDYIAPE
IREH1	RKKRSAVGTPDYLAPE
IRE3	DHKRSAVGTPDYLAPE

Figure 6. Phylogeny of AGC kinases in *Arabidopsis* and conservation of activation loop phosphorylation sites. *A*, dendrogram of *Arabidopsis thaliana* AGC kinases shows that of the 37 members of this family, not including *At*PDK1-1 and *At*PDK1-2, the largest subfamily is the VIIIa family consisting of 17 members. *B*, the consensus PDK1 phosphorylation motif derived from analysis of AGC kinases in humans is highly conserved among AGC kinases in *Arabidopsis* – font color corresponds to the subfamily designated in 4A.

motif found between the N and C lobes of the kinase domain is altered to DFD (Bogre et al., 2003). In addition to the Mg^{2+} coordination motif's alteration, a unique characteristic of the AGC VIII kinases is an insertion of 48-109 AA within their activation loop (Zegzouti et al., 2006). Plant AGC kinases are involved in but not limited to development and reproduction, for example WAG1 and WAG2 have been implicated in root development by mediating auxin transport (Santner and Watson, 2006). Likewise, AGC1-5 and AGC1-7 have been characterized and are associated with pollen tube development (Zhang et al., 2009). In addition to AGC kinases from *Arabidopsis*, AGC kinases from other organisms have been studied – Adi3 from tomato is a negative regulator of cell death and Oxi1 from rice is a positive regulator of basal disease resistance (Devarenne et al., 2006; Matsui et al., 2010).

In comparison, *Arabidopsis* and mammalian AGC kinases retain similar characteristics. The PIF motif in mammalian AGC kinases, FXXF(D/E)(F/Y) is also present in *Arabidopsis* as F(D/E)XF (Bogre et al., 2003). Similarly, the activation loop phosphorylation motif derived from human AGC kinases is conserved in *Arabidopsis* AGC kinases (Bogre et al., 2003) (Figure 6B).

In addition to the conservation of the activation loop phosphorylation site and the presence of the PIF, several of the residues that comprise the PIF binding pocket are conserved as well (Figure 7). Comparison of AtPDK1-1 and mammalian PDK shows that the PIF binding pocket residues are highly conserved and although they are not as well conserved among AGC VIIIa kinases, some residues are conserved and could be involved in forming the PIF binding pocket (Devarenne et al., 2006).

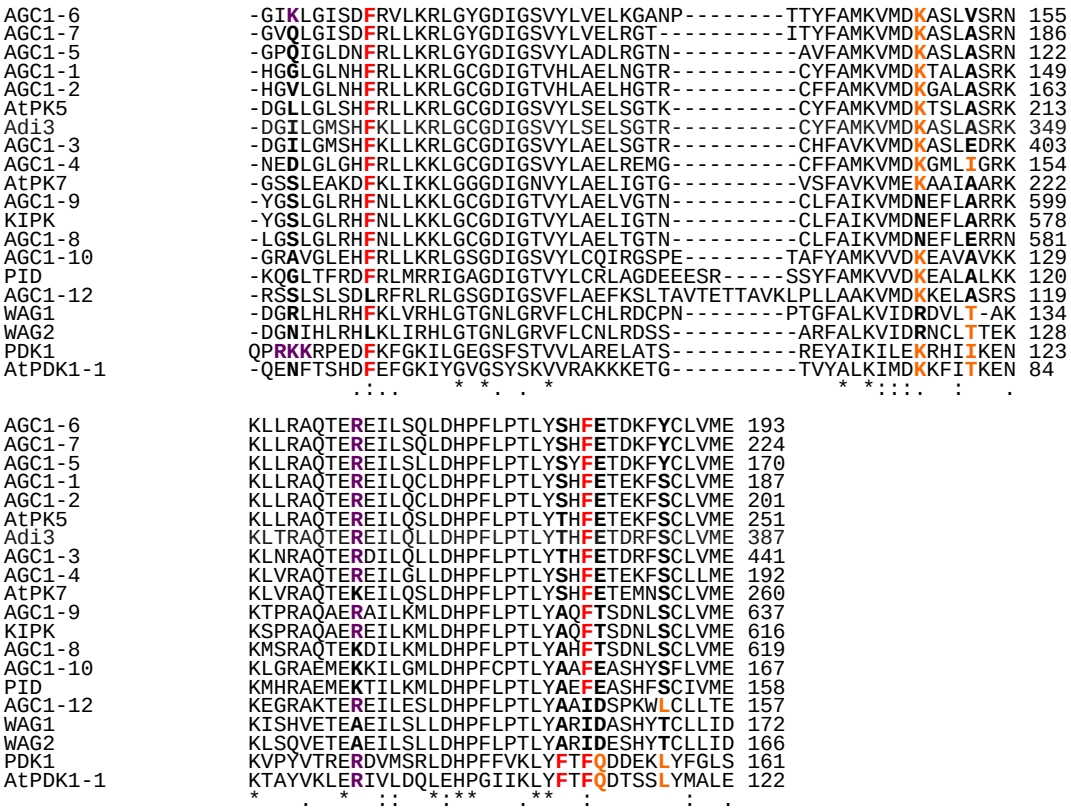

Figure 7. Alignment of PIF binding pockets. Above is the sequences of human and *Arabidopsis* PDK1 PIF-binding pockets aligned with *Arabidopsis* AGC VIIIa subfamily members and the tomato AGC kinase Adi3. Residues in purple are involved in binding the phosphate in the PIF, residues in red are involved in binding the Phe/Tyr of the PIF, residues in orange are involved in binding the first two Phe of the PIF, and residues in black are mutant residues from the PDK1 reference residues.

1.3 Tomato AGC VIIIa kinase, Adi3

1.3a Adi3, tomato cell death regulator

In tomatoes resistant to the bacterial pathogen *Pseudomonas syringae* pv. *tomato*, the host resistance protein, Pto, interacts with the avirulence protein AvrPto (Martin et al., 1993).The interaction between AvrPto and Pto initiates a signaling cascade resulting in a form of cell death known as the hypersensitive response (Morel and Dangl, 1997). The HR can be simply referred to as cell death development resulting from disease resistance and with pathogen recognition (Morel and Dangl, 1997). In a resistant plant upon perception of an avirulence protein, expression of multiple defense related genes are induced including proteins involved in biosynthesis of anti-microbial compounds (Morel and Dangl, 1997). To understand the signaling cascade initiated in response to a resistance protein interacting with an avirulence protein thoroughly, a yeast 3-hybrid screen was conducted to identify proteins involved in AvrPto-Pto signaling (Bogdanove and Martin, 2000). A total of 5 genes were identified as possibly interacting with AvrPto-Pto (Bogdanove and Martin, 2000). Based on interaction with AvrPto and Pto, these proteins were named Adi proteins – AvrPto dependent Pto interacting protein (Bogdanove and Martin, 2000). Virus induced gene silencing (VIGS) of one of the candidate genes, *Adi3,* resulted in development of cell death lesions throughout tomato leaves (Devarenne et al., 2006). Further characterization of this protein identified it as a Ser/Thr protein kinase and in particular, a member of the AGC VIIIa family of protein kinases (Devarenne et al., 2006). The investigation of Adi3 as a cell death regulator directed studies in multiple directions. First, an investigation was undertaken to identify

what components of Adi3 alter cell viability, followed by an investigation into what signaling partners Adi3 utilizes by using a yeast 2-hybrid screen of a cDNA library (Ek-Ramos et al., 2010; Avila et al., 2012).1.3b Adi3 localization and cell viability

Adi3, like other AGC VIIIa family members has a large insertion within its activation loop – 74 AA in the case of Adi3 (Devarenne et al., 2006). An Adi3 mutant with the activation loop extension deleted did not alter *auto*- or *trans*-catalytic activity of Adi3, the interaction with PDK1, or its ability to phosphorylate Adi3 (Ek-Ramos et al., 2010). However, transient expression of the Adi3 activation-loop extension mutant resulted in decreased cell viability indicating that the activation-loop extension was fundamentally important for cell viability (Ek-Ramos et al., 2010). After looking at the activation-loop extension sequence it was determined that a nuclear localization signal (^{504}PQKSKKK^{510}) was in that region of the protein (Ek-Ramos et al., 2010). Microscopy and cell viability studies revealed that two factors were important and inseparable for Adi3 – nuclear localization and phosphorylation at the activation loop serine (Ek-Ramos et al., 2010). Mutants of Adi3 that cannot be phosphorylated at the activation loop serine and lacked the activation loop extension reduced cell viability to ~20% of wild type (Ek-Ramos et al., 2010). Microscopy studies revealed that this same mutant did not localize to the nucleus like its wild type counterpart (Ek-Ramos et al., 2010). A strong correlation exists between nuclear localization, activation loop phosphorylation, and cell viability as well as nuclear localization.

1.3c Adi3 signal transduction

The investigation into signaling partners of Adi3 identified SnRK as an interacting partner (Avila et al., 2012). SnRK is a α-subunit of the SnRK1 complex, which is homologous to sucrose nonfermenting 1 (Snf1) in yeast and AMP-activated protein kinase (AMPK) in mammals. In yeast, *Snf1* was first studied in the context of mutants which were unable to metabolize sucrose, galactose, or maltose (Celenza and Carlson, 1986). In mammals, the AMPK complex can regulate metabolism by induction of fatty acid oxidation in order to produce more ATP in demanding scenarios (Luo et al., 2010). This complex is conserved as a heterotrimer made up of a catalytic β-subunit and two regulatory subunits – α and ϒ (Luo et al., 2010). Although Adi3 was found to interact with the regulatory α-subunit, SnRK, it was determined that Adi3 was able to phosphorylate the catalytic β-subunit GAL83, both *in vivo* and in *in vitro* kinase assays (Avila et al., 2012). Phosphorylation of the β-subunit by Adi3 reduces SnRK1 complex kinase activity (Avila et al., 2012). Ultimately Adi3 is a cell death suppressor requiring nuclear localization and activation loop phosphorylation, how Adi3's phosphorylation of the SnRK1 complex relates to cell death remains to be fully understood.

1.4 Protein kinase substrate identification techniques

Identifying interacting partners of protein kinases is critical to understand how a stimulus is transmitted. For example, understanding the regulation of the signaling cascade that flows through PHOT1 and PHOT2 will provide a thorough understanding of the processes activated and/or inhibited that result in a phototropic response (Briggs

and Christie, 2002). In some cases interacting partners are identified through genetic analysis using mutant plants (Christie et al., 2011).

An inherent challenge in identifying substrates of a protein kinase is that the interaction between a kinase and its substrate is expected to be transient in many cases (Ptacek et al., 2005). A successful and commonly employed method of identifying substrates and interacting partners is the yeast 2-hybrid assay – as previously mentioned, a yeast 2-hybrid screen was employed using Adi3 to identify SnRK as an interacting partner (Avila et al., 2012). The yeast 2-hybrid assay is not the only technique to employ a library-based approach; phage display is another technique that has successfully identified interacting partners of protein kinases (Watson et al., 1999). Phage display and the yeast 2-hybrid system both potentially identify interacting partners that are not necessarily substrates so if a substrate is the project goal, these techniques might not provide the desired data.

To identify substrates rather than interacting partners, the kinase of interest is mutated to use "bulky" ATP analogs, which also have a radiolabel or sulfur on the ϒ-phosphate, which is then chemically modified and detected specifically by an anti-body (Koch and Hauf, 2010; Dittrich and Devarenne, 2012). A developing technique is to use proteins printed on a plate much like a microarray, incubate the plate with a kinase and radiolabeled ATP and based on the position of the radiolabel on the plate, a potential substrate peptide can be determined (MacBeath and Schreiber, 2000).

In addition to experimental techniques, bioinformatics substrate prediction tools have been developed in part a result of the increasing volume of interaction and

phosphorylation data available (Lai et al., 2012). The fundamental issue is that predicted substrates still must be confirmed experimentally. However it does provide a starting point for investigation of a signaling network.

Although all of these approaches have drawbacks they can provide some insight into what processes a protein kinase can activate or inhibit and what processes are altered by a given stimulus.

1.5 Dissertation overview

The work detailed in this dissertation was conducted to begin the characterization of the *Arabidopsis thaliana* homologue of the tomato cell death suppressing protein, Adi3. I begin this work by investigating the non-activation loop phosphorylation site of AGC1-3 and Adi3. In work conducted with fellow lab members, we determined that the second phosphorylation site of AGC1-3 was conserved within Adi3. Additionally, this second phosphorylation site proved valuable to activation of the Adi3 substrate GAL83. I followed that work up by investigating if other AGC VIIIa protein kinases have additional, non-activation loop phosphorylation sites. The last portion of my dissertation investigates substrates of AGC1-3 in an effort to expand this project in *Arabidopsis* as well as with Adi3, by identifying potential substrates using the Kinase Client assay.

CHAPTER II

METHODS*

2.1 Cloning and site directed mutagenesis

Cloning of the Adi3, *Sl*Pdk1, and Gal83 cDNAs into pMAL-c2 and expression/purification of protein from *Escherichia coli* for N-terminal maltose binding protein (MBP) translational fusions were previously described (Devarenne et al., 2006; Avila et al., 2012). Site-directed mutagenesis was carried out using standard protocols and Pfu Turbo DNA polymerase (Stratagene). All primers used in this study for cloning and mutagenesis are listed in Table 1. The *Arabidopsis thaliana* sequence homolog to Adi3, AGC1-3 (At2g44830; accession # AY078927), was identified by BLAST of the *Arabidopsis* genome (www.arabidopsis.org) using the full-length open reading frame (ORF) sequence of Adi3. The 2298 bp full-length ORF of AGC1-3 was cloned by RT-PCR. Total mRNA was extracted from *Arabidopsis* (Col-0) leaf tissue and first strand synthesis was completed with the SuperScriptII cDNA synthesis kit (Invitrogen). The AGC1-3 ORF was amplified from first strand cDNA with primers based at the ATG start codon and the TAA stop codon using GoTaq Green (Promega). The product was cloned into pCR2.1-TOPO (Invitrogen) to confirm identity by sequencing. All AGC1-3 variants (full-length and N-terminal deletions) were cloned into a modified form of

---

* Portions of the following article have been reprinted with permission from: **Gray J, Nelson Dittrich AC, Chen S, Avila J, Giavalisco P, Devarenne TP** (2013) Two Pdk1 phosphorylation sites on the plant cell death suppressor Adi3 contribute to substrate phosphorylation. Biochim Biophys Acta **1834:** 1099-1106. Copyright 2013 © by Elsevier.

Table 1. Primers used in this study.

Gene	Primer Name	Purpose	Direction	Restriction site	Sequence
AGC1-3	AtAdi3 1.2F	Amplifying ORF from first strand synthesis	Forward		ATGCTGGAAATGGAAAGAG
AGC1-3	AtAdi3-2298R	Amplifying ORF from first strand synthesis	Reverse		TTAGAAAAACTCAAAGTCTAGAAATTTA CCACCAGATTTCGTGTCTGCTGCTG CTGC
AGC1-3	AGC1-3/1-EcoRIF	Amplifying ORF for pEG202/pJG4-5	Forward	EcoRI	CACGAATTCATGCTGGAAATGGAAA GAG
AGC1-3	AGC1-3/2298-XhoIR	Amplifying ORF for pEG202/pJG4-5	Reverse	XhoI	CACCTCGAGTTAGAAAAACTCAAAG TC
AtPDK1-1	AtPDK1-1/1-EcoRIF	Amplifying ORF for pEG202/pJG4-5/pGEX/pETMAL	Forward	EcoRI	CACGAATTCATGTTGGCAATGGAG
AtPDK1-1	AtPDK1-1/1476-XhoIR	Amplifying ORF for pEG202/pJG4-5/pGEX/pETMAL	Reverse	XhoI	CACCTCGAGTCAGCGGTTCTGAAGA GT
MBP	MBP/NdeI	Amplifying ORF for pETMAL construction	Forward	NdeI	CACCATATGAAAACTGAAGAAGGT
MBP	MBP/SpeI	Amplifying ORF for pETMAL construction	Reverse	SpeI	CACACTAGTTGAAATCCTTCCCTC
AtPDK1-1	K73QF	Mutagenesis	Forward		ACTGTGTATGCTTTACAGATTATGG ACAAAAAG
AtPDK1-1	K73QR	Mutagenesis	Reverse		CTTTTTGTCCATAATCTGTAAAGCAT ACACAGT
AGC1-3	BamHI/HA/AGC1-3F	Amplifying ORF for pGEX	Forward	BamHI	CACGGATCCATGTATCCCTACGACG TCCCCGATTATGCACTGGAAATGGA A
AGC1-3	AGC1-3/2298-SalIR	Amplifying ORF for pGEX	Reverse	SalI	CACGTCGACTTAGAAAAACTCAAAG TC

Table 1. Continued.

AGC1-3	AGC1-3 K392QF	Mutagenesis	Forward		CGATGCCATTTTGCTGTGCAAGTCATGGATAAAGCGTCT
AGC1-3	AGC1-3 K392QR	Mutagenesis	Reverse		AGACGCTTTATCCATGACTTGCACAGCAAAATGGCATCG
AGC1-3	AGC1-3 S596AF	Mutagenesis	Forward		CCTAACACACGGTCCATGGCCTTTGTTGGAACCCACGAG
AGC1-3	AGC1-3 S596AR	Mutagenesis	Reverse		CTCGTGGGTTCCAACAAAGGCCATGGACCGTGTGTTAGG
AGC1-3	AGC1-3 S596DF	Mutagenesis	Forward		CCTAACACACGGTCCATGGACTTTGTTGGAACCCACGAG
AGC1-3	AGC1-3 S596DR	Mutagenesis	Reverse		CTCGTGGGTTCCAACAAAGTCCATGGACCGTGTGTTAGG
AGC1-3	AGC1-3 K562AF	Mutagenesis	Forward		AGCATCTTCCCTAACGCAAACAAAAAAAACAAG
AGC1-3	AGC1-3 K562AR	Mutagenesis	Reverse		CTTGTTTTTTTTGTTTGCGTTAGGGAAGATGCT
AGC1-3	AGC1-3 K565AF	Mutagenesis	Forward		CCTAACGCAAACAAAGCAAACAAGTCCCGTAAA
AGC1-3	AGC1-3 K565AR	Mutagenesis	Reverse		TTTACGGGACTTGTTTGCTTTGTTTGCGTTAGG
AGC1-3	d100 AGC1-3 EcoRI	Amplifying N-terminal 100AA deletion of AGC1-3 for pETMAL	Forward	EcoRI	CACGAATTCATGAGAACGATGAAGGCC
AGC1-3	d200 AGC1-3 EcoRI	Amplifying N-terminal 200AA deletion of AGC1-3 for pETMAL	Forward	EcoRI	CACGAATTCATGCTTTCACCTGCAGAAAGC
AGC1-3	d300 AGC1-3 EcoRI	Amplifying N-terminal 300AA deletion of AGC1-3 for pETMAL	Forward	EcoRI	CACGAATTCATGGTTTTGGATTCGTTT
AGC1-3	d400 AGC1-3 EcoRI	Amplifying N-terminal 400AA deletion of AGC1-3 for pETMAL	Forward	EcoRI	CACGAATTCATGGACCGGAAGAAGTTG
AGC1-3	d225 AGC1-3 EcoRI	Amplifying N-terminal 225AA deletion of AGC1-3 for pETMAL	Forward	EcoRI	CACGAATTCATGAACACTGAAAACTCT

Table 1. Continued.

AGC1-3	d250 AGC1-3 EcoRI	Amplifying N-terminal 250AA deletion of AGC1-3 for pETMAL	Forward	EcoRI	CACGAATTCATGAATGTGAGCCCAC AT
AGC1-3	d275 AGC1-3 EcoRI	Amplifying N-terminal 275AA deletion of AGC1-3 for pETMAL	Forward	EcoRI	CACGAATTCATGGCAACAAGTACTA CT
AGC1-3	dPIF AGC1-3 XhoI	Amplifying AGC1-3 without the C-terminal PIF	Reverse	XhoI	CACCTCGAGTTAGTCTAGAAATTTAC C
AGC1-3	AGC1-3 S253AF	Mutagenesis	Forward		CCCAGTACCAATGTGGCCCCACATAG CAGTAGT
AGC1-3	AGC1-3 S253AR	Mutagenesis	Reverse		ACTACTGCTATGTGGGGCCACATTGG TACTGGG
AGC1-3	AGC1-3 S261AF	Mutagenesis	Forward		AGCAGTAGTGTTGAAGCCATGAATTT GGCTCGG
AGC1-3	AGC1-3 S261AR	Mutagenesis	Reverse		CCGAGCCAAATTCATGGCTTCAACAC TACTGCT
AGC1-3	AGC1-3 S269AF	Mutagenesis	Forward		TTGGCTCGGGCTATGGCCATTGCTAA TAGCTCT
AGC1-3	AGC1-3 S269AR	Mutagenesis	Reverse		AGAGCTATTAGCAATGGCCATAGCC CGAGCCAA
AGC1-4	5’ At5g40030 cDNA	Amplifying ORF from first strand synthesis	Forward		ATGAGTAAACAAACTCCAAATCTTG AA
AGC1-4	3’ At5g40030	Amplifying ORF from first strand synthesis	Reverse		CTAGAAGAACTCAAAATCTAAATAA GG
AGC1-4	AGC1-4 EcoRI	Amplifying ORF for pGEX	Forward	EcoRI	ACGAATTCATGAGTAAACAAACTCC AAAT
AGC1-4	AGC1-4 XhoI	Amplifying ORF for pGEX	Reverse	XhoI	ACCTCGAGCTAGAAGAACTCAAAAT C
AGC1-4	AGC1-4 K143QF	Mutagenesis	Forward		CTTTGCTATGCAAGTGATGGATAAA
AGC1-4	AGC1-4 K143QR	Mutagenesis	Reverse		CATTCCTTTATCCATCACTTTCATAGC
AGC1-4	AGC1-4 S343AF	Mutagenesis	Forward		ATGCGTGCCAACGAATGCCATAGAT CGAGC
AGC1-4	AGC1-4 S343AR	Mutagenesis	Reverse		GCTCGATCTATGGCATTCGTTGGCAC GCAT

Table 1. Continued.

AGC1-7	AGC1-7 EcoRI	Amplifying ORF for pGEX	Forward	EcoRI	ACGAATTCATGTTAACGAAGCCCGGAAAG
AGC1-7	AGC1-7 XhoI	Amplifying ORF for pGEX	Reverse	XhoI	ACCTCGAGCTAAAAGTATTCAAAGTC
AGC1-7	AGC1-7 K175QF	Mutagenesis	Forward		ACCTATTTCGCCATGCAAGTGATGGACAAGGCT
AGC1-7	AGC1-7 K175QR	Mutagenesis	Reverse		AGCCTTGTCCATCACTTGCATGGCGAAATAGGT
AGC1-7	AGC1-7 S379AF	Mutagenesis	Forward		AACGTTAAGTCAATGGCATTCGTTGGAACACAC
AGC1-7	AGC1-7 S379AR	Mutagenesis	Reverse		GTGTGTTCCAACGAATGCCATTGACTTAACGTT
PFP	PFP EcoRI	Amplifying ORF for pGEX	Forward	EcoRI	CACGAATTCATGGCCCCTGCTCTCGCC
PFP	PFP XhoI	Amplifying ORF for pGEX	Reverse	XhoI	GTGCTCGAGCTATTGAGCCCCGAGTTC
PFP	PFP T008AF	Mutagenesis	Forward		CCTGCTCTCGCCGTTGCGCGAGATCTCACCGCC
PFP	PFP T008AR	Mutagenesis	Reverse		GGCGGTGAGATCTCGCGCAACGGCGAGAGCAGG
PFP	PFP T012AF	Mutagenesis	Forward		GTTACACGAGATCTCGCCGCCGTCGGATCTCCG
PFP	PFP T012AR	Mutagenesis	Reverse		CGGAGATCCGACGGCGGCGAGATCTCGTGTAAC
PFP	PFP T008A/T012AF	Mutagenesis	Forward		GTTGCGCGAGATCTCGCCGCCGTCGGATCTCCG
PFP	PFP T008A/T012AR	Mutagenesis	Reverse		CGGAGATCCGACGGCGGCGAGATCTCGCGCAAC
PFP	PFP T008DF	Mutagenesis	Forward		CCTGCTCTCGCCGTTGACCGAGATCTCACCGCC
PFP	PFP T008DR	Mutagenesis	Reverse		GGCGGTGAGATCTCGGTCAACGGCGAGAGCAGG
PFP	PFP T012DF	Mutagenesis	Forward		GTTACACGAGATCTCGACGCCGTCGGATCTCCG
PFP	PFP T012DR	Mutagenesis	Reverse		CGGAGATCCGACGGCGTCGAGATCTCGTGTAAC
PFP	PFP T008D/T012DF	Mutagenesis	Forward		GTTGACCGAGATCTCGACGCCGTCGGATCTCCG
PFP	PFP T008D/T012DR	Mutagenesis	Reverse		GTTGACCGAGATCTCGACGCCGTCGGATCTCCG

Table 1. Continued.

Adi3	S119A	Mutagenesis	Forward		CTGGTGAAAAACGTAGCATTGAAGGGTCCTTTC
Adi3	S119A	Mutagenesis	Reverse		GAAAGGACCCTTCAATGCTACGTTTTTCACCAG
Adi3	S119D	Mutagenesis	Forward		CTGGTGAAAAACGTAGACTTGAAGGGTCCTTTC
Adi3	S119D	Mutagenesis	Reverse		GAAAGGACCCTTCAAGTCTACGTTTTTCACCAG
Adi3	S212A	Mutagenesis	Forward		GTTGTGAGATCTATGGCAATTGTCAACAGTTGC
Adi3	S212D	Mutagenesis	Reverse		GCAACTGTTGACAATTGCCATAGATCTCACAAC
Adi3	S518A	Mutagenesis	Forward		GTTGTGAGATCTATGGACATTGTCAACAGTTGC
Adi3	S518A	Mutagenesis	Reverse		GCAACTGTTGACAATGTCCATAGATCTCACAAC
Adi3	S518D	Mutagenesis	Forward		CCTAAGCCTCGAGCTGATGCAGGGTTTCAAGCTAATTCAATGCC
Adi3	S518D	Mutagenesis	Reverse		GGCATTGAATTAGCTTGAAACCCTGCATCAGCTCGAGGCTTAGG
Adi3	S651A	Mutagenesis	Forward		GCTCTAATACGTTGCGCAACACCACCTGAAGTG
Adi3	S651A	Mutagenesis	Reverse		CACTTCAGGTGGTGTTGCGCAACGTATTAGAGC
Adi3	S651D	Mutagenesis	Forward		GCTCTAATACGTTGCGATACACCACCTGAAGTG
Adi3	S651D	Mutagenesis	Reverse		CACTTCAGGTGGTGTATCGCAACGTATTAGAGC
Adi3	S680A	Mutagenesis	Forward		GGGGTTGGCAATACCGCAAAAAGAGTGGTAGGG
Adi3	S680A	Mutagenesis	Reverse		CCCTACCACTCTTTTTGCGGTATTGCCAACCCC
Adi3	S680D	Mutagenesis	Forward		GGGGTTGGCAATACCGACAAAAGAGTGGTAGGG
Adi3	S680D	Mutagenesis	Reverse		CCCTACCACTCTTTTGTCGGTATTGCCAACCCC

pET41a (Novagen), which expresses MBP-fusions rather than GST-fusion proteins. This modified pET41a was created by digestion with NdeI and SpeI to remove the GST ORF and cloning of the MBP ORF, amplified from pMAL-C2, into the same sites. Expression and purification of MBP-AGC1-3 fusion proteins expressed from the modified pET41a yielded higher protein levels compared to pMAL-C2, possibly due to the longer linker region between MBP and AGC1-3 in the modified pET41a compared to pMAL-C2. All variants of AGC1-3 used in this study were cloned into the 5′ EcoRI and 3′ XhoI sites of the modified pET41a vector, and the yeast 2-hybrid plasmids pEG202 and pJG4-5. For localization and cell viability studies, AGC1-3 was cloned in frame into the BamHI and SalI sites of pTEX-eGFP (Ek-Ramos et al., 2010), producing an N-terminal fusion of GFP.

The full-length AGC1-4 (At5g40030; accession # NM 123366) ORF was amplified from first strand synthesis product made from a total mRNA extract, just as AGC1-3. After sequencing, AGC1-4 was amplified and cloned into the EcoRI and XhoI sites of the bacterial expression vector pGEX (Amersham Biosciences).

The AtPdk1-1 cDNA (At5g04510; accession # NM_203001) has been previously described (Deak et al., 1999). The full length AtPdk1-1 ORF was amplified from first strand cDNA and cloned into pCR2.1-TOPO as with AGC1-3. The AtPdk1-1 ORF was subcloned into the EcoRI and XhoI sites of the bacterial expression vectors pGEX and pMAL-c2, and the yeast 2-hybrid plasmids pEG202 & pJG4-5.

Full-length cDNA clones of AGC1-7 (At1g79250; # NM 106575), PFP (pyrophosphate dependent PFK1) (At1g12000; accession # NM_101072), and AMP

deaminase (At2g38280; accession # NM_129384) were procured from the ABRC (Arabidopsis Biological Research Center) in the plant expression vector pUNI51. Full-length cDNAs of AGC1-7 and PFP were amplified and cloned into the EcoRI and XhoI sites of the pGEX expression plasmid. Full-length AMP deaminase was cloned into the MBP expression vector pETMAL.

2.2 Mass spectrometry

For MS analysis of Adi3 phosphorylation sites, 5 μg of MBP-Adi3 was phosphorylated by 1 μg MBP-Pdk1 in an in vitro kinase assay and samples separated by 10% SDS-PAGE as detailed below for kinase assays, except non-radiolabeled ATP was used. For sample preparation, coomassie stained gel bands were in-gel digested with trypsin overnight (Sheffield et al., 2006) and phosphopeptides were enriched using a NuTip metal oxide phosphoprotein enrichment kit according to manufacturer's instructions (Glygen, Columbia, MD).

For LC–MS/MS analysis, phosphopeptides were injected onto a capillary trap (LC Packings PepMap, Amsterdam, Netherlands) and desalted for 5 min with 0.1% v/v acetic acid at a flow rate of 3 μl/min. The samples were loaded onto an LC Packings C_{18} PepMap nanoflow HPLC column. The elution gradient of the HPLC column started at 97% solvent A, 3% solvent B and finished at 60% solvent A, 40% solvent B for 30 min. Solvent A consisted of 0.1% v/v acetic acid, 3% v/v ACN, and 96.9% v/v H_2O. Solvent B consisted of 0.1% v/v acetic acid, 96.9% v/v ACN, and 3% v/v H_2O. LC–MS/MS analysis was carried out on a LTQ Orbitrap XL mass spectrometer (Thermo Scientific, Bremen, Germany). The instrument under Xcalibur 2.07 with LTQ Orbitrap

Tune Plus 2.55 software was operated in the data dependent mode to automatically switch between MS and MS/MS acquisition. Survey scan MS spectra (from m/z 300–2000) were acquired in the orbitrap with resolution R = 60,000 at m/z 400. During collisionally induced dissociation (CID), if a phosphate neutral loss of 98, 49, 32.66 and 24.5 m/z below the precursor ion mass was detected, there was an additional activation of all four neutral loss m/z values. This multistage activation was repeated for the top five ions in a data-dependent manner. Dynamic exclusion was set to 60 s. Typical mass spectrometric conditions include a spray voltage of 2.2 kV, no sheath and auxiliary gas flow, a heated capillary temperature of 200 °C, a capillary voltage of 44 V, a tube lens voltage of 165 V, an ion isolation width of 1.0 m/z, and a normalized CID collision energy of 35% for MS/MS in LTQ. The ion selection threshold was 500 counts for MS/MS. The mass spectrometer calibration was performed according to the manufacturer's guidelines using a mixture of sodium dodecyl sulphate, sodium taurocholate, MRFA and Ultramark.

For the protein search algorithm, all MS/MS spectra were analyzed using Mascot (Matrix Science, London, UK; version 2.4). Mascot was set up to search a current *Arabidopsis* database assuming the digestion enzyme trypsin and one miscleavage. Mascot was searched with a fragment ion mass tolerance of 0.80 Da and a parent ion tolerance of 10 ppm. Iodoacetamide derivative of Cys, deamidation of Asn and Gln, oxidation of Met and phosphorylation of serine, threonine and tyrosine are specified as variable modifications. The MS/MS spectra of the identified phosphorylated

peptides were manually inspected to ensure confidence in phosphorylation site assignment.

2.3 Yeast two-hybrid assays

Y2H assays were conducted using pEG202 for the bait vector and pJG4-5 for the prey vector as described previously (Devarenne et al., 2006). Constructs were transformed into yeast strain EGY48 containing the pSH18-34 reporter vector and analyzed for LacZ gene expression on 5-bromo-4-chloro-3-indolyl-β-D-galactopyranoside-containing plates. Protein expression was confirmed by Western blot. All other procedures for the Y2H assays followed standard procedures as described previously (Golemis et al., 2008).

2.4 Recombinant protein expression and purification

For the purpose of protein purification, cells were grown in 400mL cultures of TB at 37° with shaking to an OD_{600} = 0.5-0.7. Protein expression was induced with 100uM IPTG isopropyl β-D-1-thiogalactopyranoside (IPTG) for 5 hours at 25°. Cultures were spun down at 4,000xg for 10 minutes. Cell pellets were stored at -20° until they were prepared for protein purification.

MBP fusions were resuspended in EB1 (50mM Tris, pH 8.0, 50mM NaCl, 5mM EDTA, 1% Triton X-100) volume equal to 10% of the original culture volume. GST fusion proteins were resuspended in EB2 (1X PBS, 1% Triton X-100) volume equal of 10% of the original culture volume. Resuspended protein extracts were sonicated 3 times for 30 seconds, at power setting of 10, at one-minute intervals. The sonicated samples were centrifuged at 10,000xg for 20 minutes at 4°.

EB1 or EB2 was added to the protein lysate to a total volume of 200mL and then loaded onto either a GST-Trap or MBP-Trap column. The protein was flowed over the affinity column at flow rate of 0.2mL/min using the Akta Prime FPLC System (GE Healthcare Life Sciences). The lysate was flowed over the column for a total of 500mL and then washed with 15 column volumes of the respective extraction buffer. After washing the column with 15 CV of extraction buffer, the column was washed with 25 CV with EB3 (50mM Tris, pH 8.0, 50mM NaCl, 5mM EDTA). MBP fusion proteins were eluted with EB3 with 100mM maltose (Fluka) and GST fusion proteins were eluted with EB3 supplemented with 10mM glutathione (Sigma-Aldrich). Eluted proteins were collected in 1.2mL fractions and analyzed by SDS-PAGE to identify fractions containing protein. Fractions containing protein were pooled, concentrated, and stored as 20% glycerol stocks.

2.5 Pulldown assays

For MBP-AGC1-3 and GST-AtPdk1-1 pull-down assays, cell pellets from 2 ml cultures were lysed by sonication in 500 µl of extraction buffer (50 mM Tris, pH 8.0, 50 mM NaCl, 5 mM EDTA, 0.1% Triton X-100, 1 × general protease inhibitors [Sigma]) and cell debris pelleted by centrifugation at 5000 ×*g*, 4 °C for 5 min. One hundred µg of the supernatant (total protein) from each extract was added to 50 µl of equilibrated amylose resin, the volume was adjusted to 1 ml with extraction buffer, incubated on a nutator at 4 °C for 30 min, the resin was pelleted by centrifugation at 1000 ×*g* for 1 min, and the resin was washed 3 times with 500 µl of extraction buffer. Samples were eluted from the resin with 100 µl of 1 × SDS-PAGE buffer at 95 °C for

5 min, and 5 µl of each sample was analyzed by 10% SDS-PAGE. Proteins were analyzed by Western blotting using α-GST (Santa Cruz Biotechnology) at 1:4000 or α-MBP (New England BioLabs) at 1:10,000.

2.6 Kinase assays

In vitro kinase assays were done in 30 µl reactions in kinase buffer (10 mM Tris–HCl, pH 7.5, 10 mM $MgCl_2$, 1 mM dithiothreitol [DTT]) with the protein amounts given in the figure legends. The reactions were started by the addition of 0.25 µCi of [γ-^{32}P]ATP (6000 Ci mmol^{-1}; Perkin-Elmer) and non-radiolabeled ATP to a final concentration of 20 µM per sample followed by incubation for 30 min at 30 °C. Reactions were terminated by the addition of 4 × SDS-PAGE sample buffer, and samples were resolved by 10% SDS-PAGE or 1:200 *bis*-acrylamide:acrylamide 10% SDS-PAGE. Visualization and quantification of incorporated radioactivity were done using a phosphorimager (Bio-Rad Molecular Imager) and quantification software (Bio-Rad Quantity One). For non-radioactive kinase assays, the assays were carried out as above with the omission of [γ-^{32}P]ATP. The kinase artificial substrate myelin basic protein was purchased from Sigma.

2.7 1:200 *bis*-acrylamide SDS-PAGE

10% SDS-PAGE gels with a 1:200 *bis*-acrylamide:acrylamide ratio were made by mixing the following: 2.5 ml 4 × resolving gel buffer (1.5 M Tris-base, 0.4% SDS, pH 8.8), 3.317 ml 30% acrylamide, 250 µl 2% *bis*-acrylamide, 50 µl 10% ammonium persulfate, and 5 µl N, N, N′, N′-tetramethylethylenediamine (TEMED) in a final volume

of 10 ml. These gels were used with a typical 4% acrylamide stacking gel. Gels were run at 150V for approximately 4h.

2.8 λ Phosphatase treatment

Adi3 and *Sl*Pdk1 were incubated in a 30 µl in vitro kinase assay as described above with only non-radiolabeled ATP. Following the kinase assay 4 µl of 10× λ phosphatase buffer (500mM HEPES, pH 7.5, 1M NaCl, 20mM DTT, 0.1% Brij 35) and 4µl of 10mM $MnCl_2$ were added for a final volume of 38 µl. Reactions were started with the addition of 800units (2 µl) of λ phosphatase (New England Biolabs), incubated at 30 C for 1h, and reactions were terminated by the addition of 10 µl 4× SDS-PAGE sample buffer. Samples were then resolved by 1:200 *bis*-acrylamide:acrylamide 10% SDS-PAGE as described above.

2.9 Protoplast protein expression and cell death assays

Wild type *Arabidopsis* (Col-0) were grown under an 16 hour light schedule at ~23° C for ~4-5 weeks, rosette leaves were cut off before bolting occurred and digestion of leaves was done as previously reported, with slight modifications (Yoo et al., 2007). Leaf strips were incubated in the enzyme solution (Xing et al., 2001) in the dark for no more than 16 hours and no less than 12 hours. A slightly different enzyme solution was used to facilitate effective separation of viable from dead protoplasts (see below). After digestion, the enzyme-protoplasts solution was filtered through a metal sieve, separating liberated protoplasts from undigested leaf tissue. The liberated protoplasts were collected in a 15mL round bottom Falcon tube and centrifuged with an overlay of 1mL of W5 solution (125mM $CaCl_2$, 5mM glucose, 5mM KCl, 1.5mM MES, 154mM NaCl) at

100xg for 3 minutes this step separates viable protoplasts from dead cells and extraneous debris. This W5 overlay step is the only modification to the protocol for *Arabidopsis* protoplast recovery (Yoo et al., 2007). Prior to transformation, cells were counted with a hemacytometer and concentration was adjusted to $1x10^5$ cells/mL. Transformations consisted of 200μL of protoplasts ($4x10^4$ cells), 20% PEG solution was used, and 25μg of each pTEX-eGFP plasmid were transformed after preparation by CsCl gradient. Cell viability was measured by staining of cells with 0.05% Evan's blue, a total of 200 cells were counted in four different experiments.

For localization of GFP fusion proteins, protoplasts were prepared and transformed in the same manner as in cell viability experiments. Visualization with a Zeiss Axioplan 2 fluorescent microscope enabled visualization of GFP fusions while nuclear visualization required incubation with 10μM HOECHST 33342 (Sigma) for 30 minutes.

2.10 Kinase-Client assay

This procedure was carried out as previously described with modifications, the synthetic peptide library, PEPscreen peptides (Sigma-Aldrich) contained 2100 peptides derived from phosphorylation data of *Arabidopsis* proteins (Huang and Thelen, 2012). For their role as the kinase in the KiC assay, MBP, MBP-AGC1-3, and MBP-AGC1-3^{S596D} were expressed, purified, and adjusted to a final concentration of 5 μg/μL. Each kinase was assayed for auto-catalytic activity, trypsin digested, and subjected to LC-MS/MS analysis to identify auto-catalytic residues. For the identification of substrate peptides, each kinase was incubated with ~100 peptides at a final concentration of 4.5

μM. Kinase assays with peptides were incubated at room temperature for 30 minutes and quenched by adding an equal volume of 1% formic acid/99% acetonitrile then dried by centrifugal-evaporator and frozen at -20°C. Freeze-dried-peptides were suspended in 40μL of 0.1% formic acid and loaded onto 96-well plates and placed in an autosampler. From the autosampler, 10μL of the freeze-dried peptide sample was taken and peptides were bound to a C8 Captrap then eluted with a gradient of 1-30% acetonitrile in 0.1% formic acid over 15 minutes. Peptides were separated using a "Magic 18" fused silica column and analyzed using a stand-alone LTQ-XL with a 1-40% acetonitrile gradient. Raw MS files were searched against the sequences of the peptide library, using SEQUEST.

CHAPTER III

PDK1 PHOSPHORYLATES AGC1-3 AND ADI3 AT MULTIPLE SITES*

3.1 Mass spectrometry analysis of *Sl*Pdk1 phosphorylated by Adi3

From our previous studies we have shown that *Sl*Pdk1 phosphorylates Adi3 only on Ser residues, phosphorylation of Ser539 accounts for ~ 40–50% of *Sl*Pdk1 activity on Adi3, and at least one additional Adi3 Ser residue accounts for the remaining phosphorylation by *Sl*Pdk1 (Devarenne et al., 2006). In an effort to identify the additional *Sl*Pdk1 phosphorylation site(s) on Adi3 we initially took a mass spectrometry (MS) approach. Kinase-inactive Adi3^{K337Q} was phosphorylated by *SlPdk1* using non-radiolabeled ATP, digested with trypsin, and analyzed by tandem MS/MS, which identified 20 peptides giving 49% coverage of the Adi3 protein sequence (Figure 8). This MS/MS analysis was repeated several times without, an increase in peptide coverage of Adi3. Two new phosphorylated Ser residues were found in two separate Adi3 peptides; Ser119 and Ser518 (Figure 8, Figure 9, Figure 10). The previously identified *Sl*Pdk1 phosphorylation activation site in Adi3, Ser539 (Devarenne et al., 2006), was also identified as a phosphorylated residue (Figure 8 and Figure 11).

---

* Portions of the following article have been reprinted with permission from: **Gray J, Nelson Dittrich AC, Chen S, Avila J, Giavalisco P, Devarenne TP** (2013) Two Pdk1 phosphorylation sites on the plant cell death suppressor Adi3 contribute to substrate phosphorylation. Biochim Biophys Acta **1834:** 1099-1106. Copyright 2013 © by Elsevier.

Peptides identified by MS, alternately highlighted in yellow and green, cover 345 residues giving 49% coverage of the Adi3 protein. Peptide with Ser212 phosphorylation identified by targeted MS highlighted in orange.

MERIPEVRESTRQFPIGAKVAHTFSTSKKEVGIRGFRDFDLAIPIQTW
KGKTSYQEEEDLMVDAGTIKRSDDSLEDSGSTSFHGASHPPEPVDTDL
MRPVYVPIGQNKADGKCLVKNVSLKGPFLDDLSIRMPNVKPSPSLLSP
AESLVEEPNDLGVISSPFTVPRPSQNTETSLPPDSEEKECIWDASLPP
SGNVSPLSSIDSTGVVRSMSIVNSCTSTYRSDVLMSDGMLSVDRNYES
TKGSIRGDSLESGKTSLSRASDSSGLSDDSNWSNITGSANKPHKGNDP
RWKAILAIRARDGILGMSHFKLLKRLGCGDIGSVYLSELSGTRCYFAM
KVMDKASLASRKKLTRAQTEREILQLLDHPFLPTLYTHFETDRFSCLV
MEYCPGGDLHTLRQRQPGKHFSEYAARFYAAEVLLALEYLHMLGVVYR
DLKPENVLVRDDGHIMLSDFDLSLRCAVSPTLIRISSDDPSKRGAAFC
VQPACIEPTTVCMQPACFLPRLFPQKSKKKTPKPRADSGFQANSMPEL
VAEPTSARSMSFVGTHEYLAPEIIKGEGHGSAVDWWTFGIFLHELLYG
KTPFKGSGNRATLFNVVGQQLKFPDSPATSYASRDLIRGLLVKEPQNR
LGVKRGATEIKQHPFFEGVNWALIRCSTPPEVPRPVEPDYPAKYGQVN
PVGVGNTSKRVVGADAKSGGKYLDFEFF

Potential Pdk1 phosphorylation sites on Adi3 identified by MS here: S119, S518

Pdk1 phosphorylation site on Adi3 previously identified as well as here by MS: S539

Pdk1 phosphorylation site identified by homology with *At*AGC1-3 and MS: S212

Figure 8. Adi3 peptide MS coverage and Pdk1 phosphorylation site identification. The Adi3 protein sequence showing peptides identified by MS, alternately highlighted in yellow and green, from Pdk1 phosphorylated Adi3 giving 49% coverage of the total Adi3 protein. Phosphorylation sites identified by MS or homology to AtAGC1-3 are highlighted as indicated.

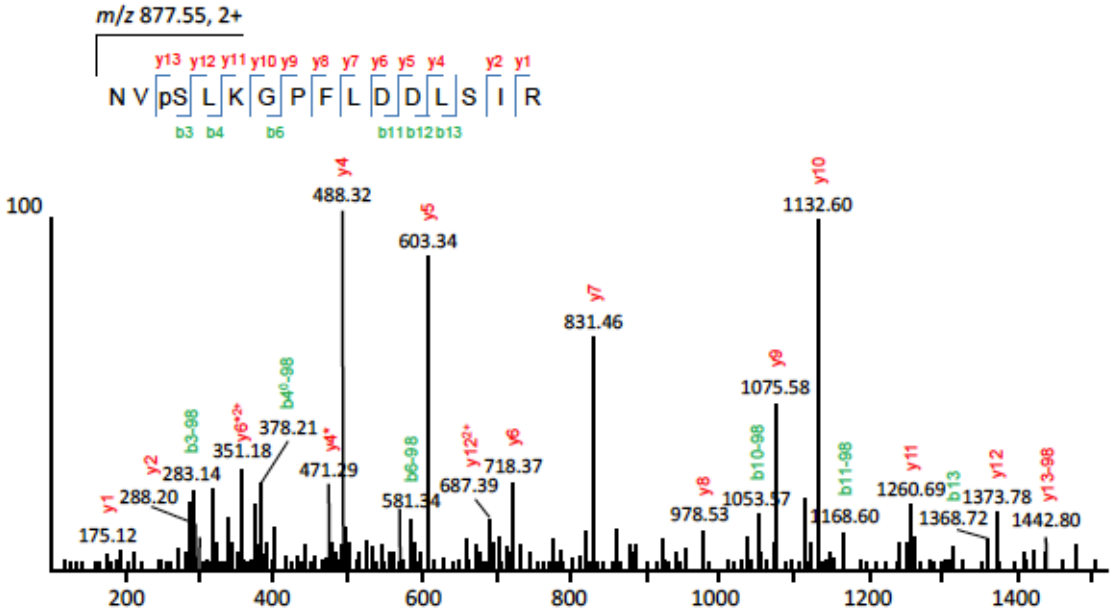

Figure 9. MS/MS spectra of Pdk1 phosphorylated Adi3 peptide with Ser119 phosphorylation. Trypsin digestion of the kinase inactive, bacterially expressed Adi3 phosphorylated by bacterially expressed Pdk1 results in a phosphorylated peptide. Analysis of this phosphorylated peptide indicates that the 3rd amino acid from the N-terminus, a serine, is phosphorylated. Analysis of full-length Adi3 protein sequence reveals that this site corresponds to Ser119. Although this peptide has another serine at position 13, it is not appear to be phosphorylated by Pdk1.

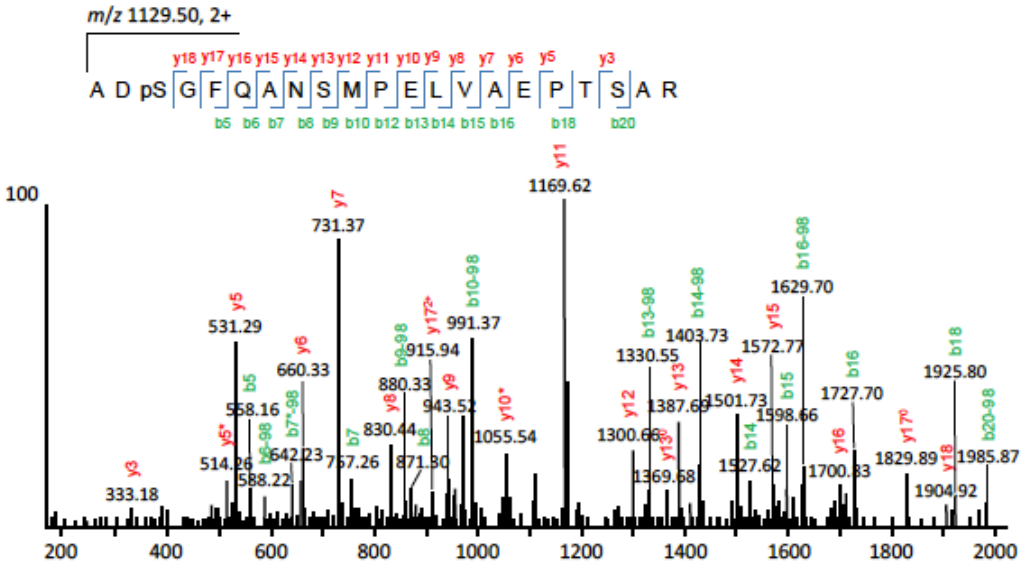

Figure 10. MS/MS spectra of Pdk1 phosphorylated Adi3 peptide with Ser518 phosphorylation. Trypsin digestion of the kinase inactive, bacterially expressed Adi3 phosphorylated by bacterially expressed Pdk1 results in a phosphorylated peptide. Analysis of this phosphorylated peptide indicates that the 3rd amino acid from the N-terminus, a serine, is phosphorylated. Analysis of full-length Adi3 protein sequence reveals that this site corresponds to Ser518. This peptide has other residues that could be phosphorylated by Pdk1 – Ser9, Thr18, and Ser19 however this spectra indicates that those residues are not phosphorylated by Pdk1.

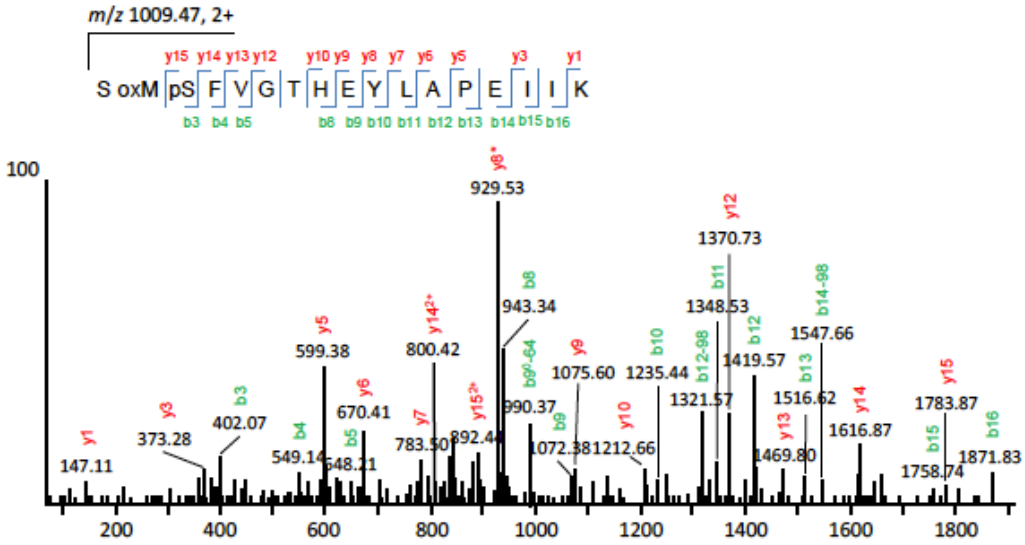

Figure 11. MS/MS spectra of Pdk1 phosphorylated Adi3 peptide with Ser539 phosphorylation. Trypsin digestion of the kinase inactive, bacterially expressed Adi3 phosphorylated by bacterially expressed Pdk1 results in a phosphorylated peptide. Analysis of this phosphorylated peptide indicates that the 3rd amino acid from the N-terminus, a serine, is phosphorylated. Analysis of full-length Adi3 protein sequence reveals that this site corresponds to Ser5139. This residue is the activation-loop residue, known to be phosphorylated by Pdk1. This peptide has other residues that could be phosphorylated by Pdk1 – Ser1, and Thr7 however this spectra indicates that those residues are not phosphorylated by Pdk1. This spectra also indicates that Met2 in the peptide is oxidized.

3.2 The MS/MS-identified phosphorylation sites do not contribute to *Sl*Pdk1 phosphorylation of Adi3 or Adi3 auto- or trans-phosphorylation

In order to confirm or deny that the phosphorylated Adi3 Ser residues identified by MS/MS were phosphorylated by *Sl*Pdk1, each residue was mutated to Ala in the kinase-inactive Adi3^{K337Q} background, the proteins incubated with *Sl*Pdk1 in an in vitro kinase assay with [γ-^{32}P]ATP, and the level of Adi3 phosphorylation quantified and compared to the level of phosphorylation for Adi3^{K337Q}. As we have seen previously (Devarenne et al., 2006), the S539A mutation reduces *Sl*Pdk1 phosphorylation of Adi3 by ~ 40% (Figure 12A, lane 4). However, the Ala mutations of the other Ser residues identified here by MS/MS did not reduce *Sl*Pdk1 phosphorylation of Adi3 and in some cases even increased phosphorylation (Figure 12, lanes 2, 3).

We have previously shown that mutation of Adi3 Ser539 to the phosphomimetic Asp greatly increases autophosphorylation and substrate phosphorylation (Devarenne et al., 2006; Ek-Ramos et al., 2010; Avila et al., 2012) supporting activation of Adi3 by *Sl*Pdk1 phosphorylation of this site. Next, we mutated the MS/MS-identified phosphorylation sites to Asp and tested autophosphorylation as well as phosphorylation of the protein kinase artificial substrate myelin basic protein. As we have seen before, the S539D mutation greatly increases Adi3 auto- and trans-phosphorylation (Figure 12B, lane 4). The S119D, mutation increased Adi3 autophosphorylation only slightly above that of wild-type and not to the extent of S539D (Figure 12B, lane 2), while S518D was slightly lower than wild-type (Figure 12B, lane 3). Similar results were seen for

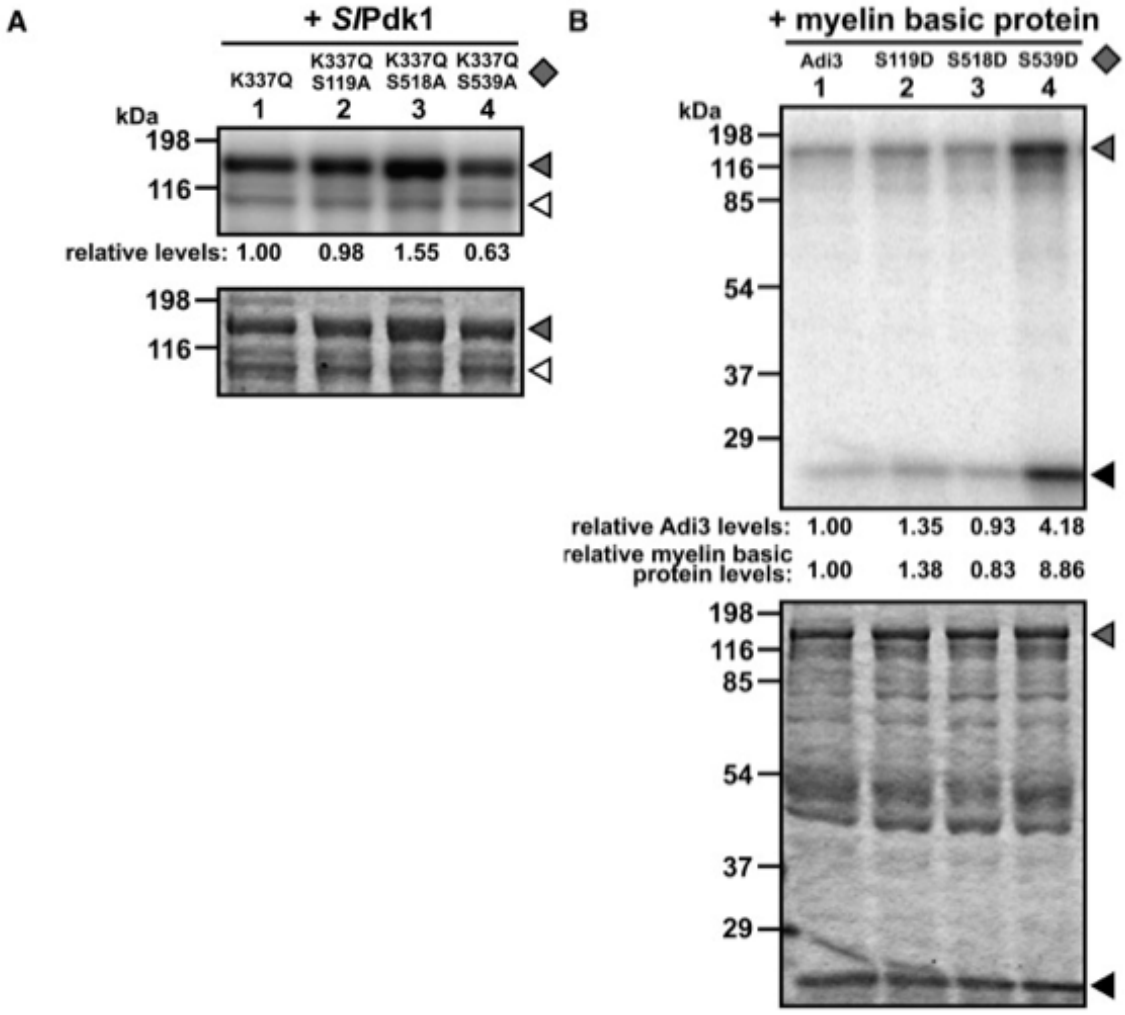

Figure 12. Contribution of MS/MS-identified Adi3 phosphorylation sites to phosphorylation by *Sl*Pdk1 and Adi3 trans-phosphorylation. In (A) and (B), the indicated proteins were incubated in an in vitro kinase assay with γ-[^{32}P]ATP. Top panel, phosphorimage; bottom panel, coomassie stained gel. Relative values of phosphorylation are given below each lane and are representative of two independent experiments. Gray diamond, form of MBP-Adi3 used in assay. Gray, open, and black triangles, location of MBP-Adi3, MBP-*Sl*Pdk1, and myelin basic protein, respectively. The following amounts of each protein were used in the assay: MPB-Adi3, 5 µg; MBP-SlPdk1, 1.0 µg; myelin basic protein, 5 µg. (A) Ala mutation of the identified phosphorylated Ser residues does not reduce Pdk1 phosphorylation of Adi3. (B) Asp mutation of the identified phosphorylated Ser residues does not increase Adi3 phosphorylation of myelin basic protein.

phosphorylation of myelin basic protein by the Asp mutations; only the S539D mutation greatly increased the phosphorylation of the substrate (Figure 12B, lane 4). These results may suggest that Ser119 and Ser518 are not bona fide *Sl*Pdk1 phosphorylation sites and may be artifacts of the in vitro kinase assay. These residues are most likely not Adi3 autophosphorylation sites since the kinase-inactive Adi3K337Q was used for the MS/MS analysis.

3.3 Identification and characterization of AGC1-3, the *Arabidopsis thaliana* sequence homologue of Adi3

At the same time we were carrying out the MS/MS analysis and characterization of the identified Adi3 phosphorylation sites described above, we began to characterize the *Arabidopsis* thaliana sequence homologue of Adi3 to identify *Arabidopsis* thaliana Pdk1 (AtPdk1) phosphorylation sites. A BLAST search of the *Arabidopsis* genome and proteome using the Adi3 cDNA and protein sequences returned gene At2g44830 (a.k.a. AGC1-3 (Bogre et al., 2003)) as the closest sequence homologue to Adi3. A comparison of AGC1-3 to Adi3 shows that they share 63.8% amino acid identity and have the same protein domains that are the hallmarks of the VIIIa group of plant AGC kinases such as a PIF, PIF binding pocket, kinase domain, and activation-loop extension (Figure 13A). AGC1-3 is 65 amino acids longer than Adi3, which is mainly localized to the region N-terminal to the kinase domain (Figure 13A).

There have been minimal studies on AGC1-3. The only experimental characterization of AGC1-3 has shown that it is a phosphorylation substrate of AtPdk1 and that its mRNA is expressed in seedlings, reproductive organs (inflorescences,

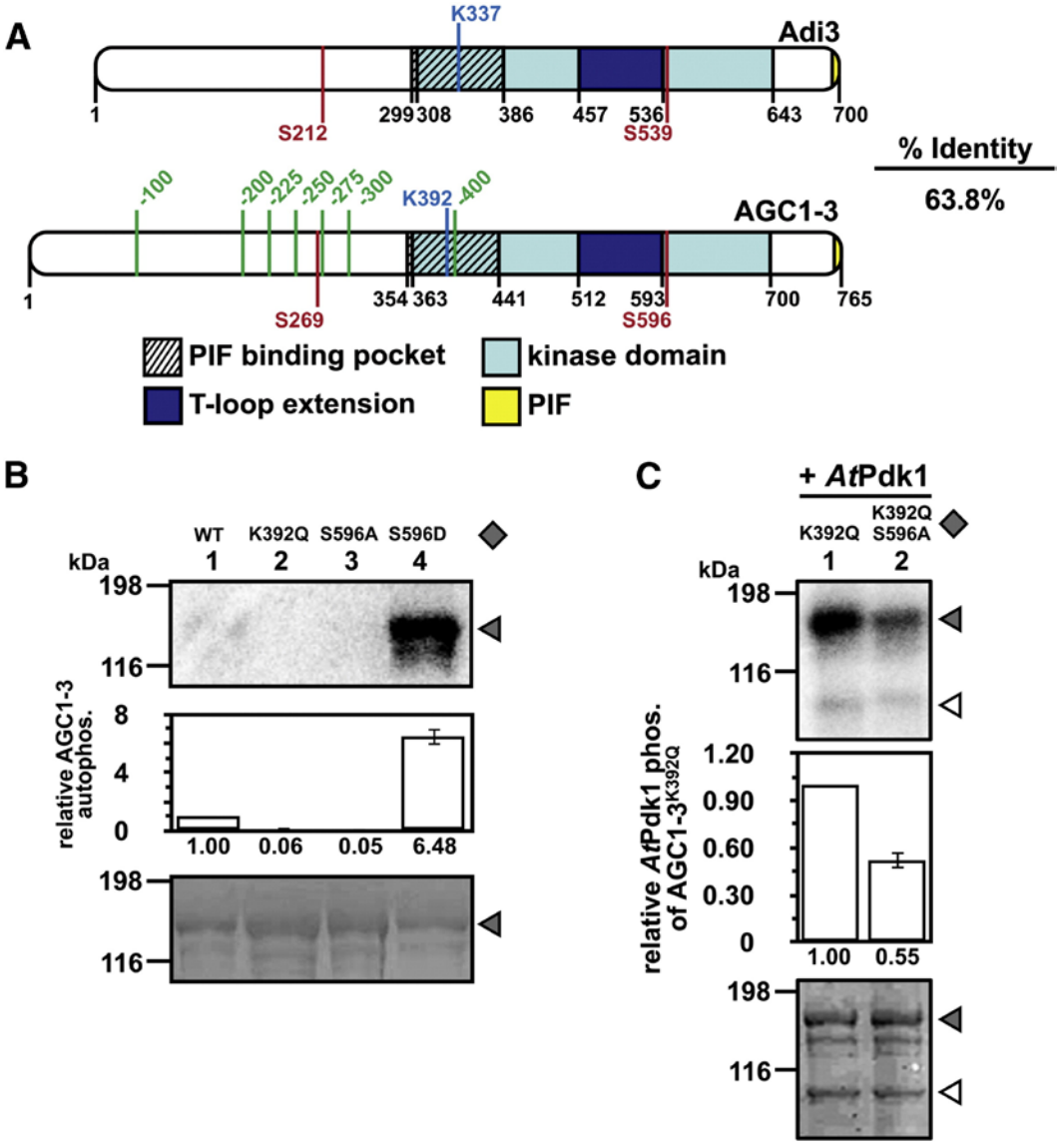

Figure 13. Auto- and AtPdk1 phosphorylation of AGC1-3. The indicated MBP-AGC1-3 proteins were incubated in an *in vitro* kinase assay with γ-[^{32}P]ATP. Top panel, phosphorimage; bottom panel, coomassie stained gel; middle panel, quantification of AGC1-3 autophosphorylation (A) or phosphorylation by AtPdk1 (B) from at least 3 independent assays. Error bars indicate standard error. Average value is shown under each column. Gray diamond, form of MBP-AGC1-3 used in assay. Gray and open triangles, location of MBP-AGC1-3 and GST-AtPdk1, respectively. The following amounts of each protein were used in the assay: MPB-AGC1-3, 8 µg, GST-AtPdk1, 4 µg. (A) AGC1-3 encodes a functional protein kinase. Analysis of wild-type, kinase-deficient, and constitutively active MBP-AGC1-3 fusion proteins by in vitro autophosphorylation assays. (B) Ser596 accounts for 45% of AtPdk1 phosphorylation of AGC1-3. Analysis of AtPdk1 phosphorylation of AGC1-3 in in vitro kinase assays.

flowers, siliques), and root (Zegzouti et al., 2006). Interestingly, AGC1-3 is not expressed in cauline leaves or stems of mature plants (Zegzouti et al., 2006). We have shown that AGC1-3 and AtPDK1 interact in a yeast two-hybrid (Y2H) assay in reciprocal combinations of the proteins as bait and prey (Figure 14, samples 2, 3) and that this interaction was dependent on the presence of the AGC1-3 PIF motif (Figure 14, sample 12).

We next tested the autophosphorylation activity of AGC1-3 using *in vitro* kinase assays. Wild-type AGC1-3 showed a low level of autophosphorylation activity (Figure 13, lane 1), whereas AGC1-3^{K392Q}, which has a mutation in the Lys residue that corresponds to the Lys337 ATP-binding residue in Adi3 (Figure 13A), did not (Figure 13A, Lane 2). Serine 596 corresponds to the conserved Pdk1 phosphorylation site in the activation loop of AGC1-3, and mutation to Ala (S596A) eliminated AGC1-3 autophosphorylation (Figure 13B, Lane 3), while mutation to Asp (S596D) greatly increased this activity (Figure 13B, Lane 4). This would suggest that phosphorylation of Ser596 contributes to full activity of AGC1-3.

Even though AGC1-3 has been shown to be phosphorylated by AtPdk1 (Zegzouti et al., 2006), the actual site(s) of phosphorylation was not identified. Thus, we tested the contribution of Ser596 to AtPdk1 phosphorylation of AGC1-3. Using the kinase deficient AGC1-3^{K392Q} it was seen that AtPdk1 can phosphorylate AGC1-3 (Figure 13C, lane 1), and the Ala mutation of Ser596 in the AGC1-3^{K392Q} background resulted

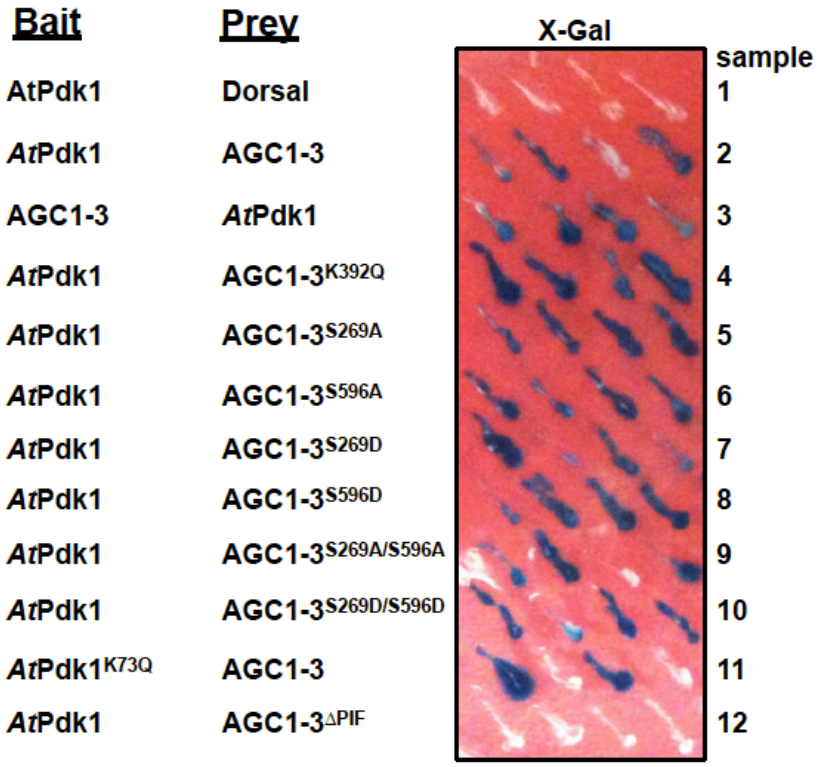

Figure 14. AGC1-3 yeast two-hybrid interactions with *At*Pdk1. The indicated bait and prey constructs were tested in the Y2H assay for expression of the *lacZ* gene on X-Gal plates (blue = interaction). The *Drosophila* protein Dorsal was used as a negative control and indicate that the *At*Pdk1/Adi3 interaction is specific.

in a loss of ~45% of the AtPdk1 phosphorylation of AGC1-3 (Figure 13C, Lane 2). Both of the AGC1-3^{K392Q} and AGC1-3^{S596A} proteins maintain interaction with AtPdk1 (Figure 13, samples 4, 5). These data would suggest that Ser596 is an AtPdk1 phosphorylation site in AGC1-3.

3.4 N-terminal truncations of AGC1-3 identify Ser269 as a second AtPdk1 phosphorylation site

Since MS/MS on *Sl*Pdk1 phosphorylated Adi3 was not successful in identifying additional phosphorylation sites, we took the alternate approach with AGC1-3 of using truncations to identify additional AtPdk1 phosphorylation sites. Successive AGC1-3 100 amino acid N-terminal deletions up to 400 amino acids, as shown in Figure 13A, were constructed in the kinase-inactive AGC1-3$^{K392Q/S596A}$ background and tested for phosphorylation by AtPdk1 (Figure 15A). After deletion of the first AGC1-3 100 amino acids, phosphorylation by AtPdk1 increased over that of the full length protein (Figure 15A Lanes 1, 2) suggesting an inhibitory function for these first 100 AGC1-3 amino acids for interaction with or phosphorylation by AtPdk1. The AGC1-3$^{\Delta 200}$ deletion protein did not change the phosphorylation by AtPdk1 compared to AGC1-3$^{\Delta 100}$ (Figure 15A, Lane 3). However, the AGC1-3$^{\Delta 300}$ deletion caused a drastic decrease in the phosphorylation of AGC1-3 by AtPdk1 (Figure 15A, Lane 4), as did the AGC1-3$^{\Delta 400}$ deletion (Figure 15A, Lane 5), suggesting that an additional AtPdk1 phosphorylation site(s) in AGC1-3 exists between amino acids 200 and 300. This was confirmed by creating further AGC1-3 N-terminal truncations of 25 amino acids based on the AGC1-3$^{\Delta 200/K392Q/S596A}$ protein and testing these proteins for AtPdk1 phosphorylation. The

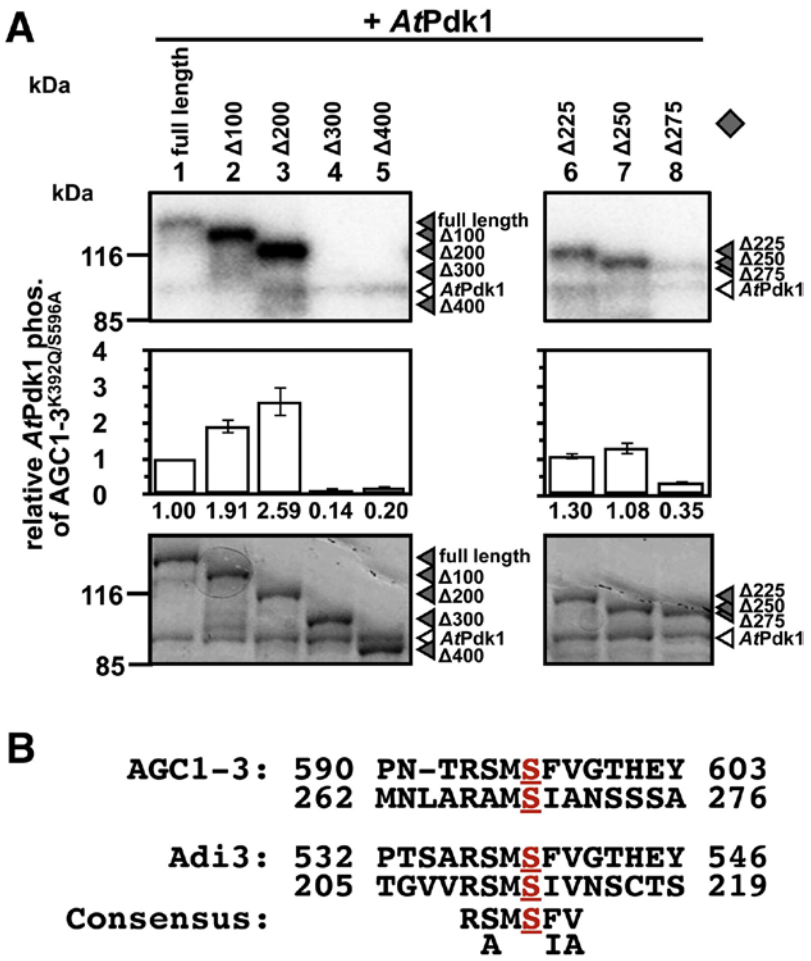

Figure 15. Identification of Ser269 as a second phosphorylation site in AGC1-3. In A and C, the indicated proteins were incubated in an in vitro kinase assay with γ-[^{32}P]ATP. Top panel, phosphorimage; bottom panel, coomassie stained gel; middle panel, quantification of AGC1-3 phosphorylation by AtPdk1 from at least 3 independent assays. Average value is shown under each column. Error bars indicate standard error. Gray diamond, form of MBP-AGC1-3 used in assay. Gray triangles, location of MBP-AGC1-3$^{K392Q/S595A}$ N-terminal truncation (B) and MBP-AGC1-3 (C) proteins. Open triangles, location of MBP-AtPdk1. The following amounts of each protein were used in the assay: MBP-AtPdk1, 4 μg; MPB-AGC1-3, 5 μg. (A) Identification of AGC1-3 Ser269 phosphorylation by AtPdk1 using kinase inactive N-terminally truncated MBP-AGC1-3$^{K392Q/S596A}$ proteins. (B) Amino acid sequences around the conserved Pdk1 phosphorylation sites in AGC1-3 (S596) and Adi3 (S539), the identified second Pdk1 phosphorylation site in AGC1-3 (S269), the homologous site in Adi3 (S212), and the consensus sequence. (C) MBP-AtPdk1 phosphorylation of MBP-AGC1-3 kinase site mutants produced in the kinase inactive K392Q background.

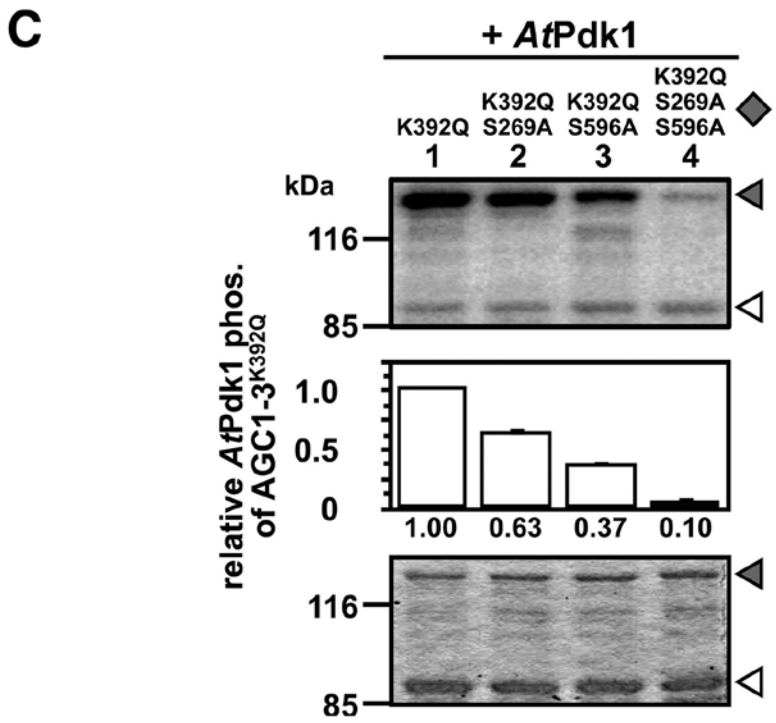

Figure 15. Continued.

AGC1-3$^{\Delta 275}$ protein had a large reduction in AtPdk1 phosphorylation indicating a second AtPdk1 phosphorylation site in AGC1-3 exists between amino acids 250 and 275. The reduction in AtPdk1 phosphorylation of the AGC1-3 N-terminal deletions was not due to a reduced interaction with AtPdk1 since all the AGC1-3 N-terminal deletions were capable of pulling down equal amounts of AtPdk1 (Figure 16). There are eight Ser residues within this amino acid 250 to 275 region of AGC1-3. However, only one Ser, Ser269, has a similar surrounding sequence as the Ser596 activation loop AtPdk1 site (Figure 15B).

In order to confirm Ser269 as an AtPdk1 phosphorylation site on AGC1-3, this amino acid was mutated to Ala in the AGC1-3^{K392Q} and AGC1-3$^{K392Q/S596A}$ backgrounds and tested for phosphorylation by AtPdk1. These proteins did not contain autophosphorylation activity (Figure 17) indicating that any phosphorylation when incubated with AtPdk1 could be attributed to AtPdk1. The AtPdk1 phosphorylation of AGC1-3$^{K392Q/S269A}$ was reduced by ~ 40% compared to AGC1-3^{K392Q} (Figure 15C, compare Lanes 1, 2) and the double phosphorylation site mutant AGC1-3$^{K392Q/S596A/S269A}$ showed a large ~90% decrease in AtPdk1 phosphorylation (Figure 15C, Lane 4). These data suggest that both Ser269 and Ser539 are the main AtPdk1 phosphorylation sites in AGC1-3, and there may be additional minor phosphorylation sites.

3.5 Adi3 Ser212 is homologous to AGC1-3 Ser269 and is a second *Sl*Pdk1 phosphorylation site

We next used the data obtained for the AGC1-3 Ser269 AtPdk1 phosphorylation site to identify a potential second *Sl*Pdk1 site in Adi3.

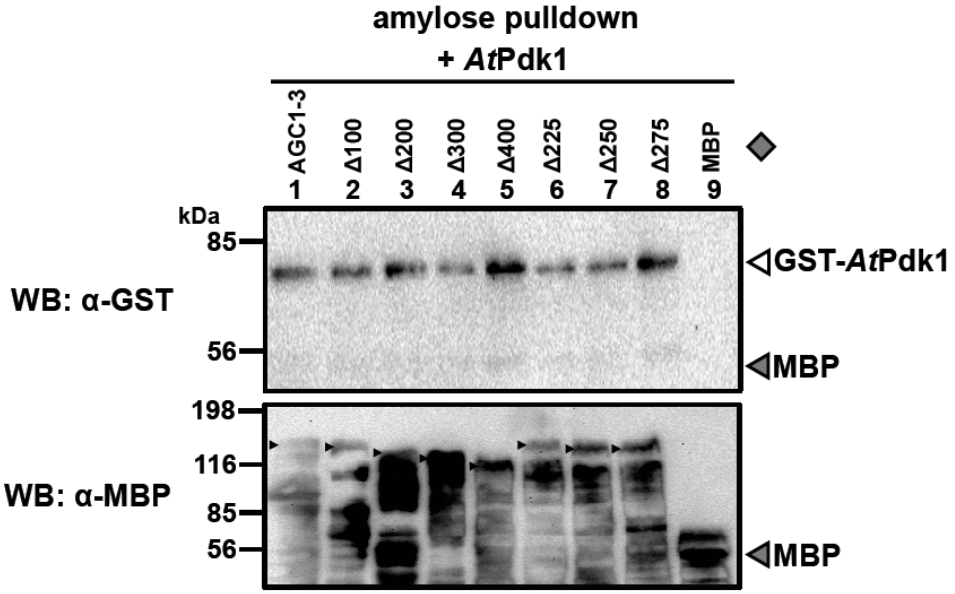

Figure 16. AGC1-3 N-terminal truncations interact with *At*Pdk1. The indicated N-terminal truncated MBP-AGC1-3$^{K337Q/S596A}$ proteins were incubated with GST-*At*Pdk1 or MBP for 1 hr at 4°C and the MBP-tagged proteins pulled down with amylose resin. Each pull-down was split into two equal fractions and analyzed for the presence of GST-Pdk1 by **α**-GST western blot (top panel) and the N-terminal truncated MBP-AGC1-3$^{K337Q/S596A}$ proteins by **α**-MBP western blot (bottom panel). Gray diamond, truncated form of AGC1-3 in the kinase inactive MBP-AGC1-3$^{K392Q/S595A}$ background used in assay. White and gray triangles, location of GST-AtPdk1 and MBP. Small black triangles on **α**-MBP western blot (bottom panel) indicate position of N-terminal truncated MBP-AGC1-3$^{K337Q/S596A}$ proteins.

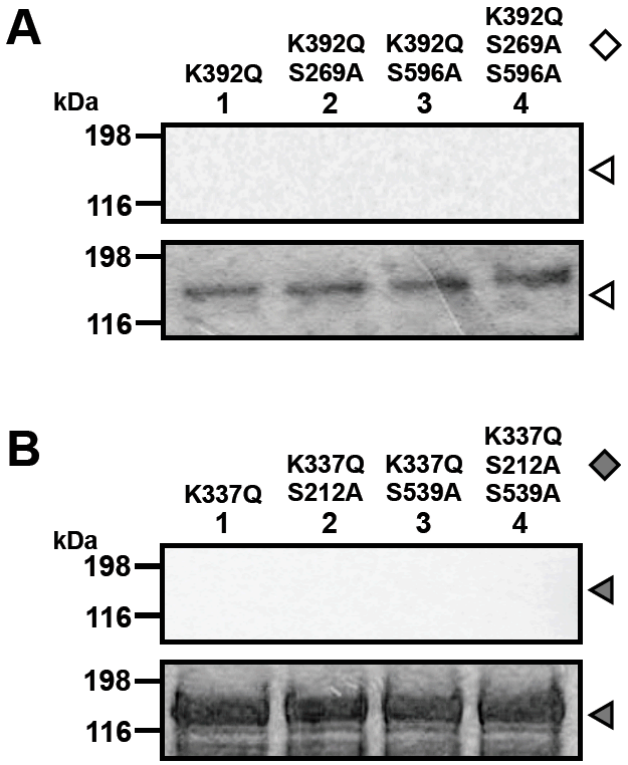

Figure 17. Autophosphorylation of the AGC1-3 S269A and S596A mutants in the kinase-inactive K392Q background and the Adi3 S212A and S539A mutants in the kinase-inactive K337Q background. In A and B, the indicated proteins were incubated in an in vitro kinase assay with γ-[32P]ATP. Top panel, phosphorimage; bottom panel, Coomassie stained gel. Gray and white diamonds, form of MBP-Adi3 or MPB-AGC1-3 used in assay, respectively. Gray and white triangles, location of MBP-Adi3 or MPB-AGC1-3, respectively . 5μg of MPB-Adi3 and 3 μg of MPB-AGC1-3 was used in the assay. (A) AGC1-3 autophosphorylation. (B) Adi3 autophosphorylation.

An alignment of the Adi3 and AGC1-3 protein sequence shows that Ser212 of Adi3 aligns with that of AGC1-3 Ser269 (Figure 15B). As with AGC1-3 Ser269, the sequence surrounding Adi3 Ser212 is similar to that around the conserved Ser539 activation loop *Sl*Pdk1 site (Figure 15B) suggesting this may be an *Sl*Pdk1 phosphorylation site. The contribution of Ser212 toward *Sl*Pdk1 phosphorylation of Adi3 was tested using in vitro kinase assays. As with AGC1-3 Ser269, Ser212 was mutated to Ala in the kinase-inactive Adi3^{K337Q} and Adi3$^{K337Q/S539A}$backgrounds and tested for phosphorylation by *Sl*Pdk1. These proteins did not contain autophosphorylation activity (Figure 17B) indicating that any phosphorylation when incubated with *Sl*Pdk1 could be attributed to *Sl*Pdk1. The *Sl*Pdk1 phosphorylation of Adi3$^{K337Q/S212A}$ was reduced by ~ 40% compared to Adi3^{K337Q} (Figure 18A, compare Lanes 1, 2) and the double phosphorylation site mutant Adi3$^{K337Q/S212A/S539A}$showed a ~ 74% reduction in *Sl*Pdk1 phosphorylation (Figure 18A, Lane 4).

Since we have previously shown that the Adi3^{S539D} phosphomimetic protein has increased autophosphorylation (Devarenne et al., 2006), the Adi3^{S212D} phosphomimetic protein was analyzed for increased autophosphorylation. The Adi3^{S212D} protein did not have increased autophosphorylation over that of wild-type protein (Figure 18B, Lanes 1, 2) and introducing the S212D mutation into the Adi3^{S539D} background did not increase autophosphorylation over that of the Adi3^{S539D} protein alone (Figure 18B, Lanes 3, 4).

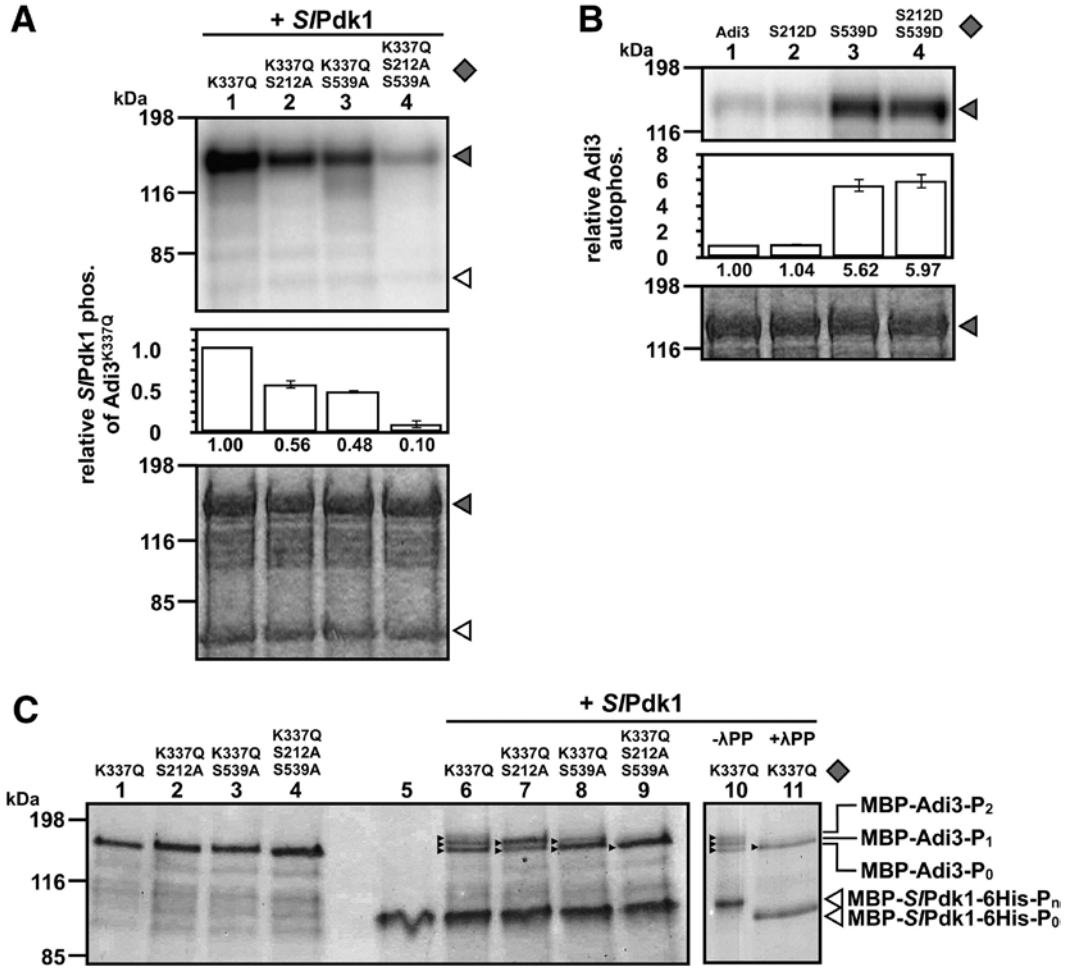

Figure 18. Evidence for Adi3 Ser212 phosphorylation by *Sl*Pdk1. In A and B, the indicated proteins were incubated in an in vitro kinase assay with γ-[^{32}P]ATP. Top panel, phosphorimage; bottom panel, coomassie stained gel; middle panel, quantification of Adi3 autophosphorylation (A) or *Sl*Pdk1 phosphorylation of Adi3 (B) from at least 3 independent assays. Average value is shown under each column. Error bars indicate standard error. Gray diamond, form of MBP-Adi3 used in assay. Gray and open triangles, location of MBP-Adi3 and *Sl*Pdk1-6His (A) or MBP-*Sl*Pdk1-6His (C), respectively. The following amounts of each protein were used in the assay: MPB-Adi3, 5 μg; MBP-*Sl*Pdk1-6His, 0.5 μg. (A) Adi3 Ser212 is phosphorylated by *Sl*Pdk1. (B) Ser212 does not contribute to Adi3 autophosphorylation. (C) Separation of *Sl*Pdk1-phosphorylated Adi3. The indicated proteins were incubated in an in vitro kinase assay with non-radiolabeled ATP followed by SDS-PAGE using a 1:200 ratio of *bis*-acrylamide:acrylamide and stained with coomassie. Different phosphorylated species of Adi3 are indicated by black arrowheads next to the band. 2 μg of both MBP-Adi3 and MBP-*Sl*Pdk1-6His was used in the assay.

These data suggest that both Ser212 and Ser539 are *Sl*Pdk1 phosphorylation sites in Adi3, there is an additional site(s) since there is still 10% of *Sl*Pdk1 phosphorylation remaining in the Adi3$^{K337Q/S539A/S212A}$ protein, and that phosphorylation of Ser212 does not contribute to Adi3 autophosphorylation.

As additional evidence that Ser212 is an *Sl*Pdk1 phosphorylation site on Adi3 we analyzed *Sl*Pdk1 phosphorylated Adi3 proteins by SDS-PAGE for the identification of Adi3 protein band shifts due to phosphorylation. The SDS-PAGE gels used in these assays contain a *bis*-acrylamide:acrylamide ratio of 1:200 rather than the standard 1:37.5 ratio. Studies from our lab and others have shown that the 1:200 gels are capable of efficiently separating phosphoproteins based on single phosphorylation events (Demmel et al., 2008; Avila et al., 2012). Adi3 proteins with the non-phosphorylatable S212A and S539A mutations in the kinase-inactive Adi3^{K337Q}background were phosphorylated by *Sl*Pdk1 and separated by 1:200 10% SDS-PAGE. The non-*Sl*Pdk1 phosphorylated proteins appeared as single protein bands (Figure 18C, Lanes 1–4), while the *Sl*Pdk1 phosphorylated proteins were separated into several different protein bands (Figure 18C, Lanes 6–9). The Adi3^{K337Q} protein appeared as three distinct protein bands (Figure 18C, Lane 6), the Adi3$^{K337Q/S212A}$ and Adi3$^{K337Q/S539A}$ proteins appeared as two distinct protein bands (Figure 18C, Lanes 7, 8), and the Adi3$^{K337Q/S2121A/S539A}$ protein appeared as a single protein band (Figure 18C, Lane 9). This would suggest that Adi3 exists in three different *Sl*Pdk1 phosphorylated forms and each Adi3 protein band corresponds to a phosphoprotein from *Sl*Pdk1 phosphorylation. The protein band seen in Adi3$^{K337Q/S212A/S539A}$ presumably contains a minor amount of *Sl*Pdk1 phosphorylation

since this protein still contains 10% of *Sl*Pdk1 phosphorylation (Figure 18A). In order to confirm these Adi3 bands as phosphoproteins, we treated *Sl*Pdk1 phosphorylated Adi3^{K337Q} with λ phosphatase to remove phosphate groups and analyzed by 1:200 10% SDS-PAGE. As seen previously, *Sl*Pdk1 phosphorylated Adi3^{K337Q} appeared as three distinct protein bands (Figure 18C, Lane 10). Treatment with λ phosphatase reduced Adi3^{K337Q} to a single protein band (Figure 18A, Lane 11). Taken together, these data indicate that the two slower migrating Adi3 bands are due to phosphorylation at Ser212 and Ser539, while the fastest migrating protein should contain a minimal amount of *Sl*Pdk1 phosphorylation. λ phosphatase treatment also shifted the migration of *Sl*Pdk1 (Figure 18C, compare Lanes 10, 11) indicating it is also phosphorylated in the assay. Interestingly, *Sl*Pdk1 did not appear as multiple phosphoprotein bands without λ phosphatase (Figure 18C, Lane 10) suggesting a single phosphorylation state for *Sl*Pdk1.

For a final piece of evidence that Ser212 is phosphorylated in Adi3 by *Sl*Pdk1 we repeated MS/MS on *Sl*Pdk1 phosphorylated Adi3^{K337Q} followed by LC–MS/MS analysis on an LTQ-Orbitrap mass spectrometer system as we previously reported (Avila et al., 2012). This analysis positively identified Ser212 phosphorylation (Figure 19), and altogether the data presented indicate that Ser212 is a second *Sl*Pdk1 phosphorylation site on Adi3.

3.6 The phosphomimetic mutation of Ser212 and Ser539 contributes to full Adi3 phosphorylation of Gal83

Since the phosphomimetic proteins Adi3^{S212D} or Adi3$^{S212D/S539D}$ did not affect Adi3 autophosphorylation, we analyzed the contribution of

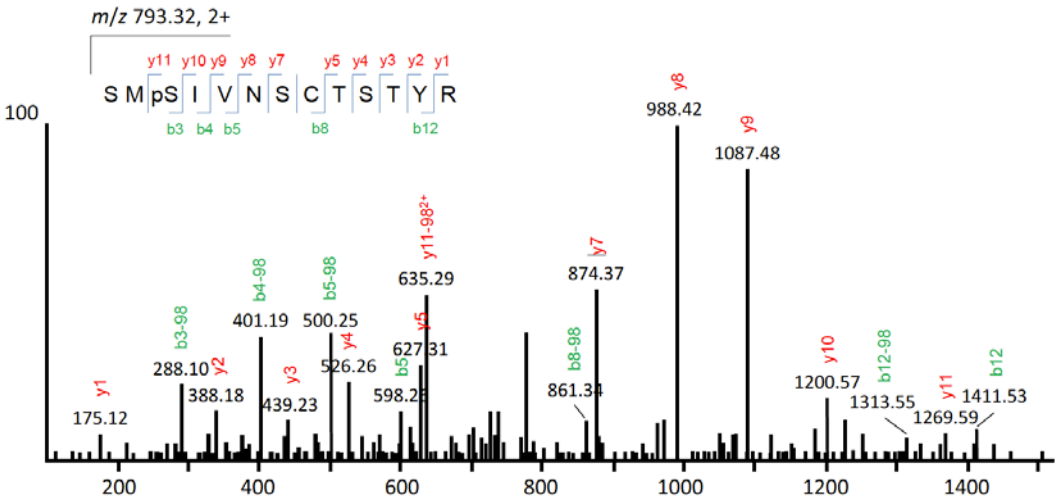

Figure 19. MS/MS spectra of Ser212 of Adi3. Trypsin digestion of the kinase inactive, bacterially expressed Adi3 phosphorylated by bacterially expressed Pdk1 results in a phosphorylated peptide. Analysis of this phosphorylated peptide indicates that the 3rd amino acid from the N-terminus, a serine, is phosphorylated. Analysis of full-length Adi3 protein sequence reveals that this site corresponds to Ser212. This peptide has other residues that could be phosphorylated by Pdk1 – Ser1, Ser7, Thr9, Ser10, and Thr11 however this spectra indicates that those residues are not phosphorylated by Pdk1.

Ser212 toward phosphorylation of an Adi3 substrate. We have previously shown that Adi3 phosphorylates Gal83, the β-subunit of the tomato SnRK1 protein complex, at Ser26 (Avila et al., 2012) and (Dittrich and Devarenne, 2012). The SnRK1 protein complex regulates metabolism under numerous situations including resistance to pathogens (Halford et al., 2003) and (Halford and Hey, 2009), and the β-subunits of this complex control cell localization, substrate specificity, and complex activity (Mitchelhill et al., 1997; Vincent and Carlson, 1999; Vincent et al., 2001; Warden et al., 2001). We have shown that Adi3 phosphorylation of Gal83 inhibits SnRK1 activity (Avila et al., 2012).

The double Adi3$^{S212D/S539D}$phosphomimetic mutant protein has similar activity on Gal83 as Adi3 that has been fully phosphorylated by *Sl*Pdk1. Phosphorylation of Gal83 by Adi3^{S212D} showed a twofold increase in Gal83 phosphorylation over wild-type Adi3 (A, compare Lanes 2 and 3), but did not phosphorylate Gal83 as strongly as Adi3^{S539D} (A, compare Lanes 3 and 4). The double phosphomimetic mutant Adi3$^{S212D/S539D}$ showed a large fourteen fold increase in Gal83 phosphorylation over wild-type Adi3 (A, compare Lanes 2 and 5), and had more Gal83 phosphorylation than either single phosphomimetic mutant (A, compare Lanes 3, 4. 5). This would suggest that phosphorylation of Ser212 contributes Adi3 substrate phosphorylation.

Our data indicate that there is an additional *Sl*Pdk1 phosphorylation site(s) on Adi3 other than Ser212 and Ser539 (Figure 18A), suggesting that this additional phosphorylation site(s) may be required for full phosphorylation of substrates by Adi3. This was tested by comparing the ability of Adi3$^{S212D/S539D}$ and *Sl*Pdk1 phosphorylated

wild-type Adi3 to phosphorylate Gal83. For this assay, one sample contained Adi3$^{S212D/S539D}$ incubated with Gal83 as in Figure 20A, while in another, wild-type Adi3 was incubated first with *Sl*Pdk1 so that Adi3 would be fully phosphorylated, and then Gal83 was added to the assay. The results showed that Adi3$^{S212D/S539D}$ phosphorylated Gal83 to a similar level as seen previously (Figure 20B, Lane 5), *Sl*Pdk1 could not phosphorylate Gal83 (Figure 20B, Lane 6), and the pre-*Sl*Pdk1-phosphorylated Adi3 phosphorylated Gal83 to roughly the same level as Adi3$^{S212D/S539D}$ (Figure 20B, Lane 7). The level of *Sl*Pdk1 phosphorylation of Adi3^{K337Q} was not affected by the incubation with Gal83 (Figure 20B, Lane 8). This would indicate that *Sl*Pdk1 phosphorylation of both Adi3 Ser212 and Ser539 is sufficient for full Gal83 phosphorylation and that any additional *Sl*Pdk1 phosphorylation sites on Adi3 do not significantly contribute to Gal83 phosphorylation.

3.7 Phosphorylation and nuclear localization of AGC1-3 is correlated to cell viability

As mentioned previously, studies of an Adi3 mutant with the activation loop extension deleted led to the identification of a nuclear localization sequence (Ek-Ramos et al., 2010). Transient expression of the Adi3 mutant with the activation loop extension deleted, as well as the activation loop serine mutated to alanine, reduced cell viability to ~18%, approximately 30% of the empty vector control (Ek-Ramos et al., 2010). Transient expression of Adi3 with point mutations within the activation loop extension (K506A/K509A) reduced cell viability to ~30%, which was ~50% of the empty vector control (Ek-Ramos et al., 2010).

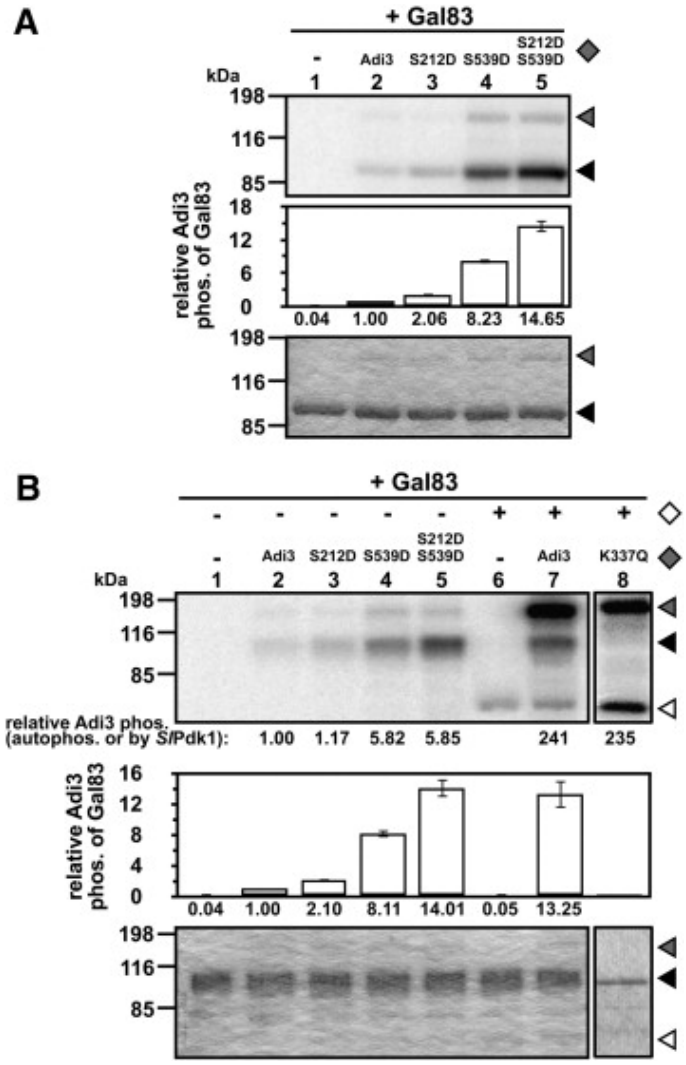

Figure 20. Activation of Adi3 kinase activity toward Gal83 through Ser212 and Ser539 phosphorylation. In A and B, the indicated proteins were incubated in an in vitro kinase assay with γ-[^{32}P]ATP. Top panel, phosphorimage; bottom panel, coomassie stained gel. Middle panel, quantification of Gal83 phosphorylation by Adi3 from at least 3 independent assays. Average value is shown under each column. Error bars indicate standard error. Gray diamond, form of MBP-Adi3 used in assay; open diamond, presence or absence of *Sl*Pdk1-6His. Gray, black, and open triangles, location of MBP-Adi3, MBP-Gal83, and *Sl*Pdk1-6His, respectively. The following amounts of each protein were used in the assay: *Sl*Pdk1-6His, 0.2 μg; MPB-Adi3, 0.4 μg; MBP-Gal83, 2 μg. (A) The Adi3$^{S212D/S539D}$ phosphomimetic mutant has increased kinase activity toward Gal83 compared to the single S212D and S539D phosphomimetic mutants. (B) Mutating either Ser212 or Ser539 to the phosphomimetic Asp increases Adi3 phosphorylation of Gal83.

Cellular fractionation and microscopy studies with a GFP fusion of the non-phosphorylatable activation loop extension deletion mutant, as well as a GFP fusion of the K506A/K509A mutant showed exclusion of the GFP signal from the nucleus and localization to many punctate cellular structures that are membranous in nature and resemble endosomal vesicles (Ek-Ramos et al., 2010). When the activation loop extension deleted mutant was then mutated at the activation loop serine to resemble a constitutively active Adi3, cell viability increased to a level slightly higher than the empty vector control, and microscopy and fractionation studies indicated that Adi3 localization was shifted back to the nucleus (Ek-Ramos et al., 2010). From these data, it is clear the nuclear localization signal within the activation loop extension and phosphorylation of the activation loop serine are both important for subcellular localization and cell viability. The NLS within the activation loop extension is conserved between Adi3 and AGC1-3 (Figure 21A). Studies were undertaken to determine how mutations of the AGC1-3 NLS and activation loop serine impact *Arabidopsis* protoplast cell viability and AGC1-3 localization. As expected, transient expression of the wild type AGC1-3 was distributed throughout the cell and did not reduce cell viability relative the empty plasmid control (Figure 21B & C). However, cell viability was reduced in the NLS, non-phosphorylatable triple mutant – K562A/K565A/S596A to ~45% or around 70% of the empty plasmid control (Figure 21B). The GFP fusion of the K562A/K565A/S596A triple mutant was localized to small punctate cellular structures, similar to Adi3 (Figure 21C). When a constitutively active, NLS mutant of AGC1-3 (K562A/K565A/S596D) was transiently expressed, cell viability was approximately

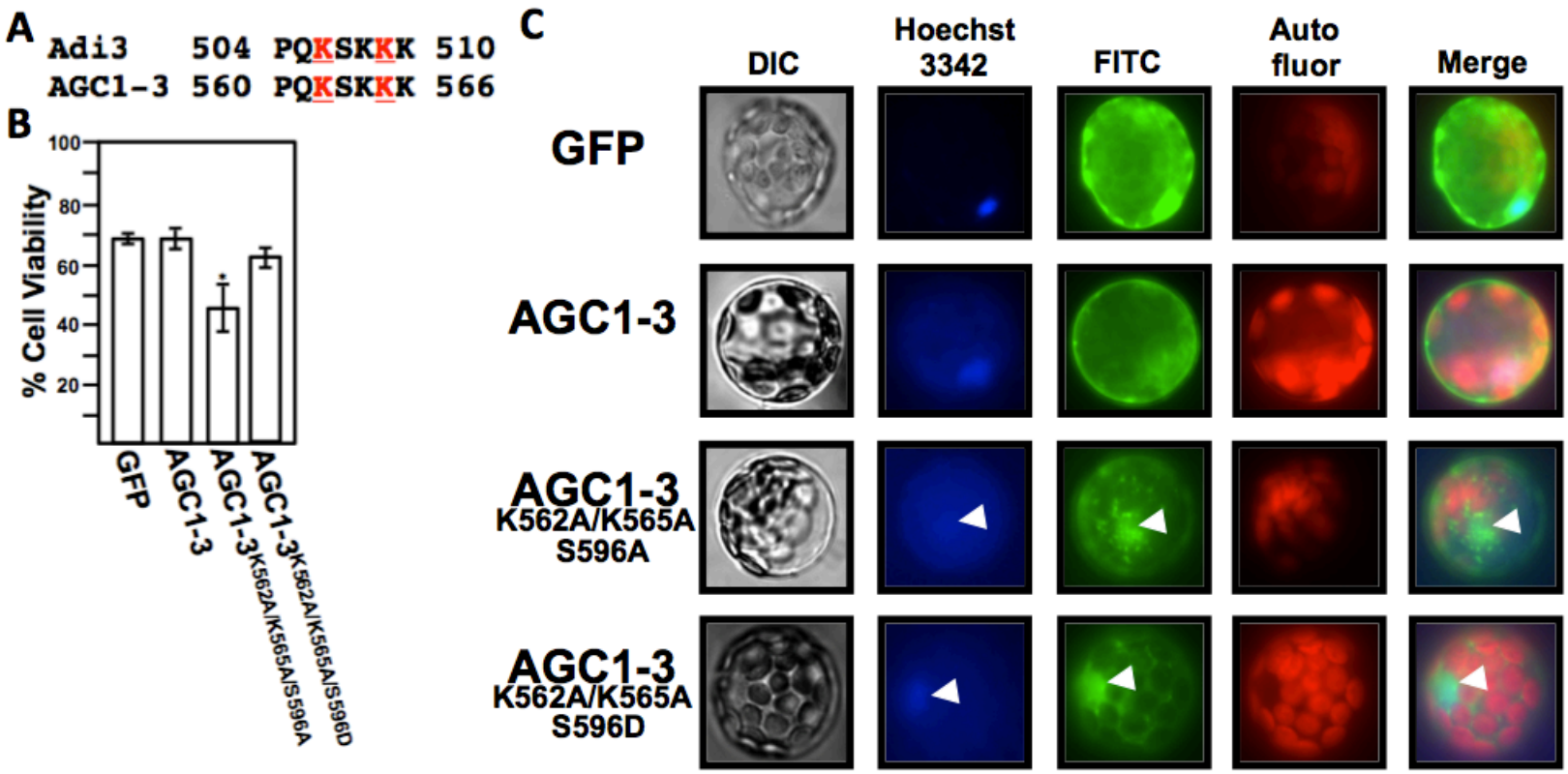

Figure 21. Subcellular localization and cell viability studies of AGC1-3. White arrows are used to indicate the nucleus in the field using the nuclear DNA stain Hoechst 3342, the FITC field, as well as the images of the autofluoresence/FITC merge. *A*, The conserved NLS within the activation loop extension of Adi3 and AGC1-3. *B*, Cell viability of protoplasts, expressing GFP-AGC1-3 NLS and activation loop mutants – cells were analyzed by Evan's blue stain of dead cells, 24hr post-transfection. *C*, Protoplasts were analyzed 24hr post-transfection for subcellular localization.

65% - essentially a ~5% reduction compared to the empty vector control (Figure 21B). GFP analysis of the K562A/K565A/S596D triple mutant indicated that expression of AGC1-3 appeared to be found in the nucleus (Figure 21C).

These results indicate that the NLS and activation loop serine are involved in localization of AGC1-3 to the nucleus. Similarly the NLS and activation loop serine are relevant to cell viability in *Arabidopsis* protoplasts. It appears that cell viability control by AGC1-3 is similar to Adi3, as are subcellular localization patterns (Ek-Ramos et al., 2010).

3.8 Other AGC VIIIa kinases have multiple Pdk1 phosphorylation sites

Considering that AGC1-3 and Adi3 have a phosphorylation site very similar to their activation loop motif, we analyzed other members of the AGC VIIIa subfamily to determine if they also have a second activation-loop-like Pdk1 phosphorylation site. Sequence analysis did not yield any obvious residues to investigate however the second AGC1-3/Adi3 site was not identified until mutagenesis studies were conducted. In a result similar to Adi3, a previous study with the rice AGC kinase Oxi1, non-activation-loop Pdk1 phosphorylation was observed but not identified (Matsui et al., 2010).

Despite the lack of obvious additional Pdk1 phosphorylation sites based on sequence analysis and alignment, AGC1-4 and AGC1-7 were selected for further analysis (Figure 22). Of the VIIIa subfamily, AGC1-4 at 55% identity is the closest relative of AGC1-3. In comparison, AGC1-7 is more distantly related but is 51% identical to AGC1-3. To determine if these proteins have additional Pdk1 phosphorylation sites they were expressed and purified as GST fusion proteins, the

Figure 22. Alignment of AGC1-3, AGC1-4, and AGC1-7. The alignment above shows AGC1-3 compared to AGC1-4 and AGC1-7. AGC1-3 and AGC1-4 are 55% identical whereas AGC1-7 and AGC1-3 are 51% identical. The activation loop serines are underlined and in red, as is the non-activation loop serine identified in AGC1-3 (Ser269). Additional AGC1-4 and AGC1-7 phosphorylation sites identified by NetPhosK are highlighted in yellow.

activation-loop serine was mutated to alanine and the ATP-binding site lysine mutated to glutamine. Using the phosphorylation site prediction tool NetPhosK (www.cbs.dtu.dk/services/NetPhosK/), several prospective phosphorylation sites were identified in AGC1-4 and AGC1-7. In the case of AGC1-4, mutation of the activation-loop residue, Ser343 eliminated virtually all phosphorylation by Pdk1 of the kinase inactive AGC1-4 mutant (Figure 23A). On the contrary, mutation of the activation-loop residue, Ser379 did not eliminate all phosphorylation of AGC1-7 by Pdk1 (Figure 23B). To narrow the scope of the search, only sites with an Arg in the -3 position upstream of the phosphorylatable residue were considered based on the Pdk1 phosphorylation motifs. Several residues were identified in AGC1-4 & AGC1-7 that had an Arg in the -3 position relative to a Ser or Thr (Figure 23C & D). The motifs surrounding the two residues identified in AGC1-4 are similar to motifs surrounding residues in AGC1-7, Thr161 and Thr455 of AGC1-4 are similar to Thr193 and Thr492, respectively, in AGC1-7 (Figure 23C & D). Considering that AGC1-4 is not phosphorylated outside of the activation loop serine and AGC1-7 is, Thr193 and Thr492 are unlikely to be phosphorylated by Pdk1 (Figure 23D). The residues that meet the -3 Arg criteria in AGC1-7 are Ser109 and Thr472 and thus are prospective Pdk1 phosphorylation sites. Although investigation of non-activation loop Pdk1 phosphorylation sites within other AGC VIIIa protein kinases concluded without identifying those residues, Ser109 phosphorylation was reported in a recent phosphoproteomic analysis of mature *Arabidopsis* pollen (Mayank et al., 2012). In comparison to other AGC VIIIa protein

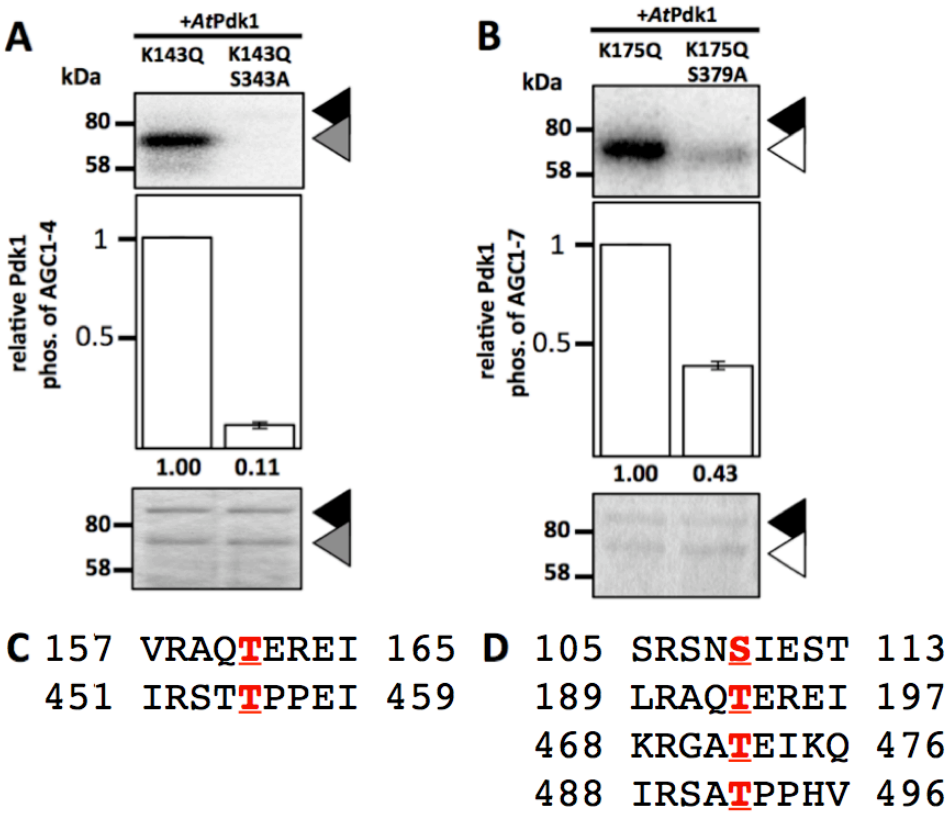

Figure 23. Pdk1 phosphorylation of AGC1-4 and AGC1-7 reveals additional phosphorylated residues. In the above figure, kinase inactive mutants of AGC1-4 and AGC1-7 are mutated at their activation loop serine by *At*Pdk1. *A*, phosphorylation of AGC1-4 (gray arrows) by Pdk1 (black arrows) is reduced by ~90% when the activation loop serine is mutated to the non-phosphorylatable alanine. The possibility remains that AGC1-4 is phosphorylated at other residues by Pdk1 however these residues are relatively insignificant to the overall phosphorylation of AGC1-4 by Pdk1. *B*, phosphorylation of AGC1-7 (white arrows) by Pdk1 (black arrows) is reduced by only ~60% indicating that other residues are phosphorylated by Pdk1. *C* & *D*, potential residues phosphorylated by Pdk1 in AGC1-4 and AGC1-7 respectively.

kinases, Ser109 of AGC1-7 resembles the activation loop serines of AGC1-8, AGC1-9, and KIPK all are preceded by RSN like AGC1-7. Although this non-activation loop phosphorylation site is phosphorylated *in vivo*, whether or not Pdk1 is responsible is unknown.

3.9 Discussion

The data presented here identify a second *Sl*Pdk1 phosphorylation site in Adi3, Ser212, that is required for full phosphorylation of the Gal83 substrate. Initially, we identified Ser212 by comparison with AGC1-3, the *Arabidopsis* sequence homologue to Adi3, and subsequently phosphorylation of Ser212 was identified by MS/MS. Previously, high-throughput studies of *Arabidopsis* suspension cells treated with the flagellin peptide, *flg22* implicated Ser137 and/or Ser138 as phosphorylated on AGC1-3 (Nakagami et al., 2010). Our studies indicate that *At*Pdk1 does not phosphorylate Ser137 and/or Ser138, *in vitro*. Studies regarding AGC1-3's role in cell death regulation, cellular localization, and substrate identification are ongoing. However initial evidence supports AGC1-3 as the functional homologue of Adi3. Addition experiments of this nature are ongoing, however we have not been successful in obtaining a T-DNA knockout line of AGC1-3, suggesting that a homozygous knockout of AGC1-3 may be lethal (not shown). This would support, but is not conclusive of a function for AGC1-3 similar to Adi3 in cell death suppression. Identification of AGC1-3 substrates would also help to gauge the function of this kinase. Experiments are currently ongoing toward this end. Once AGC1-3 substrates are identified, it will be of importance to test the

contribution of Ser269 phosphorylation toward substrate phosphorylation for comparison with Adi3.

Similar to Adi3, there appears to be a correlation between cell-death suppression, subcellular localization of AGC1-3, activation-loop phosphorylation, and the NLS of AGC1-3 (Figure 21). Previous work has supported AGC1-3 as a dynamic protein, a phosphoproteomic analysis of cultured *Arabidopsis* cells treated with *flg22*, AGC1-3 was located at the PM and phosphorylated at the activation loop serine (Nuhse et al., 2007). Meanwhile, in a study of protein movement in response to cold treatment, a fragment of AGC1-3 was identified in isolated nuclei in a 2-D gel (Bae et al., 2003). With the small amount of AGC1-3 publicly available data and localization data these from these GFP-AGC1-3 studies, AGC1-3 appears to be a dynamic protein with differential localization and phosphorylation states.

We also observed that the Ala mutation of AGC1-3 activation site (S596) eliminated autophosphorylation activity (Figure 13B), while we have previously seen that the Adi3 activation site Ala mutation (S539A) does not eliminate autophosphorylation (Devarenne et al., 2006) and (Ek-Ramos et al., 2010). Differences in the effects of activation site Ala mutation in mammalian AGC kinases also range from inactivation to no effect on catalytic activity. For example, the activation site Ala mutations in PKCα and β isotypes produce an inactive protein, while in the PKCδ isotype the activation site Ala mutation maintains activity (Parekh et al., 2000) and (Stempka et al., 1997). Thus, it appears that the plant AGC kinases contain many of the properties that have been seen in mammalian AGC kinases.

Our data also indicate that there is an additional Pdk1 phosphorylation site(s) on Adi3 that accounts for approximately 10% of the total Pdk1 phosphorylation. Given the difficulty we have experienced in identifying Adi3 peptides by MS/MS, it seems that other conventional methods such as Ala scanning mutagenesis and/or phosphopeptide mapping may be useful in this effort. Since our studies have shown that Ser539 and Ser212 are required for full substrate phosphorylation by Adi3, any additional Pdk1 phosphorylation sites on Adi3 may be involved in stabilizing the Adi3 protein, controlling Adi3 autophosphorylation, or regulating phosphorylation of substrates other than Gal83. It should also be noted that it still needs to be determined if these Adi3 residues are phosphorylated by Pdk1 in plant and if they have the same function in vivo as we have shown here by in vitro assays.

It is interesting to note the differences seen here for a plant AGC kinase compared to mammalian AGC kinases. The three main phosphorylation sites found on mammalian AGC kinases (activation site, PIF site, turn motif site) are all phosphorylated by different kinases and each has a different role in AGC kinase regulation (Pearce et al., 2010) and (Hauge et al., 2007). In the case of plants, or at least for Adi3, AGC1-3, and AGC1-7, it appears that Pdk1 is responsible for the multiple phosphorylation events on AGC kinases and at least two of these are required for full kinase activity on substrates. It will be of importance to determine all Pdk1 phosphorylation sites on Adi3 and determine their roles in activity or conformation stabilization.

CHAPTER IV

IDENTIFICATION OF AGC1-3 SUBSTRATES

4.1 Identification of AGC1-3 and AGC1-3^{S596D} substrates with the KiC assay

In order to define other components involved in the signaling regulated by AGC1-3, a collaboration with Nagib Ahsan, a post-doctoral researcher in Dr. Jay Thelen's lab at the University of Missouri, was established. Using both the wild type AGC1-3 and the constitutively active mutant AGC1-3^{S596D} in the KiC assay, substrate peptides were identified along with their corresponding full-length proteins. Any substrates of AGC1-3 are also potential substrates of Adi3, thus data derived from studies with AGC1-3 will also potentially benefit Adi3 signaling.

4.2 Autophosphorylation of AGC1-3

Prior to peptide library screening with the KiC assay, AGC1-3 and AGC1-3^{S596D} were assayed to identify auto-phosphorylation sites of each respective protein. After incubation with ATP, each protein was trypsin digested and analyzed by MS/MS. When incubated with ATP, AGC1-3 auto-phosphorylates at two residues, Ser^{516} and Thr^{518} (Figure 24). On the contrary, MS/MS analysis did not support AGC1-3^{S596D} auto-phosphorylation of Ser^{516} and Thr^{518}; however it did support phosphorylation of Ser^{81} and Ser^{131} (Figure 25). All four of these phosphorylation sites are unique and are not present in the PhosPhAt database.

4.2 Peptides phosphorylated by AGC1-3

Using the KiC assay, a total of 26 peptides were identified as potential substrates of wild type AGC1-3

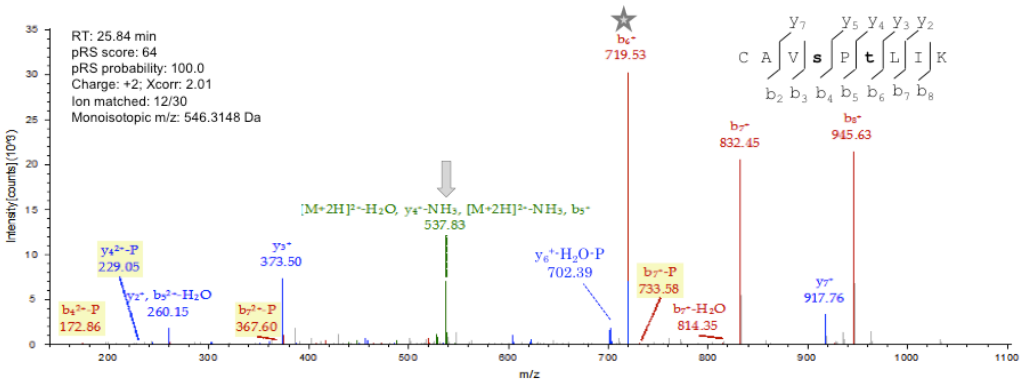

Figure 24. MS/MS spectra of auto-phosphorylation of AGC1-3. Trypsin digestion of the wild-type, bacterially expressed AGC1-3 phosphorylates itself at several residues. Analysis of this phosphorylated peptide indicates that the 4th amino acid from the N-terminus, a serine, is phosphorylated. Likewise, the 5th amino acid from the N-terminus, a threonine, is phosphorylated. These two phosphorylated residues correspond to Ser516 and Ser518.

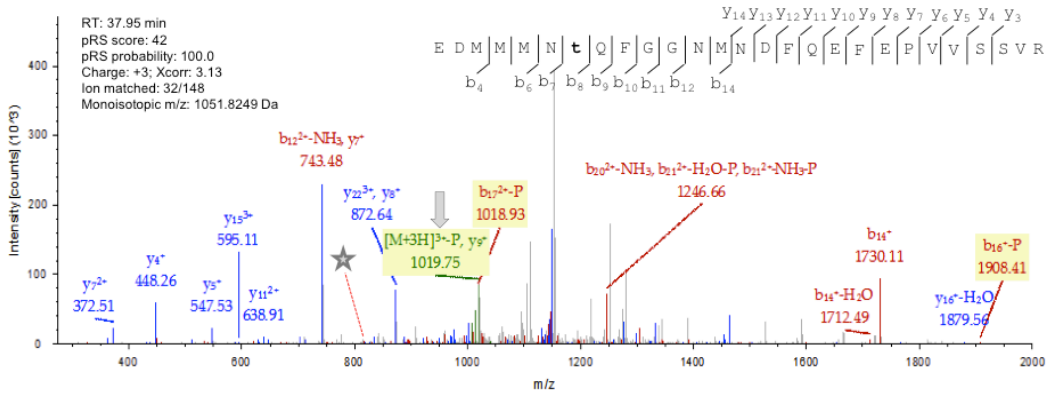

Figure 25. MS/MS spectra of auto-phosphorylation of AGC1-3^{S596D}. Trypsin digestion of the constitutively active, bacterially expressed AGC1-3 phosphorylates itself at one residue. Analysis of this phosphorylated peptide indicates that the 7th amino acid from the N-terminus, a threonine, is phosphorylated. Thr7 in this peptide corresponds to Thr81 in the full-length AGC1-3 protein.

(Table 2). All peptide sequences were subjected to BLASTp searches of the *Arabidopsis* genome. From the BLASTp searches, AGIs (Arabidopsis Genome Identification) were identified, with their annotated genes. The PhosPhAt database was searched to determine if *in vivo* MS data was available for any of the candidate proteins (http://phosphat.mpimp-golm.mpg.de). The PhosPhAt database is a collection of *Arabidopsis* MS data collected from publications as well as unpublished data. Of the 26 AGC1-3 phosphorylated peptides in the KiC dataset, all but 2 of the proteins have supporting data from PhosPhAt. Of the 24 remaining peptides, 19 have at least one phosphorylated residue identified in the KiC assay that is also found in the PhosPhAt database (Table 2). Although AGC1-3 is a Ser/Thr kinase, 5 KiC peptides have phosphorylated tyrosines and one of those 5 is present in the PhosPhAt database (Table 2). The protein in question is a GDSL-like lipase/acylhydrolase with a Thr phosphorylated immediately before the phosphorylated Tyr (At3g62280). Thus although unexpected, AGC1-3 could possibly phosphorylate tyrosines on certain substrates.

4.3 19 peptides are phosphorylated by AGC1-3^{S596D}

The same protocol was used for peptides phosphorylated by AGC1-3^{S596D} – first a BLASTp search, then followed by PhosPhAt searches. All of the 19 peptides phosphorylated by AGC1-3^{S596D}, 11 had PhosPhAt results indicating the phosphorylated residue from the KiC assay is also phosphorylated within the PhosPhAt database (Table 3). In a result similar to the wild type protein, several of the phosphorylated peptides have phosphorylated tyrosines. Of the five that have phosphorylated tyrosines, the peptide that appears to be phosphorylated by

Table 2. AGC1-3 phosphorylated peptides. The peptides identified as being phosphorylated by AGC1-3 as well as their *Arabidopsis* genome identifiers, if the protein is phosphorylated according to data in the PhosPhAt database, as well as the peptide in the PhosPhAt database. Phosphorylated residues are identified in bold red font.

Peptide	AGI	Annotation	PhosPhAt	PhosPhAt Peptide
SRMEKAAEQGSALAAAVEGV	At3g52950	CBS/octicosapeptide/Phox/Bemp1	No	Not Covered
AAL**S**KTFKSPIVDTIQSL	At2g29680	Cell division control 6	No	Not Covered
SRDLGSVAN**S**PPRV**T**VT	At3g18630	Uracil DNA glycosylase	Yes	DLGSVAN**S**PPR
EHLKM**T**Y**Y**LSPYLDSLSPNF	At3g62280	GDSL-like lipase/acylhydrolase	Yes	M**T**Y**Y**L**S**P**Y**LD**S**L**S**PNFK
VRPI**S**PKSPVASASAF	At2g38280	AMP deaminase - embryonic factor 1	Yes	A**S**VHGA**S**SIRK**T**G**S**FVRPI**S**PK
EVFDLELMRETQ**S**VGDE	At3g51740	Infloresence meristem receptor-like kinase 2	Yes	EEW**T**NEVFDLELMRE**T**Q**S**VGDELLNTLK
SS**S**REPFSGGSDNANYETAL	At2g19470	Casein Kinase I-Like 5	Yes	RVVD**T**S**S**REPF**S**GG**S**DNAN**Y**E**T**ALK
PMNKPVEKVGS**T**EEIE	At3g04820	Pseudouridine synthase family protein	Yes	VG**ST**EEIEDESMK
FESAAL**S**LKDV**S**PGNVM	At5g35910	Polynucleotidyl transferase	Yes	DV**S**PGNVMDK
EYPDRMMM**T**F**S**VFPS	At5g44340	beta-tubulin	Yes	MMM**T**FSVFPSPK
MVTREASLEG**Y**QLLN	At5g45275	Major facilitator superfamily	No	EA**S**LEGYQLLNDDVVR
E**T**L**T**LRQSSFGSKCEL	At3g23890	Topoisomerase II	Yes	E**T**LTLRQ**S**SFGSK
LADEVKEPL**T**IEDAVL	At5g35750	Histidine Kinase	Yes	EPL**T**IEDAVLK
QPRNISGSMQSPR**S**PSS	At5g06140	Arabidopsis thaliana sorting nexin 1	Yes	**S**P**S**S**H**P**Y**LSVSVTDPVK
VRRSLSLNFDS**Y**PEDE	At2g31270	Cyclin dependent kinase	No	**S**L**S**LNFDSYPEDER
TVSSDGRQ**T**PTVQIPR	At5g50020	DHHC-type zinc finger	Yes	NSHPPEEELCYDTTVSSDGRQ**T**PTVQIPR
TSAGVRGSPNN**Y**FR**S**EGQN	At3g02180	Spiral1-like 3	No	TSAGVRG**S**PNNYFR
MMKEIQRNPSNLNL**Y**LQ	At1g62740	HOP2	No	NP**S**NLNLYLQDQR
LQNLAGQR**S**DVLENLTPN	At4g26110	Nucleosome assembly protein 1	Yes	LQNLAGQR**S**DVLENLTPNVR
AKIQVDDDVI**S**LDGMDPLR	At1g77110	Auxin efflux carrier	Yes	IQVDDDVI**S**LDGMDPLRTETETDVNGR
LYEYKGFVADD**S**DIESPR	At5g19390	REN1 - Rho GTPase activating protein	Yes	GFVADD**S**DIE**S**PRDTNGPR
AQERGVPVT**S**SQNGDALRAM	At2g01180	Phosphatidic acid phosphatase	Yes	GVPVTS**S**QNGDALR
IIDG**S**PPP**S**PK	At2g37340	Zinc-knuckle protein 33	Yes	IIDG**S**PPP**S**PK
I**T**S**S**DIKLEGAV**T**S**S**DIEAR	At1g04860	Ubiquitin-specific protease 2	No	SLNNLA**S**S**S**DIEDQCSGSGSITSDIKLEGAVT**S**DIEAR
KSVVEL**T**NG**S**SEDGRELS	At1g54080	Oligouridylate-binding protein 2	Yes	**S**VVEL**T**NG**S**S**S**EDGR
SYTTVR**T**LL**S**ILRISAA	At4g02060	Minichromosome maintenance	Yes	**T**LL**S**ILRISAALAR

Table 3. Peptides phosphorylated by AGC1-3^{S596D}. Peptides phosphorylated by the constitutively active mutant of AGC1-3. 19 peptides are phosphorylated by AGC1-3^{S596D} and 11 of the peptides have supporting data available in the PhosPhAt database.

Peptide	AGI	Annotation	PhosPhAt	PhosPhAt Peptide
SRMEKAAEQGSALAAAVEGV	At3g52950	CBS/octicosapeptide/Phox/Bemp1	No	Not Covered
AALSKTFKSPIVDTIQSL	At2g29680	Cell division control 6	No	Not Covered
SMGASTLQATSPKKAAG	At1g01550	BYPASS1 – auxin transport inhibitor	No	SMGASTLQATSPK
RPVDLYKAIFSDDSEDDE	At5g23080	TATA binding protein interacting protein	No	Not Covered
EHLKMTYLSPYLDSLSPNF	At3g62280	GDSL-like lipase/acylhydrolase	Yes	MTYLSPYLDSLSPNFK
NLFGAYSNGGESANKRQ	At1g14850	Similar to nucleoporin	No	NLFGAYSNGGESANK
LADEVKEPLTIEDAVL	At5g35750	Histidine kinase	Yes	EPLTIEDAVLK
VTWTAMVSGGYLRSKQLSI	At2g35030	Pentatricopeptide repeat	Yes	NVVTWTAMVSGYLRSK
RTDAHYLLYIADSLTTEL	At2g32415	Polynucleotidyl transferase	No	YARTDAHYLLYIADSLTTELK
VTRDKTAVGSOENAPAK	At1g12000	Pyrophosphate dependent PFK	Yes	DLTAVGSPENAPAK
MVTREASLEGYQLLN	At5g45275	Major facilitator superfamily	No	EASLEGYQLLNDDVVR
VRPISPKSPVASASAF	At2g38280	AMP deaminase	Yes	TGSFVRPISPK
VSSSNGGNGYPSISEKFG	At5g18500	Protein kinase	Yes	VDEVSSSNGGNGYPSISEK
GAPSSSGGVSGGDELIRITY	At3g48760	DHHC zinc finger	Yes	HGAPSSSGGVSGGDELIR
HVSTVVKGTPGYLDPEY	At1g06840	LRR protein kinase	Yes	GTPGYLDPEYFLTHQLTDK
AQERGVPVTSSQNGDALRAM	At2g01180	Phosphatidate phosphatase	No	GVPVTSSQNGDALR
NQTPTQSVVSAPTSTL	At1g75990	26S Proteasome Regulatory Subunit S3	Yes	DNQTPTQSVVSAPTSTLQNLK
MNDLLKGSFELPRGQSS	At5g08080	Syntaxin of plants 132	Yes	MNDLLKGSFELPR
AKIQVDDDVISLDGMDPLR	At1g77110	Auxin efflux carrier	Yes	IQVDDDVISLDGMDPLRTETETDVNGR

AGC1-3^{S596D} happens to be the same peptide phosphorylated by AGC1-3 - a GDSL-like lipase/acylhydrolase (At3g62280).

4.4 AGC1-3^{S596D} phosphorylates pyrophosphate-dependent phosphofructokinase

One peptide identified in the KiC screen for peptides phosphorylated by AGC1-3^{S596D} was a 17 amino acid peptide, phosphorylated at two residues, Thr2 and Thr6 (Figure 26). A BLASTp search of the *Arabidopsis* genome presents a 100% hit for pyrophosphate dependent phosphofructokinase (PFP) (At1g12000) (Table 3). The two residues implicated, Thr2 and Thr6 of the peptide, correspond to Thr8 and Thr12 of the full-length protein. A search for this protein in the PhosPhAt database reveals phosphorylated peptides. Two different phosphoproteomic analyses identified Thr12 and Ser16 phosphorylation, but none of the reported peptides covered Thr8 (Reiland et al., 2009; Reiland et al., 2011).

Although the peptide data from the KiC assay implicates PFP as an AGC1-3 substrate, the full-length protein must be assayed to confirm phosphorylation by AGC1-3. For these studies, AGC1-3 was incubated with a GST-PFP fusion protein for 60 minutes. In a parallel reaction, AGC1-3 was activated by pre-incubation with *At*Pdk1 for 30 minutes followed by the addition of GST-PFP and subsequent incubation for 30 minutes. Incubation of PFP with radiolabeled ATP produced no visible radiolabeled protein – identical to PFP with *At*Pdk1 and ATP (Figure 27, lane 1 & 4). Meanwhile, incubation of PFP with AGC1-3 and ATP produced 2-fold increase compared to the negative control (Figure 27, lane 2). The most profound difference resulted from pre-incubation of AGC1-3 with *At*Pdk1 and ATP followed by the addition of PFP

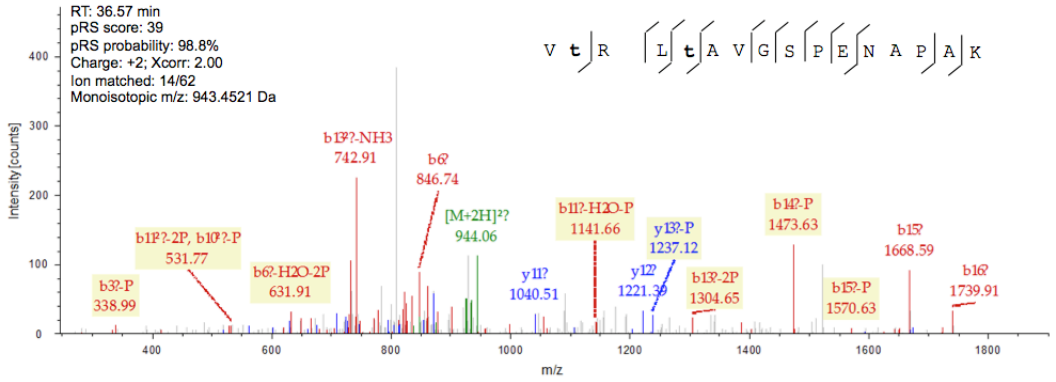

Figure 26. Mass spectra of At1g12000 peptide. The above spectra comes from the KiC assay with the constitutively active AGC1-3 and the peptide library. This peptide in particular corresponds to At1g12000 – pyrophosphate dependent phosphofructokinase (PFP). This peptide is phosphorylated at Thr2 and Thr5, which correspond to Thr8 and Thr12 in the full-length protein.

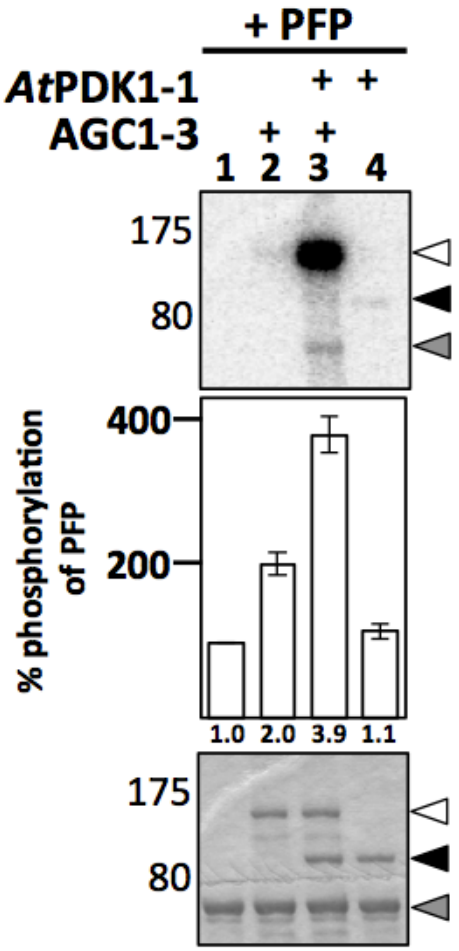

Figure 27. AGC1-3 and *At*Pdk1 activated AGC1-3 phosphorylation of PFP. The indicated proteins were incubated in an in vitro kinase assay with γ-[^{32}P]ATP. Top panel, phosphorimage; bottom panel, coomassie stained gel. Middle panel, quantification of PFP phosphorylation by AGC1-3 from at least 3 independent assays. Average value is shown under each column. Error bars indicate standard error. Open triangle, form of MBP-AGC1-3 used in assay; black triangle, presence or absence of MBP-*At*Pdk1; Gray triangle, form of GST-PFP used in assay. The AGC1-3 pre-incubated with *At*Pdk1 has increased phosphorylation of PFP, compared to PFP incubated with AGC1-3 (lane 2), PFP alone (lane 1), and PFP incubated with *At*Pdk1 (lane 4).

(Figure 27, lane 3). The peptide for PFP was found in the KiC assay with AGC1-3^{S596D} but not AGC1-3, therefore it is not particularly surprising that AGC1-3 pre-incubated with *At*Pdk1 phosphorylates PFP to a greater degree than AGC1-3 without *At*Pdk1 pre-incubation.

Based on the KiC assay, AGC1-3^{S596D} phosphorylates PFP at Thr8 and Thr12, a double mutant of PFP$^{T8A/T12A}$ was expressed and assayed with AGC1-3, pre-incubated with *At*Pdk1. The anticipated result was a total loss of phosphorylation. However, both the double mutant and wild type protein were phosphorylated at approximately the same level by AGC1-3. This result indicates that AGC1-3 phosphorylates PFP at another residue(s), though whether or not AGC1-3 phosphorylates at Thr8 and Thr12 in the full-length protein remains to be discovered; the nature of the GST-fusion conceivably precludes Thr8 and Thr12 phosphorylation.

4.5 Impact of phosphorylation on PFP activity

In order to analyze the impact of phosphorylation of Thr8 and Thr12 on PFP activity, wild type PFP and PFP$^{T8D/T12D}$ were purified as GST-fusions. PFP activity was evaluated in the same way that PFK1 activity is monitored, with slight modifications. Activity of PFP can be measured by coupling its activity to the oxidation of NADH as previously described (Kimmel and Reinhart, 2000). The only difference between the assay for PFK1 activity and PFP activity is PPi is used in place of ATP as the substrate. All of the components of the reaction were confirmed to be functional, however neither PFP nor PFP$^{T8D/T12D}$ were catalytically active (data not shown). This lack of activity is potentially attributable to the absence of a regulatory α-subunit.

4.6 Discussion

The data presented here identify a total of 26 and 19 peptides as substrates of AGC1-3 and AGC1-3^{S596D}, respectively. Annotated as a Ser/Thr protein kinase, AGC1-3 phosphorylates peptides at serines, threonines, and somewhat surprisingly, tyrosines. Of the 26 peptides phosphorylated by AGC1-3, 8 peptides are also phosphorylated by AGC1-3^{S596D}, the constitutively active mutant. While 8 peptides are substrates to both AGC1-3 and AGC1-3^{S596D}, it is somewhat surprising that there are peptides that are substrates of AGC1-3 but not AGC1-3^{S596D}. The difference in substrate peptides is surprising based on the phosphorylation of GAL83 by Adi3 and Adi3^{S539D}. It is entirely possible that some of these full-length proteins are substrates of both AGC1-3 and AGC1-3^{S596D} however the peptide was not identified in the MS/MS analysis. Ultimately if the interaction between AGC1-3 and its substrates is comparable to Adi3 and GAL83, the substrates will undergo modest phosphorylation by AGC1-3 and significantly higher phosphorylation by AGC1-3^{S596D} and AGC1-3$^{S269D/S596D}$. However the possibility does exist that AGC1-3 and AGC1-3^{S596D} are structurally different enough from one another that their substrates are unique. This, however, is worth pursuing through *in vitro* kinase assays with full-length proteins, rather than further work with peptides.

After conducting BLASTp searches of the *Arabidopsis* genome with the substrate peptide sequences, all peptides were matched to genes in the *Arabidopsis* genome. Additional analysis of the peptide sequences and full-length protein sequences in the PhosPhAt database revealed phosphopeptides for many of the substrates (Table 2 & Table 3). In many cases, the phosphopeptides identified in the KiC assay are identical

to phosphopeptides identified in previous *in vivo* phosphoproteomic studies reported in the PhosPhAt database (Nuhse et al., 2007; Nakagami et al., 2010). The presence of a phosphopeptide in both the KiC dataset and the PhosPhAt database suggests that the KiC-identified substrates could be *in vivo* substrates of AGC1-3 or AGC1-3$^{S596D.}$

After analyzing the substrate peptide sequences and the proteins that have those peptide sequences, AGC1-3 may have substrates involved in many different fundamental processes, like metabolism and transcription. In the KiC assay with AGC1-3^{S596D}, several particularly interesting proteins were identified. A 17 AA peptide, phosphorylated at Thr2 and Thr6, corresponds to the N-terminus of a 566 AA protein, pyrophosphate-dependent phosphofructokinase (PFP) (At1g12000) (detailed below in "Literature review of PFP"). The two residues implicated in the KiC assay correspond to Thr8 and Thr12 of PFP. In an *in vitro* kinase assay with AGC1-3 and AGC1-3 + *At*Pdk1, it is apparent that when activated by *At*Pdk1, AGC1-3 does phosphorylate PFP (Figure 27). In reference to the PhosPhAt database, Thr12 is phosphorylated in a peptide within the PhosPhAt database. On the contrary, no peptides in the PhosPhAt database cover Thr8. After mutagenesis of PFP to create PFP$^{T8A/T12A}$ and subsequent *in vitro* kinase assays, it is apparent that AGC1-3 activated by *At*Pdk1 does not phosphorylate those two residues (Figure 28). Although experiments have not been conducted to analyze this residue, the PhosPhAt database indicates that Ser16 is phosphorylated – whether or not AGC1-3 phosphorylates that residue remains to be seen. Currently wild-type PFP phosphorylated by *At*Pdk1 activated AGC1-3 is being analyzed by MS/MS. One possible explanation for why the PFP$^{T8A/T12A}$ protein is phosphorylated at the same level

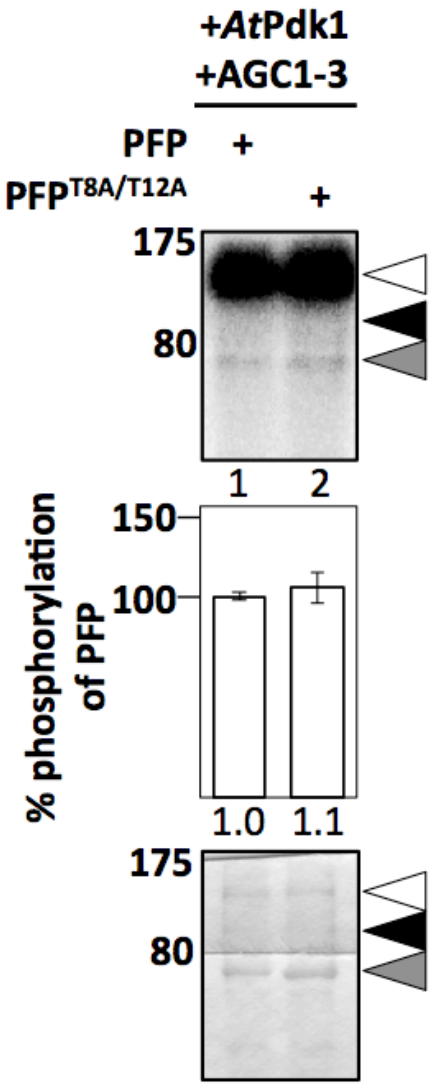

Figure 28. AGC1-3 phosphorylation of PFP and PFP$^{T8A/T12A}$. The indicated proteins were incubated in an in vitro kinase assay with γ-[^{32}P]ATP. Top panel, phosphorimage; bottom panel, coomassie stained gel. Middle panel, quantification of PFP phosphorylation by AGC1-3 from at least 3 independent assays. Average value is shown under each column. Error bars indicate standard error. Open triangle, form of MBP-AGC1-3 used in assay; black triangle, presence or absence of MBP-*At*Pdk1; Gray triangle, form of GST-PFP used in assay. AGC1-3 phosphorylation of PFP (lane 1) is comparable to phosphorylation of PFP$^{T8A/T12A}$ (lane 2).

as PFP is that PFP is expressed as a N-terminal GST-fusion protein, and since the phosphorylation sites are on the N-terminus, access to them may be impeded. Expressing PFP with an affinity-tag on its C-terminus will eliminate the possibility of N-terminal fusion protein interference. However, it is clear that since AtPdk1-activated AGC1-3 phosphorylates PFP and PFPT8A/T12A at the same level, there are other phosphorylation sites – possibly Ser16 but possibly elsewhere in the protein. Initial work into catalytic activity of PFP and PFP$^{T8A/T12A}$ was unsuccessful as no activity was observed. Once the AGC1-3 phosphorylation of PFP is resolved, experiments with PFP and the impact of phosphorylation of PFP should be resumed.

In this chapter, I have described the results of the KiC assay used to identify substrates of AGC1-3 and its constitutively active mutant AGC1-3^{S596D}. Substrates ranging from involvement in central metabolism to cell cycle control were identified in this screen. Many of the substrate phosphopeptides have supporting phosphopeptide data from *in vivo* phosphoproteomic analyses – whether or not the *in vivo* phosphorylation is done by AGC1-3 is unknown.

With AGC1-3's connection to cell-death regulation, the substrates present interesting possible narratives. For instance does, AGC1-3 phosphorylation of the gene product of At1g75990, 26S proteasome regulatory subunit S3, change proteasome activity? Likewise, does phosphorylation of PFP increase enzyme activity in an effort to deplete the cell of resources – could PFP activation be a link to the HR? Ultimately there are several additional levels to this project and successful utilization of the data

generated from the KiC assay. First and foremost, phosphorylation of these substrates must be confirmed *in vitro* and then, *in vivo*.

4.7 Supplemental literature review of PFP

4.7a Phosphofructokinase

Phosphofructokinase 1 (PFK1) is an enzyme often investigated for an insight into allostery as well as its role in glucose metabolism (Mosser et al., 2012). PFK1 produces fructose 1,6-bisphosphate (F1,6BP) by transferring the ϒ-phosphate from ATP to fructose 6-phosphate (F6P) (Mosser et al., 2012). PFK1 is a key regulatory step in glycolysis and requires ATP, F6P, and Mg^{2+} for catalysis (Mosser et al., 2012). As a regulatory step in glycolysis it is highly regulated, by a multitude of effectors. For example, it is activated by AMP and ADP, while it is inhibited by phosphoenolpyruvate (Mosser et al., 2012) (Figure 29A). F6P is also phosphorylated by the enzyme phosphofructokinase 2 (PFK2), to produce fructose 2,6-bisphosphate (F26BP) (Kotlarz and Buc, 1981) (Figure 29B). F26BP is an activator of PFK1 and is dephosphorylated by F26BPase to produce F6P, which PFK1 can once again use in glycolysis (El-Maghrabi et al., 1982). Both PFK1 and PFK2 are ATP dependent phosphofructokinases and are highly conserved in all organisms able to utilize glucose as a fuel source.

4.7b Pyrophosphate dependent phosphofructokinase (PFP)

An enzyme that is similar to PFK1 and PFK2 but not nearly as ubiquitous is pyrophosphate dependent phosphofructokinase (PFP) (Bruchhaus et al., 1996). PFP activity has been reported in a number of plants, bacteria, and algae

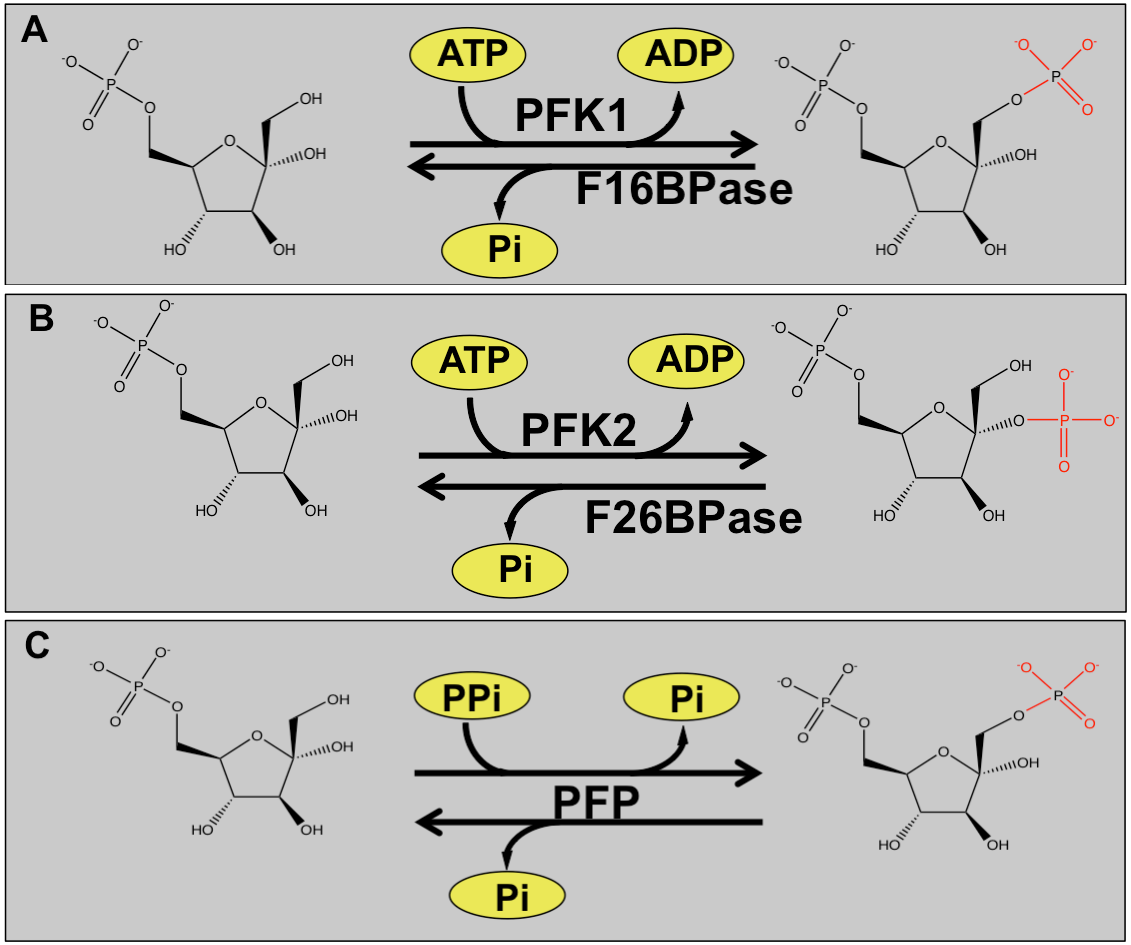

Figure 29. Catalytic activities of PFK1, PFK2, and PFP. All three of these enzymes utilize fructose 6-phosphate *A*, PFK1 and *C*, PFP both make fructose 1,6-bisphosphate, meanwhile *B*, PFK2 produces fructose 2,6-bisphosphate. The significant difference is the dephosphorylation of F16BP and F26BP rather than requiring a specific phosphatase, PFP can catalyze this reaction itself.

(Carnal and Black, 1983; Nielsen et al., 2004). One of the most profound differences between PFP and PFK1 is substrate preference. Unlike PFK1, PFP uses inorganic pyrophosphate as a substrate to phosphorylate F6P and yield F16BP (Wong et al., 1990) (Figure 29C). However that is only half of the capacity of PFP because of its ability to also utilize inorganic phosphate as a substrate in the reciprocal reaction, dephosphorylation of F16BP to produce PPi (Vincent et al., 2001) (Figure 29). Since PFP can catalyze reciprocal reactions, it is likely under strict regulation – possibly in multiple ways like PFK1 (Mosser et al., 2012).

PFP and PFK1 are quite dissimilar in primary and higher order structure, comparison of PFP (At1g12000; accession # NM_101072) and PFK1 (At4g29220; accession # NM_119066) from *Arabidopsis thaliana* reveals only 15% identity (Figure 30). The active sites of PFP and PFK1 have similarities, each is made up of 17 invariant residues (Shirakihara and Evans, 1988; Moore et al., 2002) (Figure 30). Of the 17 invariant residues, 12 of them are conserved between PFP and PFK1 (Shirakihara and Evans, 1988; Moore et al., 2002) (Figure 30). Study of PFP from the protist *Entamoeba histolytica* revealed a single active site residue was responsible for substrate specificity (Chi and Kemp, 2000). Three active site residues of PFK1 make up a DGS triplet and in PFP, that triplet is DDS (Figure 30). Mutation of *E histolytica* PFP DDS to DGS enables utilization of ATP approximately 4,000x more efficiently and essentially eliminates PPi as a substrate (Chi and Kemp, 2000). A Gly-Asp mutation is a significant mutation and produces a significant change in enzyme activity.

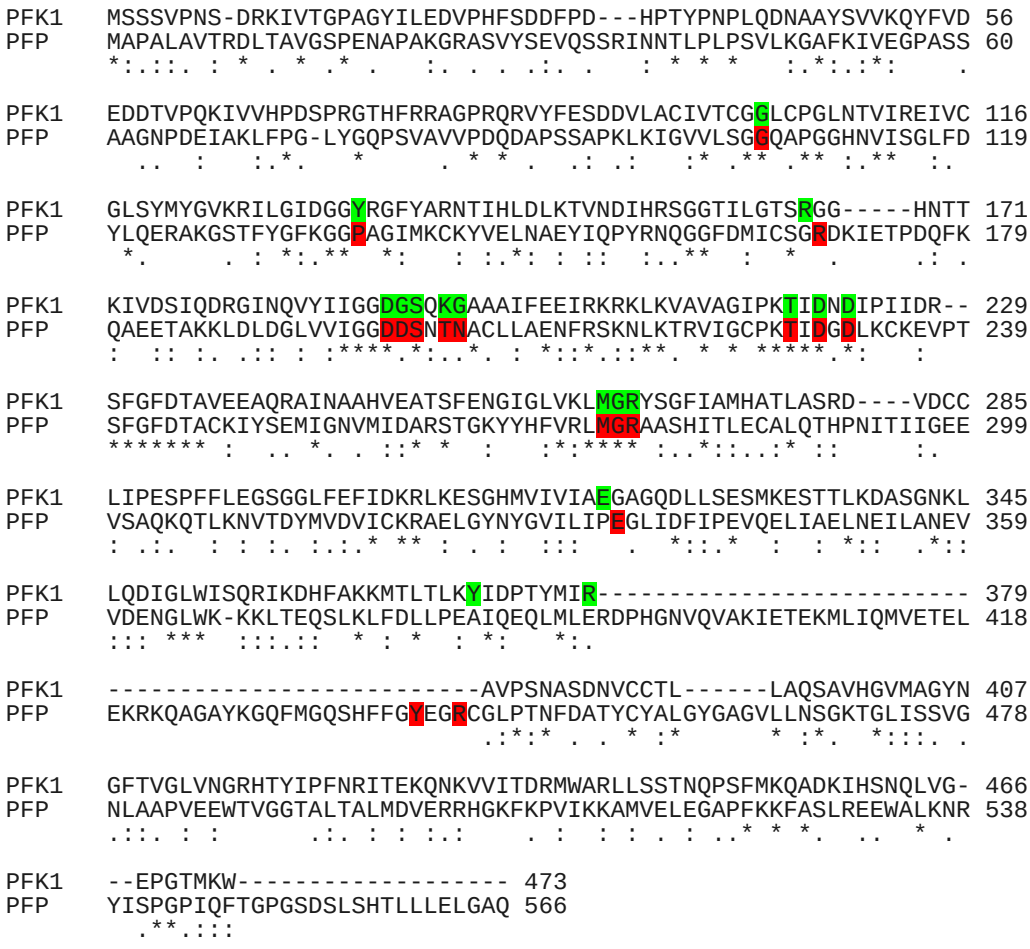

Figure 30. Sequence alignment of *Arabidopsis* PFP and PFK1. Alignment of PFK1 and PFP from *Arabidopsis thaliana*. 17 invariant residues of PFK1 are highlighted in green, 17 invariant residues of PFP are highlighted in red.

A structural comparison of PFK1 and PFP reveals that PFP is typically an $(\alpha\beta)_2$ heterotetramer or a heterodimer ($\alpha\beta$) made up of a regulatory α-subunit and a catalytic β-subunit, whereas PFK1 is more commonly a homotetramer (Carlisle et al., 1990; Moore et al., 2002). The organization of subunits is significant because bacterial PFK1 subunits make contacts that compose the active site of the enzyme (Ladror et al., 1991). Whether or not the α- and β-subunits of PFP make contacts that compose the active site is unknown.

Regarding the role(s) PFP plays in central metabolism, a consensus has yet to emerge. In the actinomycete, *Amycolatopsis methanolica*, PFP and PFK1 are both present, however their activity varies based on carbon source (Alves et al., 2001). When grown on glucose, PFP specific activity is 180mU/mg whereas PFK1 is 0mU/mg (Alves et al., 2001). Analysis of roots from plants unable to form symbiotic relationships with mycorrhizal fungi, PFP activity is significantly increased in response to phosphate starvation (Murley et al., 1998). In both of these circumstances, PFP responds to nutrient availability – altering activity based on carbon source and phosphate availability, however if these sorts of responses are universal remains to be seen.

4.7c Regulation of PFP and enzymes of central metabolism by phosphorylation

PFPs are divided into two categories, those whose activity is independent of F26BP (termed type I PFPs) and those that are activated by F26BP (termed type II PFPs) (Bruchhaus et al., 1996). In contrast, there is no subclassification of PFK1 as they are all allosterically activated by F26BP to increase flow of metabolites through glycolysis (Bruchhaus et al., 1996; Dang, 2013).

Currently there is no data regarding the impact phosphorylation has on PFP activity; protein phosphorylation, however, does have physiological relevance to PFK1 and other enzymes of central metabolism. In the mollusk *Mytilus galloprovincialis*, phosphorylation of PFK1 has been reported to increase enzyme activity three- to four-fold (Fernandez et al., 1998). On the contrary, phosphorylation of rabbit PFK1 does not appear to have any affect on enzyme activity (Foe and Kemp, 1984). It has been shown that 85kDa PFK1 from *Aspergillus niger* is proteolytically cleaved, eliminating PFK1 activity (Mesojednik and Legisa, 2005). However, PFK1 activity is recovered *in vitro* when the resulting 49kDa product is phosphorylated by protein kinase A (Mesojednik and Legisa, 2005). How often PFK1 undergoes proteolytic cleavage and subsequent phosphorylation *in vivo* is not clear, nor what conditions could produce this degradation (Mesojednik and Legisa, 2005). However, this is an additional example of phosphorylation of PFK1 activating enzyme activity. Much of the research pertaining to regulation of PFK1 is centered on inhibition/activation by metabolites like citrate and F26BP.

4.7d PFP in plants

PFP has been identified in a number of different plants including *Solanum lycopersicum*, *Zea mays*, and *Arabidopsis thaliana* (Nielsen et al., 2004; Obiadalla-Ali et al., 2004; Guo et al., 2012). Plant PFPs are class II enzymes because they are allosterically activated by F26BP (Bruchhaus et al., 1996; Nielsen et al., 2004). F26BP levels seem to introduce a highly complex control of PFP. In rice seedlings and in carrots, reduced oxygen levels lead to an increase of F26BP levels which are speculated

to activate PFP to facilitate adaptation of glycolysis to lower oxygen concentrations (Nielsen et al., 2004). In contrast, increased oxygen levels in potato tubers also result in increased F26BP levels, possibly to activate PFP (Nielsen et al., 2004). F26BP activation of PFP is not specifically directed in the gluconeogenic or glycolytic direction, in fact F26BP has been shown to activate in both directions (Nielsen et al., 2004). Ultimately the physiological role and importance of PFP remains to be clearly elucidated – however it does provide a unique metabolic alternative to ATP-driven glycolysis and gluconeogenesis.

Unlike its prokaryotic counterparts, PFP in plants exists as an $(\alpha\beta)_2$ heterotetramer consisting of regulatory (α) and catalytic (β) subunits (Moore et al., 2002). How each subunit contributes to complex activity has not been explicitly defined through *in vitro* studies, however studies of the hard-endosperm maize mutant, QPM (quality protein maize) and tomato suggest both subunits are required for enzyme activity (Wong et al., 1990; Guo et al., 2012). In warm climates, QPM is more successful than the soft-endosperm maize mutant, *opaque2*; a significant difference between QPM and *opaque2* lines is the expression level of the α-subunit of PFP (Guo et al., 2012). The significance of higher levels of the α-subunit is that in a heat stressed environment, ATP-dependent HSPs burden the cell by utilizing ATP that would otherwise be used for other cellular processes (Guo et al., 2012). While HSP levels are lower in QPM, PFP levels are elevated and induced in response to heat stress. Therefore PFP activity could reduce the ATP-requirement of glycolysis, thus enabling HSP activity without impeding central metabolism (Guo et al., 2012). Additionally, glycolytic PFP activity is increased in the

QPM endosperm while the reverse activity, dephosphorylation of F16BP, is reduced 100-fold compared to wild-type (Guo et al., 2012). QPM provides an example where the α-subunit expression is increased in an environment where the cell would benefit from increased PFP activity.

Meanwhile, the PFP heterodimer (αβ) can be purified from tomato and remains active in both glucogenic and glycolytic directions (Wong et al., 1990). When purified as individual components, the β-subunit exhibited ~70% lower specific activity than the αβ heterodimer (Wong et al., 1990). The reduced activity could be an indication that both subunits must be present for PFP activity. To date, no *in vitro* analysis of the requirements for catalytic activity have been devised but perhaps both the α- and β-subunits are required for enzyme activity. Sequence alignment of the catalytic β-subunit of PFPs from different plants (*Arabidopsis thaliana*, *Medicago truncalatula*, *Solanum tuberosum*, and *Sorghum bicolor*) demonstrates high sequence conservation, approximately 80% identical (Figure 31).

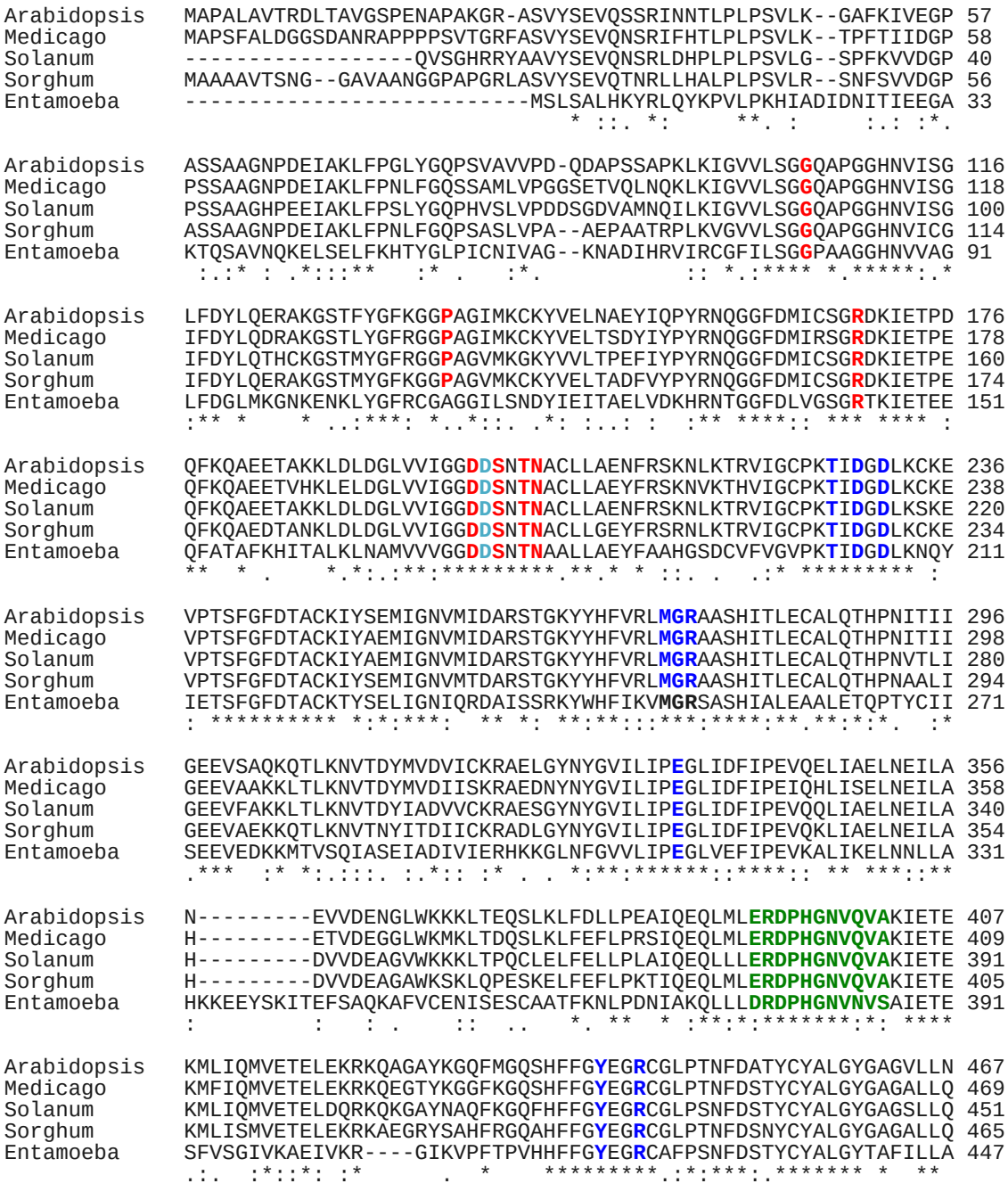

Figure 31. Alignment of 4 plant PFPs with PFP from the protist *Entamoeba histolytica*. Alignment of plant PFPs with *E histolytica* PFP active site residues are highlighted in blue, active site residues involved in PPi binding are highlighted in red, and additional residues involved in PPi binding are highlighted in green. The substrate-specifying residue is in teal.

```
Arabidopsis   SGKTGLISSVGNLAAPVEEWTVGGTALTALMDVERRHGKFKPVIKKAMVELEGAPFKKFA 527
Medicago      SGKTGLISSVGNLCAPVEEWTVGGTALTSLMDVERRHGKFKPVIKKAMVELEEAPFKKFA 529
Solanum       SGKTGLISSVGNLAAPVEELTVGGTALTALMDVERRHGKFKPVIKKAMVELEGAPFKKFA 511
Sorghum       SGKTGLISSVGNLAAPVQEWTVGGTALTSLMDVERRHGKFKPVIKKAMVELDAAPFKKYA 525
Entamoeba     LKKTGQICCISGLQKPAEEWICGGVPLTIMMNMEQRNGEMKPVIKKALVEIEGKPFKFYQ 507
                 *** *.:..*  *.:*   **..** :*::*:*:*::*******:**::  *** :

Arabidopsis   SLREEWALKNRYISPGPIQFTGPG--SDSLSHTLLLELGAQ- 566
Medicago      SLRDEWALKNCYISPGPIQFTGPG--SDAISHTLLLELGAQA 569
Solanum       SKREEWALNNRYINPGPIQFVGPV--ANKVNHTLLLELGVDA 551
Sorghum       SMRDEWAIKNRYISPGPIQFSGPG--SDDSNHTLMLELGAEL 565
Entamoeba     SKRAQWASAEDFVFPGAIQYFGPSEVCDQPTKTLLLEQN--- 546
              * * :**  : :: **.**: **   .:  .:**:** .
```

Figure 31. Continued.

CHAPTER V

CONCLUSIONS AND FUTURE DIRECTIONS

5.1 Chapter III conclusions and future directions

In Chapter III, I successfully identified a second major Pdk1 phosphorylation site on AGC1-3, in addition to the conserved activation-loop serine. Previously an attempt to map Pdk1-phosphorylated residues on Adi3 with MS/MS was conducted, and although other residues were identified, subsequent analysis demonstrated Adi3 was still phosphorylated by Pdk1. With this knowledge, I explored the PhosPhAt database to see if any high-throughput studies identified AGC1-3 phosphorylation sites, which could possibly be phosphorylated by Pdk1. Within the PhosPhAt database, one of two residues was identified as a phosphorylated residue in AGC1-3 (Ser137 or Ser138). Around this same time I read a paper detailing the use of reductive mutants to study the interaction between AvrPtoB and Pto (Xiao et al., 2007). I determined that a similar approach could be used to identify AGC1-3 phosphorylation sites by making N-terminal deletions. These studies implicated Ser269 as a Pdk1 phosphorylation site on AGC1-3. Mutagenesis and MS/MS confirmed Pdk1 phosphorylates the conserved site in Adi3, Ser212. Subsequent studies revealed the importance of this second site in Adi3 substrate activation.

5.1a Investigate AGC1-3 phosphorylation in vivo

Considering that Ser269 and Ser212 were both identified with recombinant proteins, they must be confirmed *in vivo*. For MS analysis of a protein, several mg are required, and recovering enough AGC1-3 from transient expression in protoplasts or any

other system could be problematic. To address problems involved with recovering enough protein for MS, a tandem affinity purification (TAP) plasmid was developed to purify protein complexes from transgenic plants (Rubio et al., 2005). The plasmid has a T-DNA that will overexpress a 9xMyc-6xHis fusion protein in plants and has been utilized to purify protein complexes as well as for post-translational modification analysis (Rubio et al., 2005). By using this system in transgenic plants, the tagged protein can be purified from the native system and will be under physiological conditions. Perhaps this plasmid would provide the appropriate system to recover enough AGC1-3 for MS analysis. If AGC1-3 could successfully be purified, a tool like this would enable further analysis of the AGC1-3 phosphorylation state, for example under different biotic and abiotic stresses. Additionally, cellular fractionation of a transgenic plant would enable detection of what phosphorylated species exists in different cellular compartments.

In addition to identifying a non-activation loop phosphorylation site on AGC1-3, I investigated if additional Pdk1 phosphorylation sites could be found in other AGC VIIIa kinases. I investigated AGC1-4 and AGC1-7 and found Pdk1 phosphorylates AGC1-7 at other residue(s) in addition to the activation loop serine. On the other hand, Pdk1 does not phosphorylate AGC1-4 at any other residues. Additional phosphorylation of AGC1-7 by Pdk1 indicates that Pdk1 does have at least one additional *in vitro* phosphorylation motif. Through a more in-depth analysis of the AGC VIIIa kinases, more examples of Pdk1 phosphorylation of non-activation loop residues might be identified. Currently three *Arabidopsis* AGC VIIIa kinases have been analyzed (AGC1-

3, AGC1-4, & AGC1-7) and of those proteins, Pdk1 phosphorylates two of them at non-activation loop residues. There is a strong chance that another Pdk1 phosphorylation motif or set of phosphorylation motifs exist in *Arabidopsis*. How common these are and how they alter AGC VIIIa kinase activity remains to be seen.

5.1b Investigation of cell viability of AGC1-3

In this study I determined that like Adi3, the NLS and phosphorylation of the activation loop are critical to AGC1-3's suppression of cell death and nuclear localization. In order to further investigate the role of AGC1-3 as a regulator of cell death, I would develop transgenic *Arabidopsis* lines with AGC1-3 mutants under the control of an inducible promoter, like the hormone estradiol. With an inducible promoter, a number of factors can be evaluated, for instance how long after induction does a mutant induce cell death. Likewise mutant induced cell death can be analyzed at different developmental stages when protein expression is not constitutive. In studies of cell death induced by Adi3 and AGC1-3 mutants, viability was evaluated 24hr after transfection (Ek-Ramos et al., 2010). With inducible promoters, protein expression can be started and terminated or sustained indefinitely. Some Adi3 mutants might induce cell death. However it could take longer than 24 hours to develop.

An alternative approach would be to develop an RNAi transgenic plant that reduces expression of AGC1-3. If a phenotype develops from transcript reduction, the resulting plant can be used in complementation assays with Adi3. Presumably, wild type Adi3 can complement the phenotype of AGC1-3, and with that, mutants of Adi3 can be used in additional complementation tests. Certain mutants of Adi3 would not be capable

of recovering the AGC1-3 RNAi phenotype, for instance the kinase inactive Adi3 would not be expected to recover the phenotype, nor would the activation loop extension mutants. It would be interesting to see if an Adi3^{S212D} mutant could complement but Adi3$^{S212D/S539D}$ could not. Complementation of AGC1-3 knockdown phenotypes would allow flexibility to determine what are essential components of AGC1-3 and Adi3 for cell death suppression.

5.2 Chapter IV conclusions and future directions

The KiC assay provided a list of potential substrates that will be useful for the study of AGC1-3 for years to come. A total of 37 unique proteins were implicated as substrates of AGC1-3 or AGC1-3^{S596D} – previous studies have shown these proteins have diverse subcellular localizations and enzymatic functions. Differential subcellular localization of these substrates could be an indication that phosphorylation by AGC1-3 is involved in localization. How phosphorylation by AGC1-3 impacts a given substrate's activity and localization remains to be thoroughly researched. Confirmation of phosphorylation by AGC1-3 followed by investigation of how phosphorylation impacts localization and protein function will provide a greater understanding of AGC1-3's function.

5.2a Investigate phosphorylation of substrates

The most important thing to do with the KiC data is to verify phosphorylation of these full-length proteins by AGC1-3, AGC1-3^{S596D}, or AGC1-3 activated by *At*Pdk1. A number of the substrate peptides identified in the KiC assay were phosphorylated on Tyr residues. AGC1-3 phosphorylation of Tyr residues was unexpected, so confirmation of

this function will be important to confirm or dismiss. Beyond confirming phosphorylation by AGC1-3, it will be important to see if the AGC1-3$^{S269D/S596D}$ mutant has higher *trans*-catalytic activity than the AGC1-3^{S596D} mutant, as is the case with Adi3. As substrates of Adi3, it would be interesting to analyze their activity and phosphorylation state in the context of infection by *Pseudomonas syringae* pv. *tomato*. With the data from the KiC assay, I assembled a table of tomato homologues and indicated whether or not the phosphorylated residue is conserved. Unfortunately, there is not a database similar to PhosPhAt for tomato, so I cannot see if the tomato homologues are phosphorylated.

5.2b Co-localization of AGC1-3 with substrates

From my work, AGC1-3 exhibits different localization patterns – it is in the nucleus when phosphorylated at the activation loop serine, in spite of mutations to a nuclear localization signal. In contrast, AGC1-3 is absent from the nucleus when phosphorylation of the activation loop serine is prevented, and its nuclear localization signal is mutated. Based on these pieces of data, AGC1-3 changes subcellular localization, therefore it is conceivable that when in different places of the cell, AGC1-3 is exposed to different substrates. One of the great advantages of working with *Arabidopsis* is the treasure trove of publicly available data in multiple different sources as has previously been mentioned – the PhosPhAt database, which has an overwhelming amount of MS protein phosphorylation data. Similar to PhosPhAt, the SubCellular Proteomic Database (SuBA) (http://suba.plantenergy.uwa.edu.au/) is a repository of MS subcellular localization data, collected from published data. Twenty of the 26 substrates

of AGC1-3 are supported by MS data identifying these proteins in the following locations: cytosol (Lee et al., 2005; Ito et al., 2011), PM (Benschop et al., 2007; Mitra et al., 2009; Zhang and Peck, 2011), mitochondria (Klodmann et al., 2011), extracellular (Bayer et al., 2006), nucleus (Calikowski et al., 2003; Tillemans et al., 2005), and plastid (Kleffmann et al., 2004; Ferro et al., 2010) (Table 4). Thirteen of 19 AGC1-3^{S596D} substrates have MS data that implicates their subcellular localization as well (Table 5). The significance of this is that review of the SuBA database showed that several PM localized proteins were phosphorylated at the same residue(s) identified in the KiC assay (Benschop et al., 2007). The data from PhosPhAt and SuBA do not stand-alone. However, these observations present the foundation for a narrative of AGC1-3 phosphorylation of several substrates. One potential substrate of AGC1-3^{S596D} is annotated as a DHHC zinc finger protein (DZFP) (At3g48760). Previously, zinc finger proteins have been reported in the nucleus as well as the cytosol (Pomeranz et al., 2010). DZFP was also identified in a phosphoproteomic analysis of the plasma membrane and is phosphorylated at the same residue that was identified in the KiC assay (Benschop et al., 2007). Though it must be confirmed, this presents the possibility that AGC1-3 co-localizes with and phosphorylates DZFP, perhaps to direct DZFP back to the nucleus.

In a proteomic analysis of the plasma membrane, PFP was identified while another proteomic analysis identified it in the cytosol. Co-localization of AGC1-3 and PFP could occur at either the PM or in the cytosol. Considering that MS data support PFP being in different locations, it will be interesting to see if localization, phosphorylation, and activity can be correlated.

Table 4. Subcellular localization of substrates phosphorylates by AGC1-3. A X denotes MS data is available identifying that protein at the listed subcellular location, a ~~X~~ denotes MS data is available identifying the implicated AGC1-3 phosphorylated residue is present at the listed subcellular location.

AGI	Cytosol	PM	Mitochondria	Nucleus	Plastid	Extracellular
At3g52950		X	X			
At2g29680						
At3g18630		X				
At3g62280						
At2g38280	X	X				
At3g51740		X				X
At2g19470	X					
At3g04820	X	X				
At5g35910	X					
At5g44340	X	X		X	X	
At5g45275		X				
At3g23890		X				
At5g35750						
At5g06140	X					
At2g31270						
At5g50020		~~X~~				
At3g02180						
At1g62740	X	X				
At4g26110	X	X				
At1g77110		~~X~~				
At5g19390						
At2g01180		X				
At2g37340	X					
At1g04860					X	
At1g54080		X				
At4g02060	X			X		

Table 5. Subcellular localization of AGC1-3^{S596D} phosphorylated substrates. A X denotes MS data is available identifying that protein at the listed subcellular location, a ~~X~~ denotes MS data is available identifying the implicated AGC1-3 phosphorylated residue is present at the listed subcellular location.

AGI	Cytosol	PM	Mitochondria	Nucleus	Plastid	Extracellular
At3g52950		X	X			
At2g29680						
At1g01550		X				
At5g23080						
At3g62280						
At1g14850	X	X		X	X	
At5g35750						
At2g35030						
At2g32415						
At1g12000	X	X				
At5g45275		X				
At2g38280	X	X				
At5g18500		~~X~~				
At3g48760		~~X~~				
At1g06840		~~X~~				
At2g01180		X				
At1g75990	X	X				
At5g08080	X	X				
At1g77110		~~X~~				

While characterization of PFP has commenced –phosphatidic acid phosphatase (PAP) is also in the initial stages of characterization. PFP was selected for more or less two reasons – I had never heard of pyrophosphate-dependent phosphofructokinase, I'd only heard of ATP-dependent phosphofructokinase and Adi3 regulates the SnRK complex, so there is already some precedent for AGC1-3/Adi3 to be connected to sugar metabolism. Phosphatidic acid phosphatase was selected for characterization because phosphatidic acid (PA) is a lipid singaling molecule that *At*Pdk1 binds via its PH domain – binding of PA activates *At*Pdk1 (Deak et al., 1999; Camehl et al., 2011). A very interesting scenario is presented: AGC1-3 could regulate an enzyme that controls the signaling molecule that indirectly regulates AGC1-3. From an anecdotal standpoint, characterizing PAP and the possible phosphorylation by AGC1-3 is an interesting project. PAP has been fairly well characterized, and in fact, phosphorylation of PAP has been investigated to an extent. In yeast, knockouts of the PAP homologue, Pah1p are highly susceptible to fatty acid-induced toxicity (Pascual and Carman, 2013). With respect to their phosphorylation state, dephosphorylation of Pah1p stimulates PAP activity (Pascual and Carman, 2013). Reviewing the list of potential substrates is a pleasant burden – when looking at the list of substrates, a new way to look at cell death regulation is considered. With that said, PFP is an interesting enzyme, with a possible grounding in stress response or at least in sustaining glycolysis in ATP-limiting environments, based on increased expression levels in QPM compared to opaque2 (Guo et al., 2012).

5.2c Utilize KiC data for studies with Adi3

With all of the data acquired from the KiC assay, it can be utilized for studies of Adi3 and AvrPto/Pto signaling. Each of the AGC1-3 substrates in *Arabidopsis* has a homologous protein in tomato, and in many cases, the phosphorylated residue(s) identified in the KiC assay are conserved in the tomato proteins (Table 6). Just as the role of phosphorylation by AGC1-3 can be characterized in *Arabidopsis*, study of these proteins in tomato will provide setting to study phosphorylation state and activity of proteins in response to pathogen attack.

5.3 Final conclusions

In this dissertation, I present work that implicates AGC1-3 as the *Arabidopsis thaliana* homologue of the tomato cell death regulator, Adi3. I also used AGC1-3 to conclusively identify a second Pdk1 phosphorylation site, in addition to the AGC1-3 activation-loop serine. This second Pdk1 phosphorylation site is conserved in Adi3 and was shown to contribute to substrate phosphorylation by Adi3. With the KiC assay, 37 potential AGC1-3 substrates that comprise diverse functions were identified. The data acquired from the KiC assay is extremely exciting, as well – essentially every single peptide presents a unique project to develop. For example, prior to substrate identification, I was completely unaware of the enzyme pyrophosphate-dependent phosphofructokinase (PFP). Continuance of studies related to the KiC assay will develop a greater understanding of AGC1-3's function as a cell death regulator. Future studies should be directed toward the implications of AGC1-3 phosphorylation of PFP, Adi3

Table 6. Tomato homologues of KiC assay substrates. Results from the KiC assay with AGC1-3 and AGC1-3^{S596D} were used in BLASTp searches of the tomato genome. Of the 37 peptides, the phosphorylated residue is conserved in 26 of the tomato homologues.

AGI	Accession	Highest Identity	Phosphorylation site conserved?
At3g52950	XP_004252207.1	73%	Yes
At2g29680	XP_004241172.1	57%	Yes
At3g18630	XP_004231528.1	64%	No
At3g62280	XP_004230336.1	55%	No
At2g38280	XP_004246317.1	78%	Yes
At3g51740	XP_004246299.1	66%	No
At2g19470	XP_004235583.1	64%	Yes
At3g04820	XP_004230110.1	64%	No
At5g35910	XP_004248555.1	49%	No
At5g44340	XP_004235778.1	91%	Yes
At5g45275	XP_004246045.1	68%	No
At3g23890	XP_004229644.1	66%	Yes
At5g35750	XP_004239224.1	56%	Thr-Ser
At5g06140	XP_004246487.1	78%	Yes
At2g31270	XP_004240635.1	46%	No
At5g50020	XP_004231755.1	49%	Yes
At3g02180	XP_004232154.1	51%	Yes
At1g62740	XP_004245731.1	73%	Yes
At4g26110	XP_004239291.1	69%	Yes
At1g77110	XP_001234199.1	68%	Yes
At5g19390	XP_004250893.1	70%	Yes
At2g01180	XP_004238889.1	65%	Yes
At2g37340	XP_004239756.1	61%	Ser-Thr
At1g04860	XP_004247858.1	41%	Yes
At1g54080	XP_004241874.1	73%	Yes
At4g02060	XP_004229395.1	84%	Yes
At5g08080	XP_004249403.1	50%	Yes
At1g01550	XP_004248056.1	56%	No
At5g23080	XP_004236099.1	62%	Yes
At1g14850	XP_004242776.1	72%	Yes
At2g35030	XP_004242982.1	38%	Yes
At2g32415	XP_004248555.1	38%	No
At1g12000	XP_004243522.1	81%	No
At5g18500	XP_004229895.1	52%	No
At3g48760	XP_004241453.1	57%	Yes
At1g06840	XP_004247017.1	66%	Yes
At1g75990	XP_004231054.1	80%	Thr-Ser

phosphorylation of a PFP homologue in tomato and the implications of these events in response to abiotic and biotic stress.

REFERENCES

Alessi DR, James SR, Downes CP, Holmes AB, Gaffney PR, Reese CB, Cohen P (1997) Characterization of a 3-phosphoinositide-dependent protein kinase which phosphorylates and activates protein kinase Bα. Curr Biol **7:** 261-269

Alves AM, Euverink GJ, Santos H, Dijkhuizen L (2001) Different physiological roles of ATP- and PP(i)-dependent phosphofructokinase isoenzymes in the methylotrophic actinomycete *Amycolatopsis methanolica*. J Bacteriol **183:** 7231-7240

Anthony RG, Henriques R, Helfer A, Meszaros T, Rios G, Testerink C, Munnik T, Deak M, Koncz C, Bogre L (2004) A protein kinase target of a PDK1 signalling pathway is involved in root hair growth in *Arabidopsis*. EMBO J **23:** 572-581

Attwood PV, Besant PG, Piggott MJ (2011) Focus on phosphoaspartate and phosphoglutamate. Amino Acids **40:** 1035-1051

Avila J, Gregory OG, Su D, Deeter TA, Chen S, Silva-Sanchez C, Xu S, Martin GB, Devarenne TP (2012) The β-subunit of the SnRK1 complex is phosphorylated by the plant cell death suppressor Adi3. Plant Physiol **159:** 1277-1290

Bae MS, Cho EJ, Choi EY, Park OK (2003) Analysis of the *Arabidopsis* nuclear proteome and its response to cold stress. Plant J **36:** 652-663

Balendran A, Casamayor A, Deak M, Paterson A, Gaffney P, Currie R, Downes CP, Alessi DR (1999) PDK1 acquires PDK2 activity in the presence of a synthetic peptide derived from the carboxyl terminus of PRK2. Curr Biol **9:** 393-404

Barth LG, Jaeger L (1950) The role of adenosine-tri-phosphate in phosphate transfer from yolk to other proteins in the developing frog egg. I. General properties of the transfer system as a whole. J Cell Physiol **35:** 413-435

Bayer EM, Bottrill AR, Walshaw J, Vigouroux M, Naldrett MJ, Thomas CL, Maule AJ (2006) *Arabidopsis* cell wall proteome defined using multidimensional protein identification technology. Proteomics **6:** 301-311

Belham C, Wu S, Avruch J (1999) Intracellular signalling: PDK1--a kinase at the hub of things. Curr Biol **9:** R93-96

Benschop JJ, Mohammed S, O'Flaherty M, Heck AJ, Slijper M, Menke FL (2007) Quantitative phosphoproteomics of early elicitor signaling in *Arabidopsis*. Mol Cell Proteomics **6:** 1198-1214

Besant PG, Attwood PV, Piggott MJ (2009) Focus on phosphoarginine and phospholysine. Curr Protein Pept Sci **10:** 536-550

Biondi RM, Cheung PC, Casamayor A, Deak M, Currie RA, Alessi DR (2000) Identification of a pocket in the PDK1 kinase domain that interacts with PIF and the C-terminal residues of PKA. EMBO J **19:** 979-988

Biondi RM, Kieloch A, Currie RA, Deak M, Alessi DR (2001) The PIF-binding pocket in PDK1 is essential for activation of S6K and SGK, but not PKB. EMBO J **20:** 4380-4390

Biondi RM, Komander D, Thomas CC, Lizcano JM, Deak M, Alessi DR, van Aalten DM (2002) High resolution crystal structure of the human PDK1 catalytic domain defines the regulatory phosphopeptide docking site. EMBO J **21:** 4219-4228

Biondi RM, Nebreda AR (2003) Signalling specificity of Ser/Thr protein kinases through docking-site-mediated interactions. Biochem J **372:** 1-13

Bogdanove AJ, Martin GB (2000) AvrPto-dependent Pto-interacting proteins and AvrPto-interacting proteins in tomato. Proc Natl Acad Sci U S A **97:** 8836-8840

Bogre L, Okresz L, Henriques R, Anthony RG (2003) Growth signalling pathways in *Arabidopsis* and the AGC protein kinases. Trends Plant Sci **8:** 424-431

Boursnell JC, Dewey HM, Wormall A (1948) The chemical and immunological properties of phosphorylated proteins. Biochem J **43:** 84-90

Briggs WR, Christie JM (2002) Phototropins 1 and 2: versatile plant blue-light receptors. Trends Plant Sci **7:** 204-210

Bruchhaus I, Jacobs T, Denart M, Tannich E (1996) Pyrophosphate-dependent phosphofructokinase of *Entamoeba histolytica*: molecular cloning, recombinant expression and inhibition by pyrophosphate analogues. Biochem J **316 (Pt 1):** 57-63

Burnett G, Kennedy EP (1954) The enzymatic phosphorylation of proteins. J Biol Chem **211:** 969-980

Calikowski TT, Meulia T, Meier I (2003) A proteomic study of the *Arabidopsis* nuclear matrix. J Cell Biochem **90:** 361-378

Calleja V, Alcor D, Laguerre M, Park J, Vojnovic B, Hemmings BA, Downward J, Parker PJ, Larijani B (2007) Intramolecular and intermolecular interactions of protein kinase B define its activation in vivo. PLoS Biol **5:** e95

Camehl I, Drzewiecki C, Vadassery J, Shahollari B, Sherameti I, Forzani C, Munnik T, Hirt H, Oelmuller R (2011) The OXI1 kinase pathway mediates *Piriformospora indica*-induced growth promotion in *Arabidopsis*. PLoS Pathog **7:** e1002051

Carlisle SM, Blakeley SD, Hemmingsen SM, Trevanion SJ, Hiyoshi T, Kruger NJ, Dennis DT (1990) Pyrophosphate-dependent phosphofructokinase. Conservation of protein sequence between the α- and β-subunits and with the ATP-dependent phosphofructokinase. J Biol Chem **265:** 18366-18371

Carnal NW, Black CC (1983) Phosphofructokinase activities in photosynthetic organisms : the occurrence of pyrophosphate-dependent 6-phosphofructokinase in plants and algae. Plant Physiol **71:** 150-155

Carnero A (2010) The PKB/AKT pathway in cancer. Curr Pharm Des **16:** 34-44

Casamayor A, Torrance PD, Kobayashi T, Thorner J, Alessi DR (1999) Functional counterparts of mammalian protein kinases PDK1 and SGK in budding yeast. Curr Biol **9:** 186-197

Celenza JL, Carlson M (1986) A yeast gene that is essential for release from glucose repression encodes a protein kinase. Science **233:** 1175-1180

Chi A, Kemp RG (2000) The primordial high energy compound: ATP or inorganic pyrophosphate? J Biol Chem **275:** 35677-35679

Chittenden RH, Folin O, Gies WJ, Koch W, Osborne TB, Osborne TB, Levene PA, Mandel JA, Mathews AP, Mendel LB (1908) Joint Recommendations of the Physiological and Biochemical Committees on Protein Nomenclature. Science **27:** 554-556

Christie JM, Yang H, Richter GL, Sullivan S, Thomson CE, Lin J, Titapiwatanakun B, Ennis M, Kaiserli E, Lee OR, Adamec J, Peer WA, Murphy AS (2011) phot1 inhibition of ABCB19 primes lateral auxin fluxes in the shoot apex required for phototropism. PLoS Biol **9:** e1001076

Currie RA, Walker KS, Gray A, Deak M, Casamayor A, Downes CP, Cohen P, Alessi DR, Lucocq J (1999) Role of phosphatidylinositol 3,4,5-trisphosphate in regulating the activity and localization of 3-phosphoinositide-dependent protein kinase-1. Biochem J **337 (Pt 3):** 575-583

Czech MP, Klarlund JK, Yagaloff KA, Bradford AP, Lewis RE (1988) Insulin receptor signaling. Activation of multiple serine kinases. J Biol Chem **263:** 11017-11020

Dang CV (2013) Role of aerobic glycolysis in genetically engineered mouse models of cancer. BMC Biol **11:** 3

Deak M, Casamayor A, Currie RA, Downes CP, Alessi DR (1999) Characterisation of a plant 3-phosphoinositide-dependent protein kinase-1 homologue which contains a pleckstrin homology domain. FEBS Lett **451:** 220-226

Demmel L, Beck M, Klose C, Schlaitz AL, Gloor Y, Hsu PP, Havlis J, Shevchenko A, Krause E, Kalaidzidis Y, Walch-Solimena C (2008) Nucleocytoplasmic shuttling of the Golgi phosphatidylinositol 4-kinase Pik1 is regulated by 14-3-3 proteins and coordinates Golgi function with cell growth. Mol Biol Cell **19:** 1046-1061

Devarenne TP, Ekengren SK, Pedley KF, Martin GB (2006) Adi3 is a Pdk1-interacting AGC kinase that negatively regulates plant cell death. EMBO J **25:** 255-265

Dittrich AC, Devarenne TP (2012) An ATP analog-sensitive version of the tomato cell death suppressor protein kinase Adi3 for use in substrate identification. Biochim Biophys Acta **1824:** 269-273

Eckhart W, Hutchinson MA, Hunter T (1979) An activity phosphorylating tyrosine in polyoma T antigen immunoprecipitates. Cell **18:** 925-933

Ek-Ramos MJ, Avila J, Cheng C, Martin GB, Devarenne TP (2010) The T-loop extension of the tomato protein kinase AvrPto-dependent Pto-interacting protein 3 (Adi3) directs nuclear localization for suppression of plant cell death. J Biol Chem **285:** 17584-17594

El-Maghrabi MR, Claus TH, Pilkis J, Fox E, Pilkis SJ (1982) Regulation of rat liver fructose 2,6-bisphosphatase. J Biol Chem **257:** 7603-7607

Fernandez M, Cao J, Villamarin JA (1998) In vivo phosphorylation of phosphofructokinase from the bivalve mollusk *Mytilus galloprovincialis*. Arch Biochem Biophys **353:** 251-256

Ferro M, Brugiere S, Salvi D, Seigneurin-Berny D, Court M, Moyet L, Ramus C, Miras S, Mellal M, Le Gall S, Kieffer-Jaquinod S, Bruley C, Garin J, Joyard J, Masselon C, Rolland N (2010) AT_CHLORO, a comprehensive chloroplast proteome database with subplastidial localization and curated information on envelope proteins. Mol Cell Proteomics **9:** 1063-1084

Foe LG, Kemp RG (1984) Isozyme composition and phosphorylation of brain phosphofructokinase. Arch Biochem Biophys **228:** 503-511

Frodin M, Antal TL, Dummler BA, Jensen CJ, Deak M, Gammeltoft S, Biondi RM (2002) A phosphoserine/threonine-binding pocket in AGC kinases and PDK1 mediates activation by hydrophobic motif phosphorylation. EMBO J **21:** 5396-5407

Golemis EA, Serebriiskii I, Finley RL, Jr., Kolonin MG, Gyuris J, Brent R (2008) Interaction trap/two-hybrid system to identify interacting proteins. Curr Protoc Mol Biol **Chapter 20:** Unit 20 21

Guo X, Ronhovde K, Yuan L, Yao B, Soundararajan MP, Elthon T, Zhang C, Holding DR (2012) Pyrophosphate-dependent fructose-6-phosphate 1-phosphotransferase induction and attenuation of Hsp gene expression during endosperm modification in quality protein maize. Plant Physiol **158:** 917-929

Halford NG, Hey S, Jhurreea D, Laurie S, McKibbin RS, Paul M, Zhang Y (2003) Metabolic signalling and carbon partitioning: role of Snf1-related (SnRK1) protein kinase. J Exp Bot **54:** 467-475

Halford NG, Hey SJ (2009) Snf1-related protein kinases (SnRKs) act within an intricate network that links metabolic and stress signalling in plants. Biochem J **419:** 247-259

Hanks SK (2003) Genomic analysis of the eukaryotic protein kinase superfamily: a perspective. Genome Biol **4:** 111.1-111.7

Hanks SK, Quinn AM, Hunter T (1988) The protein kinase family: conserved features and deduced phylogeny of the catalytic domains. Science **241:** 42-52

Hauge C, Antal TL, Hirschberg D, Doehn U, Thorup K, Idrissova L, Hansen K, Jensen ON, Jorgensen TJ, Biondi RM, Frodin M (2007) Mechanism for activation of the growth factor-activated AGC kinases by turn motif phosphorylation. EMBO J **26:** 2251-2261

Heidelberger M, Davis, Barnard, Treffers, Henry P. (1941) Phosphorylated egg albumin. Journal of the American Chemical Society **63:** 498-503

Hill MM, Hemmings BA (2002) Inhibition of protein kinase B/Akt. implications for cancer therapy. Pharmacol Ther **93:** 243-251

Huang Y, Thelen JJ (2012) KiC assay: a quantitative mass spectrometry-based approach for kinase client screening and activity analysis [corrected]. Methods Mol Biol **893:** 359-370

Huebner VD, Matthews HR (1985) Phosphorylation of histidine in proteins by a nuclear extract of *Physarum polycephalum* plasmodia. J Biol Chem **260:** 16106-16113

Ito J, Batth TS, Petzold CJ, Redding-Johanson AM, Mukhopadhyay A, Verboom R, Meyer EH, Millar AH, Heazlewood JL (2011) Analysis of the *Arabidopsis* cytosolic proteome highlights subcellular partitioning of central plant metabolism. J Proteome Res **10:** 1571-1582

Kimmel JL, Reinhart GD (2000) Reevaluation of the accepted allosteric mechanism of phosphofructokinase from *Bacillus stearothermophilus*. Proc Natl Acad Sci U S A **97:** 3844-3849

Kleffmann T, Russenberger D, von Zychlinski A, Christopher W, Sjolander K, Gruissem W, Baginsky S (2004) The *Arabidopsis thaliana* chloroplast proteome reveals pathway abundance and novel protein functions. Curr Biol **14:** 354-362

Klodmann J, Senkler M, Rode C, Braun HP (2011) Defining the protein complex proteome of plant mitochondria. Plant Physiol **157:** 587-598

Koch A, Hauf S (2010) Strategies for the identification of kinase substrates using analog-sensitive kinases. Eur J Cell Biol **89:** 184-193

Kotlarz D, Buc H (1981) Regulatory properties of phosphofructokinase 2 from *Escherichia coli*. Eur J Biochem **117:** 569-574

Krebs EG, Beavo JA (1979) Phosphorylation-dephosphorylation of enzymes. Annu Rev Biochem **48:** 923-959

Ladror US, Gollapudi L, Tripathi RL, Latshaw SP, Kemp RG (1991) Cloning, sequencing, and expression of pyrophosphate-dependent phosphofructokinase from *Propionibacterium freudenreichii*. J Biol Chem **266:** 16550-16555

Lai AC, Nguyen Ba AN, Moses AM (2012) Predicting kinase substrates using conservation of local motif density. Bioinformatics **28:** 962-969

Lawlor MA, Mora A, Ashby PR, Williams MR, Murray-Tait V, Malone L, Prescott AR, Lucocq JM, Alessi DR (2002) Essential role of PDK1 in regulating cell size and development in mice. EMBO J **21:** 3728-3738

Lee JY, Taoka K, Yoo BC, Ben-Nissan G, Kim DJ, Lucas WJ (2005) Plasmodesmal-associated protein kinase in tobacco and *Arabidopsis* recognizes a subset of non-cell-autonomous proteins. Plant Cell **17:** 2817-2831

Luo Z, Zang M, Guo W (2010) AMPK as a metabolic tumor suppressor: control of metabolism and cell growth. Future Oncol **6:** 457-470

MacBeath G, Schreiber SL (2000) Printing proteins as microarrays for high-throughput function determination. Science **289:** 1760-1763

Martin GB, Brommonschenkel SH, Chunwongse J, Frary A, Ganal MW, Spivey R, Wu T, Earle ED, Tanksley SD (1993) Map-based cloning of a protein kinase gene conferring disease resistance in tomato. Science **262:** 1432-1436

Matsui H, Miyao A, Takahashi A, Hirochika H (2010) Pdk1 kinase regulates basal disease resistance through the OsOxi1-OsPti1a phosphorylation cascade in rice. Plant Cell Physiol **51:** 2082-2091

Mayank P, Grossman J, Wuest S, Boisson-Dernier A, Roschitzki B, Nanni P, Nuhse T, Grossniklaus U (2012) Characterization of the phosphoproteome of mature *Arabidopsis* pollen. Plant J **72:** 89-101

Mesojednik S, Legisa M (2005) Posttranslational modification of 6-phosphofructo-1-kinase in *Aspergillus niger*. Appl Environ Microbiol **71:** 1425-1432

Metz HE, Houghton AM (2011) Insulin receptor substrate regulation of phosphoinositide 3-kinase. Clin Cancer Res **17:** 206-211

Mitchelhill KI, Michell BJ, House CM, Stapleton D, Dyck J, Gamble J, Ullrich C, Witters LA, Kemp BE (1997) Posttranslational modifications of the 5'-AMP-activated protein kinase β1 subunit. J Biol Chem **272:** 24475-24479

Mitra SK, Walters BT, Clouse SD, Goshe MB (2009) An efficient organic solvent based extraction method for the proteomic analysis of *Arabidopsis* plasma membranes. J Proteome Res **8:** 2752-2767

Moore SA, Ronimus RS, Roberson RS, Morgan HW (2002) The structure of a pyrophosphate-dependent phosphofructokinase from the Lyme disease spirochete *Borrelia burgdorferi*. Structure **10:** 659-671

Mora A, Komander D, van Aalten DM, Alessi DR (2004) PDK1, the master regulator of AGC kinase signal transduction. Semin Cell Dev Biol **15:** 161-170

Morel JB, Dangl JL (1997) The hypersensitive response and the induction of cell death in plants. Cell Death Differ **4:** 671-683

Mosser R, Reddy MC, Bruning JB, Sacchettini JC, Reinhart GD (2012) Structure of the apo form of *Bacillus stearothermophilus* phosphofructokinase. Biochemistry **51:** 769-775

Murley VR, Theodorou ME, Plaxton WC (1998) Phosphate starvation-inducible pyrophosphate-dependent phosphofructokinase occurs in plants whose roots do not form symbiotic associations with mycorrhizal fungi. Physiologia Plantarum **103:** 405-414

Nakagami H, Sugiyama N, Mochida K, Daudi A, Yoshida Y, Toyoda T, Tomita M, Ishihama Y, Shirasu K (2010) Large-scale comparative phosphoproteomics identifies conserved phosphorylation sites in plants. Plant Physiol **153:** 1161-1174

Newgard CB, Hwang PK, Fletterick RJ (1989) The family of glycogen phosphorylases: structure and function. Crit Rev Biochem Mol Biol **24:** 69-99

Nielsen TH, Rung JH, Villadsen D (2004) Fructose-2,6-bisphosphate: a traffic signal in plant metabolism. Trends Plant Sci **9:** 556-563

Nuhse TS, Bottrill AR, Jones AM, Peck SC (2007) Quantitative phosphoproteomic analysis of plasma membrane proteins reveals regulatory mechanisms of plant innate immune responses. Plant J **51:** 931-940

Obata T, Yaffe MB, Leparc GG, Piro ET, Maegawa H, Kashiwagi A, Kikkawa R, Cantley LC (2000) Peptide and protein library screening defines optimal substrate motifs for AKT/PKB. J Biol Chem **275:** 36108-36115

Obiadalla-Ali H, Fernie AR, Kossmann J, Lloyd JR (2004) Developmental analysis of carbohydrate metabolism in tomato (*Lycopersicon esculentum* cv. Micro-Tom) fruits. Physiol Plant **120:** 196-204

Okajima K, Kashojiya S, Tokutomi S (2012) Photosensitivity of kinase activation by blue light involves the lifetime of a cysteinyl-flavin adduct intermediate, S390, in the photoreaction cycle of the LOV2 domain in phototropin, a plant blue light receptor. J Biol Chem **287:** 40972-40981

Paoletti E, Moss B (1972) Protein kinase and specific phosphate acceptor proteins associated with *Vaccinia virus* cores. J Virol **10:** 417-424

Paradis S, Ailion M, Toker A, Thomas JH, Ruvkun G (1999) A PDK1 homolog is necessary and sufficient to transduce AGE-1 PI3 kinase signals that regulate diapause in *Caenorhabditis elegans*. Genes Dev **13:** 1438-1452

Parekh DB, Ziegler W, Parker PJ (2000) Multiple pathways control protein kinase C phosphorylation. EMBO J **19:** 496-503

Pascual F, Carman GM (2013) Phosphatidate phosphatase, a key regulator of lipid homeostasis. Biochim Biophys Acta **1831:** 514-522

Pearce LR, Komander D, Alessi DR (2010) The nuts and bolts of AGC protein kinases. Nat Rev Mol Cell Biol **11:** 9-22

Pomeranz MC, Hah C, Lin PC, Kang SG, Finer JJ, Blackshear PJ, Jang JC (2010) The *Arabidopsis* tandem zinc finger protein AtTZF1 traffics between the nucleus and cytoplasmic foci and binds both DNA and RNA. Plant Physiol **152:** 151-165

Ptacek J, Devgan G, Michaud G, Zhu H, Zhu X, Fasolo J, Guo H, Jona G, Breitkreutz A, Sopko R, McCartney RR, Schmidt MC, Rachidi N, Lee SJ, Mah AS, Meng L, Stark MJ, Stern DF, De Virgilio C, Tyers M, Andrews B,

Gerstein M, Schweitzer B, Predki PF, Snyder M (2005) Global analysis of protein phosphorylation in yeast. Nature **438:** 679-684

Rangone H, Poizat G, Troncoso J, Ross CA, MacDonald ME, Saudou F, Humbert S (2004) The serum- and glucocorticoid-induced kinase SGK inhibits mutant huntingtin-induced toxicity by phosphorylating serine 421 of huntingtin. Eur J Neurosci **19:** 273-279

Reiland S, Finazzi G, Endler A, Willig A, Baerenfaller K, Grossmann J, Gerrits B, Rutishauser D, Gruissem W, Rochaix JD, Baginsky S (2011) Comparative phosphoproteome profiling reveals a function of the STN8 kinase in fine-tuning of cyclic electron flow (CEF). Proc Natl Acad Sci U S A **108:** 12955-12960

Reiland S, Messerli G, Baerenfaller K, Gerrits B, Endler A, Grossmann J, Gruissem W, Baginsky S (2009) Large-scale *Arabidopsis* phosphoproteome profiling reveals novel chloroplast kinase substrates and phosphorylation networks. Plant Physiol **150:** 889-903

Rimington C (1927) The Phosphorus of caseinogen: Constitution of phosphopeptone. Biochem J **21:** 1187-1193

Rimington C, Kay HD (1926) Some phosphorus compounds of milk: The liberation of phosphorus from caseinogen by enzymes and other agents. Biochem J **20:** 777-790

Rubio V, Shen Y, Saijo Y, Liu Y, Gusmaroli G, Dinesh-Kumar SP, Deng XW (2005) An alternative tandem affinity purification strategy applied to *Arabidopsis* protein complex isolation. Plant J **41:** 767-778

Santner AA, Watson JC (2006) The WAG1 and WAG2 protein kinases negatively regulate root waving in *Arabidopsis*. Plant J **45:** 752-764

Sheffield J, Taylor N, Fauquet C, Chen S (2006) The cassava (*Manihot esculenta* Crantz) root proteome: protein identification and differential expression. Proteomics **6:** 1588-1598

Shirakihara Y, Evans PR (1988) Crystal structure of the complex of phosphofructokinase from *Escherichia coli* with its reaction products. J Mol Biol **204:** 973-994

Stempka L, Girod A, Muller HJ, Rincke G, Marks F, Gschwendt M, Bossemeyer D (1997) Phosphorylation of protein kinase C δ (PKC δ) at threonine 505 is not a prerequisite for enzymatic activity. Expression of rat PKC δ and an alanine 505 mutant in bacteria in a functional form. J Biol Chem **272:** 6805-6811

Tillemans V, Dispa L, Remacle C, Collinge M, Motte P (2005) Functional distribution and dynamics of *Arabidopsis* SR splicing factors in living plant cells. Plant J **41:** 567-582

Vincent O, Carlson M (1999) Gal83 mediates the interaction of the Snf1 kinase complex with the transcription activator Sip4. EMBO J **18:** 6672-6681

Vincent O, Townley R, Kuchin S, Carlson M (2001) Subcellular localization of the Snf1 kinase is regulated by specific β subunits and a novel glucose signaling mechanism. Genes Dev **15:** 1104-1114

Warden SM, Richardson C, O'Donnell J, Jr., Stapleton D, Kemp BE, Witters LA (2001) Post-translational modifications of the β-1 subunit of AMP-activated protein kinase affect enzyme activity and cellular localization. Biochem J **354:** 275-283

Watson JA, Rumsby MG, Wolowacz RG (1999) Phage display identifies thioredoxin and superoxide dismutase as novel protein kinase C-interacting proteins: thioredoxin inhibits protein kinase C-mediated phosphorylation of histone. Biochem J **343 Pt 2:** 301-305

Wong JH, Kiss F, Wu MX, Buchanan BB (1990) Pyrophosphate Fructose-6-P 1-Phosphotransferase from tomato fruit : Evidence for change during ripening. Plant Physiol **94:** 499-506

Xiao F, He P, Abramovitch RB, Dawson JE, Nicholson LK, Sheen J, Martin GB (2007) The N-terminal region of *Pseudomonas* type III effector AvrPtoB elicits Pto-dependent immunity and has two distinct virulence determinants. Plant J **52:** 595-614

Xing T, Malik K, Martin T, Miki BL (2001) Activation of tomato PR and wound-related genes by a mutagenized tomato MAP kinase kinase through divergent pathways. Plant Mol Biol **46:** 109-120

Yamaguchi H, Wang HG (2001) The protein kinase PKB/Akt regulates cell survival and apoptosis by inhibiting Bax conformational change. Oncogene **20:** 7779-7786

Yoo SD, Cho YH, Sheen J (2007) *Arabidopsis* mesophyll protoplasts: a versatile cell system for transient gene expression analysis. Nat Protoc **2:** 1565-1572

Zegzouti H, Li W, Lorenz TC, Xie M, Payne CT, Smith K, Glenny S, Payne GS, Christensen SK (2006) Structural and functional insights into the regulation of *Arabidopsis* AGC VIIIa kinases. J Biol Chem **281:** 35520-35530

Zhang Y, He J, McCormick S (2009) Two *Arabidopsis* AGC kinases are critical for the polarized growth of pollen tubes. Plant J **58:** 474-484

Zhang ZJ, Peck SC (2011) Simplified enrichment of plasma membrane proteins for proteomic analyses in *Arabidopsis thaliana*. Proteomics **11:** 1780-1788